Gene expression profiling in different stages of development of *Arabidopsis thaliana* leaf trichomes at the single cell level

Elektronisch veröffentlicht auf dem
Publikationsserver der Universität Potsdam:
http://opus.kobv.de/ubp/volltexte/2008/1747/
urn:nbn:de:kobv:517-opus-17474
[http://nbn-resolving.de/urn:nbn:de:kobv:517-opus-17474]

MAX-PLANCK-GESELLSCHAFT

Max-Planck-Institut
für Molekulare Pflanzenphysiologie

Universität Potsdam

Gene expression profiling in different stages of development of *Arabidopsis thaliana* leaf trichomes at the single cell level

Dissertation
zur Erlangung des akademischen Grades
"doctor rerum naturalium"
(Dr. rer. nat.)
in der Wissenschaftsdisziplin Molekularbiologie

eingereicht an der
Mathematisch-Naturwissenschaftlichen Fakultät
der Universität Potsdam

von
Sergiy Kryvych

Potsdam
Oktober 2007

For my father

"Publish or perish"
Popular saying among scientists today

"Knowledge of some principles easily compensates ignorance of some facts"
Claude-Adrien Helvetius, French philosopher

"Electronics is the science of contacts"
Saying

CONTENTS

FIGURES…… 6
COMMONLY USED ABBREVIATIONS…… 7
1. INTRODUCTION…… 8
1.1. Trichomes of *Arabidopsis thaliana*…….... 8
1.1.1 Trichome development…….. 9
1.1.2 Regulation of trichome development……..... 10
1.1.3 Cell cycle alterations during trichome development……. 11
1.1.3.1 Cell cycle regulation in plants……. 11
1.1.3.2 Regulation of the switch between mitotic and endoreduplication cycles in developing trichomes……... 14
1.2 Single cell analysis…….. 15
1.2.1 Methods of the single cell sampling……... 16
1.2.1.1 Non-invasive methods……. 17
1.2.1.2 Minimally invasive methods…… 17
1.2.1.3 Invasive sampling methods…… 18
1.2.2 Amplification methods used for single cell transcript profiling…….. 19
1.3 Aims of this thesis…… 21
2. MATERIALS AND METHODS……..... 22
2.1 Commonly used equipment, kits and consumables……. 22
2.1.1. Equipment…… 22
2.1.2. Consumables……... 22
2.1.3. Kits…….. 23
2.2. Plant material……. 23
2.3. Plant growth…… 23
2.4. Single Cell Sampling…… 24
2.5. Single cell PCR amplification……. 24
2.6. Single cell sampling control reactions……. 25
2.7. Probe generation for array hybridization……. 26
2.8. Filter array hybridization……. 26
2.8.1 Array hybridization and evaluation……... 26
2.8.1.1.Reference hybridization…….. 26
2.8.1.2.Complex hybridization…… 27
2.8.1.3.Data processing…….. 27
2.9. Affymetrix GeneChip hybridization…….. 27
2.10. Real-time RT-PCR……. 28
2.11. Genomic DNA isolation…… 28
2.12. RNA extraction using TRIzol protocol……. 29
2.13. Construction of promoter::β-glucuronidase fusions……... 29
2.14. Bacteria transformation and growth……... 32
2.15. *Arabidopsis thaliana* transformation……... 32
2.16. Histochemical analysis of plants transformed with promoter::GUS constructs…. 32
2.17. Promoter analysis…….. 32
2.18. PCR-based screening for homozygous knockout (KO) plant lines……. 33
2.19. Microscopic analysis of the knockout plant lines…….. 34
2.20. Gas chromatography-mass spectrometry (GC-MS)…….. 34
3. RESULTS……... 36
3.1. Workflow……. 36
3.2. Single cell sampling and array hybridization……... 36
3.3. Affymetrix GeneChip hybridization…… 40

3.4. Candidate gene selection and validation of single cell gene expression profiling.. 41
3.4.1. Real-time RT-PCR……43
3.4.2. The construction of promoter::*GUS* plant lines…….. 44
3.5. Knockout and RNAi plant lines……. 50
3.5.1. Phenotypic analysis of knockout and RNAi plant lines ……. 53
3.6. Metabolite profiling of *gh3.5* mutants (SALK_151766 T-DNA insertion line)… 55
3.7. In silico analysis of promoter cis-regulatory elements of candidate genes…… 57
4. DISCUSSION…… 61
4.1. Single cell sampling and array hybridization…….. 61
4.2. Candidate gene selection and validation of single cell gene expression profiling.. 63
4.2.1. GASA4……. 64
4.2.2. *At3g16980* ……65
4.2.3. *GH3.5* ……67
4.3. Analysis of knockout and RNAi plant lines…… 69
4.4. In silico analysis of promoter cis-regulatory elements of candidate genes…….. 72
4.5. Investigating potential functions for candidate genes in developing trichomes…...73
5. SUMMARY AND CONCLUSIONS…… 75
6. OUTLOOK……. 77
REFERENCES……. 78
APPENDICES…….. 89
APPENDIX A……. 89
APPENDIX B……. 91
APPENDIX C……. 92
LIST OF PUBLICATIONS AND PRESENTATIONS……... 104
ACKNOWLEDGEMENTS…….. 105

FIGURES

Figure 1.1 Leaf trichomes of Arabidopsis……... 8
Figure 1.2 Scheme of trichome development stages……... 9
Figure 1.3 Scheme of trichome patterning……10
Figure 1.4 Model for G1–S and G2–M transitions in plants…… 12
Figure 1.5 Endoreduplication in trichomes……15
Figure 1.6 Single cell sampling procedure using glass microcapillary…… 17
Figure 2.1 Principle of the SMART technology……25
Figure 2.2 Principle of the GATEWAY™ cloning technology…… 31
Figure 3.1 Visualization of trichome initial cells using the *pGL2::GFP* localization……...37
Figure 3.2 Sampling of single leaf epidermal cells…….. 37
Figure 3.3 Functional categorization of genes expressed in pavement, trichome initial and mature trichome cells…… 38
Figure 3.4 Visualisation of differential expression of the genes between two cell types using MAPMAN…… 39
Figure 3.5 Biotin-labelled cRNA derived from 10 single pavement cells……..41
Figure 3.6 Results of the single cell real-time RT-PCR…… 44
Figure 3.7 GUS staining in *pAt3g16980::GUS* and *pGASA4::GUS* transformants at day 6 and day 9…… 45
Figure 3.8 GUS staining in *pGH3.5::GUS* transformants at days 6 to 21……46
Figure 3.9 GUS staining in *pAt3g16980::GUS* and *pGASA4::GUS* transformants at day 14 and day 21 …… 47
Figure 3.10 GUS staining in iflorescence of *pAt3g16980::GUS*, *pGASA4::GUS*, and *pGH3.5::GUS* transformants…….. 48
Figure 3.11 GUS staining in leaf trichomes of pAt3g16980::*GUS*, p*GASA4*::*GUS* and p*GH3.5::GUS* transformants…… 49
Figure 3.12 T-DNA insertion sites in *At3g16980* and *At4g27260* (*GH3.5*)……. 50
Figure 3.13 Verification of the T-DNA insertion position in the genomes of SALK_151766 (*gh3.5*) and SALK_002430 (*At3g16980*) plant lines using PCR…… 51
Figure 3.14 Verification of specific GST presence in the plants transformed with RNAi construct for *GH3.5*……. 53
Figure 3.15 Phenotype of the plants carrying T-DNA insertion in *At3g16980* gene (SALK_002430) and *gh3.5* plants (SALK_151766)…… 54
Figure 3.16 Phenotype of the *gh3.5 RNAi* plants during their course of development……. 54
Figure 3.17 Changes in metabolite content in *gh3.5* (SALK_151766) when compared to wild type control plants……. 56
Figure 4.1 Possible roles of candidate genes in trichome development and cell cycle regulation in developing trichomes……. 74

COMMONLY USED ABBREVIATIONS

ABA	abscisic acid
BLAST	Basic Local Alignment Search Tool
bp	base pairs
BR	Brassinosteroids
CAK	CDK-activating kinase
CDK	cyclin-dependent kinase
cDNA	complementary DNA
CKI	cyclin-dependent kinase inhibitors
cRNA	complementary RNA
CYC	cyclin
DNA	deoxyribonucleic acid
dsRNA	double-stranded RNA
FAS	Fluorescence-Activated Sorting
GA	gibberellic acid
GC-MS	gas chromatography- mass spectrometry
GFP	Green Fluorescent Protein
GST	gene-specific tag
GUS	β-glucuronidase reporter gene
ICK	Inhibitor of CDK
kb	kilo bases
KO	knock-out
KRP	Kip-Related Protein
LB	Laura Bertani medium
LCM	Laser- Capture Microdissection
mRNA	messenger RNA
nt	nucleotides
PCR	Polymerase Chain Reaction
PTGS	Post-Transcriptional Gene Silencing
RB	retinoblastoma protein
RNA	ribonucleic acid
RNAi	RNA interference
RT	reverse transcriptase
RT-PCR	Reverse-Transcription Polymerase Chain Reaction
SA	salicylic acid
T-DNA	Transferred DNA
T_m	Melting temperature
v/v	volume per volume
w/v	weight per volume
WT	wild type
YEB	yeast extract nutrient broth

1. INTRODUCTION

1.1 Trichomes of *Arabidopsis thaliana*

Shoot epidermal hairs are known as trichomes (a term that is derived from the Greek word for hairs, *trichos*). Trichomes are found in most plants and can be single-celled or multicellular, secretory or nonglandular (Esau, 1977; Uphof, 1962). The functions ascribed to trichomes range from protecting the plant against insect herbivores and UV light to reducing transpiration and increasing tolerance to freezing (Johnson, 1975; Mauricio and Rausher, 1997).

Trichomes of Arabidopsis are single-celled structures of epidermal origin normally present on leaves, stems, and sepals. They are normally absent from roots, hypocotyls, cotyledons, petals, stamens, and carpels. The morphology of trichomes varies from unbranched spikes on stems and sepals, to structures containing two to five branches, found on the leaves (Fig 1.1). Most trichome mutations affect all of the trichomes on a plant. This suggests that while different trichomes may have different morphologies, the same genes control their development.

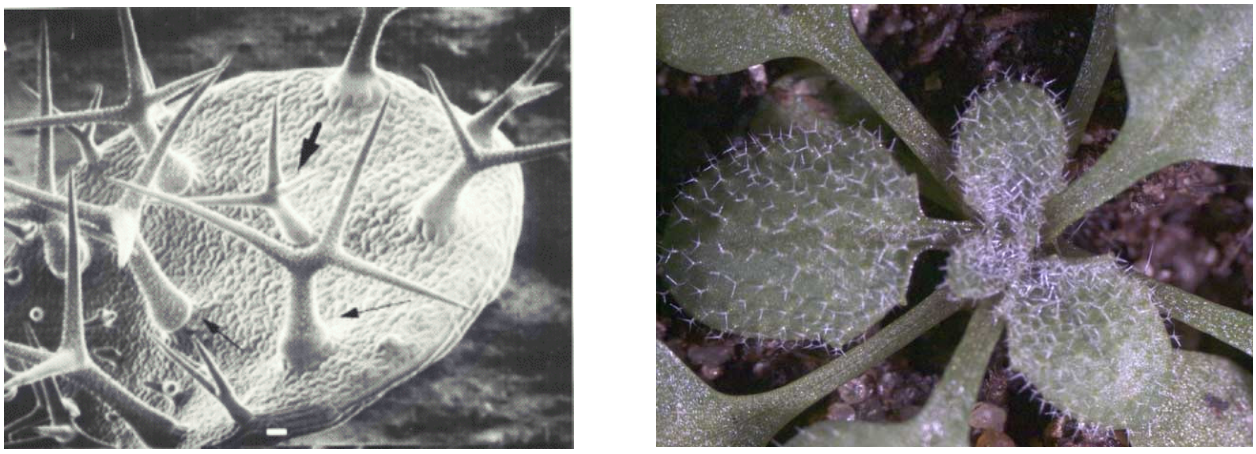

Figure 1.1 Leaf trichomes of Arabidopsis Left: scanning electron micrograph (*after* Marks, 1997). Thick arrow denotes developing trichome, thin arrows denote mature trichomes. Earlier stages of trichome development (bulging, initiation of branching) can also be seen. Right: trichomes on rosette leaves of 3-week-old Arabidopsis plant.

Leaf trichomes are easily accessible for sampling. Trichomes are a suitable model system to study various aspects of cell differentiation including cell fate determination, cell cycle regulation, cell polarity induction and cell expansion growth (Hülskamp, 1994; Hülskamp, 2004; Marks, 1997; Szymanski et al., 2000).

1.1.1 Trichome development

Trichome development proceeds as a wave across the epidermal surface on the leaf (Hülskamp et al., 1994; Marks, 1994). The first trichome initiates on the tip of the adaxial surface of the first primordium after it achieves a length of approximately 100 μm (Larkin et al., 1996; Marks, 1997). As trichomes mature at the leaf tip, new trichomes emerge progressively toward the base of the leaf. In addition, new trichomes initiate between developing trichomes that have been separated from one another by dividing epidermal cells. Trichome initiation is found only in regions where epidermal cell division is occurring.

The first detectable step in the commitment to the trichome cell fate is a cessation of cell division. Trichome initial cells start endoreduplication cycles and eventually reach ploidy levels of 32C (Hülskamp et al., 1994; Inze and De Veylder, 2006; Melaragno et al., 1993). Cells surrounding a developing trichome continue to divide normally. After the committed cell radially expands to a diameter that is approximately twofold greater than the surrounding cells, it begins to expand preferentially on its outer surface to form a stalk (Marks, 1994). As the stalk forms, diffuse growth throughout the cell results in continued radial expansion. The nucleus migrates into the aerial portion of the stalk shortly before secondary protuberances (Hülskamp et al., 1994), which subsequently expand into the branches, emerge from the aerial tip. During branch formation, the nucleus migrates to the base of the last branch that forms (Hülskamp et al., 1994). Expansion ceases when a trichome reaches a height of 200–300 μm and a base diameter of approximately 50 μm (Marks, 1997). During trichome maturation the cell wall thickens to approximately 5 μm, and the trichome surface becomes covered with papillae. In addition, the epidermal cells around the base of a trichome acquire a distinct rectangular shape. These surrounding cells are known as socket cells (Hülskamp et al., 1994) or basal cells. A schematic representation of the stages of the trichome development is presented in Fig 1.2.

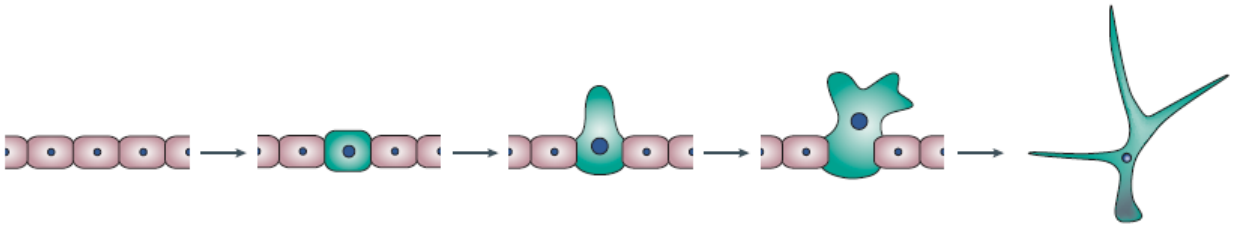

Figure 1.2 Scheme of trichome development stages (*after* Hülskamp, 2004). Initiation is followed by radial expansion in the plane of epidermis; afterwards stalk formation takes place. Shortly before branch initiation the nucleus of the developing trichome migrates to the branching area. Further expansion, branch formation and maturation complete the development of the trichome.

1.1.2 Regulation of trichome development

Most trichome mutations affect all plant trichomes, yet do not affect other key aspects of plant development. This allows efficient isolation of trichome specific mutants. Indeed, using mutants, complementation, and misexpression most of the trichome patterning genes as well as genes involved in trichome development and differentiation have been identified (recently reviewed by Hülskamp, 2004; Schellmann and Hülskamp, 2005). These genes include positive regulators of trichome development *GLABRA 1* (*GL1*) encoding MYB-related transcription factor, *GLABRA 3* (*GL3*) and *ENHANCER OF GL3* (*EGL3*) both encoding basic helix–loop–helix protein, *TRANSPARENT TESTA GLABRA1* (*TTG1*) (WD40 protein) and *GLABRA 2* (*GL2*), encoding homeodomain leucine-zipper protein. Negative regulators *TRIPTYCHON* (*TRY*), *CAPRICE* (*CPC*) and *CAPRICE TRIPTYCHON1* (*ETC1*) encode single repeat MYB proteins without obvious transcriptional-activation domain.

It has been hypothesized that trichome patterning is based on a mutual-inhibition mechanism (Hulskamp and Schnittger, 1998; Larkin, 2003; Scheres, 2002; Schiefelbein, 2003): cells that are initially equivalent produce a trichome-promoting factor (or factors) that activates a factor (or factors) that suppresses trichome development in neighbouring cells (Figure 1.3). In this scenario, these inhibiting factors (or as yet unknown signals induced by them) travel to neighbouring cells, perhaps via plasmodesmata, and arrest trichome development there. However, the exact mechanism of such cell-to-cell communication is still unknown.

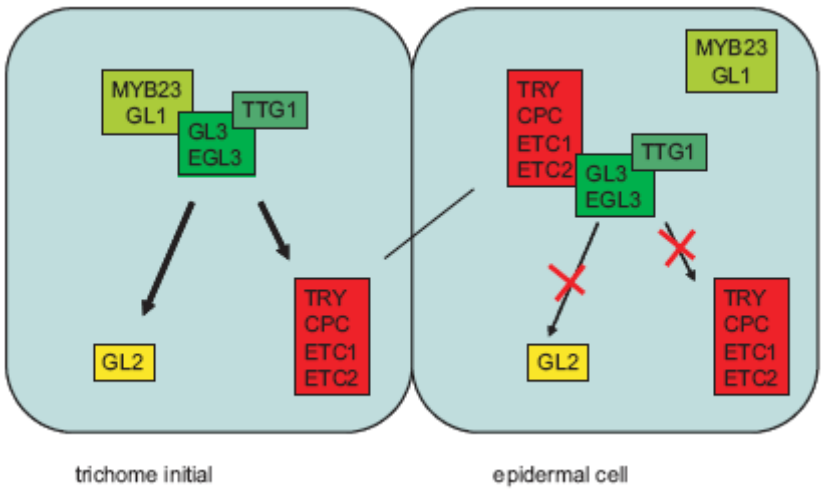

Figure 1.3 Scheme of trichome patterning (*after* Schellmann and Hülskamp, 2005). Epidermal cells that eventually express *GLABRA2* (*GL2*) in the shoot become trichomes. It is postulated that in those cells that express this gene, a trimeric active complex is formed that consists of a MYB-related transcription factor (GLABRA1 (GL1)), a basic helix–loop–helix protein (GLABRA3 (GL3), the homologous ENHANCER OF GL3 (EGL3)) and a WD40 protein (TRANSPARENT TESTA GLABRA1 (TTG1)). This active complex is thought to activate GL2 and the expression of the negative regulators TRIPTYCHON (TRY), CAPRICE (CPC), CAPRICE TRIPTYCHON1 (ETC1) and CAPRICE TRIPTYCHON2 (ETC2). These travel into the neighbouring cells where they compete with the MYB-related transcription factor GL1 for binding to the complex; binding inactivates the complex causing arrest of trichome development in the neighbouring cell. Activators of trichome fate are depicted in green shades, inhibitors are in red.

1.1.3 Cell cycle alterations during trichome development

1.1.3.1 Cell cycle regulation in plants

The cell cycle is a highly ordered process that results in the formation of two daughter cells and is usually divided into four phases: G1, S (DNA replication), G2 and M (karyo- and cytokinesis) (Fig 1.4). Ensuring that each new daughter cell receives a full complement of the hereditary material requires the correct alternation between S phase and M phase. The basic control mechanisms that regulate the progression through the cell cycle are remarkably well conserved through evolution. The main drivers of the cell cycle in yeast, mammals and plants are a class of highly conserved serine/threonine kinases known as the cyclin-dependent kinases (CDKs). Different CDK-cyclin complexes phosphorylate numerous substrates at key G1-to-S and G2-to-M transition points, triggering the onset of DNA replication and mitosis, respectively.

Little is known to date on the interaction of CDKs with cyclins (Inze and De Veylder, 2006). Interestingly, plants contain many more cyclins than have been described in other organisms (Vandepoele et al, 2002; Wang et al, 2004). For example *Arabidopsis thaliana* contains at least 32 cyclins with a putative role in cell cycle progression. Arabidopsis gene annotation identified 10 A, 11 B, 10 D and one H cyclins (Vandepoele et al, 2002; Wang et al, 2004). D-type cyclins are thought to regulate the G1/S transition and appear to act as integrators of various signals; A-type cyclins are of importance for the S/M phase control; B-type cyclins generally play a role in the G2/M transition and intra-M phase control (Fig 1.4); and the H-type cyclin is part of the CDK-activating kinase. Although much of this is speculation, the expression of plant cyclins, more specifically D-type cyclins, has been shown to be modulated by plant growth factors, such as cytokinins, brassinosteroids, sucrose and gibberellins (Stals and Inzé, 2001) (Fig 1.4). Some D-type cyclins probably act as key switches in triggering hormonal effects (Cockcroft et al., 2000; Riou-Khamlichi et al., 1999).

Plant CDK/cyclin complex activity is regulated by phosphorylation/dephosphorylation and by interactions with regulatory proteins in a manner similar to that in yeasts and animals. Phosphorylation of a tyrosine residue of A-type CDK has been shown to down-regulate CDKA activity under cytokinin deprivation, osmotic stress, or DNA damage (Inze and De Veylder, unpublished; Schuppler et al., 1998; Zhang et al., 1996). Some evidences suggest that a phosphatase capable of activating CDK/cyclin complexes is present in higher plants (Landrieu et al., 2004).

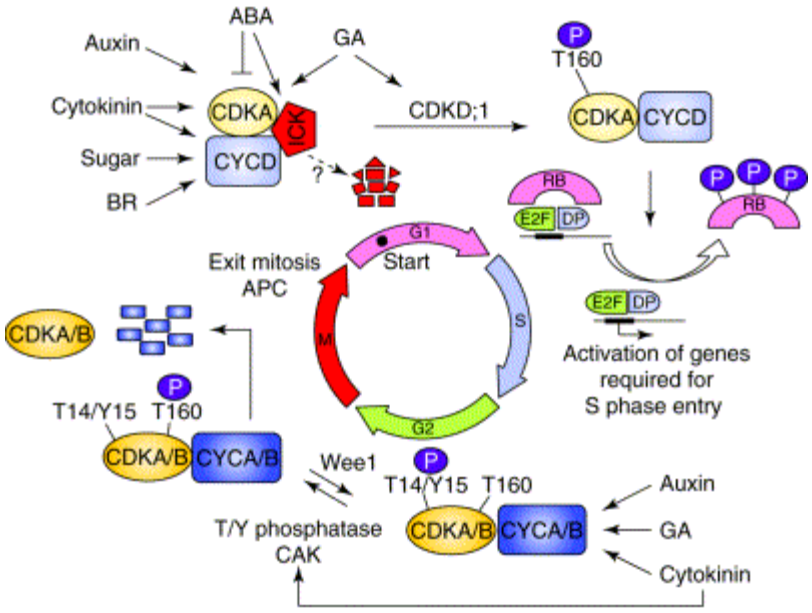

Figure 1.4 Model for G1–S and G2–M transitions in plants This model is based on results obtained in plant model systems and on parallels with the mammalian cell-cycle control (*after* Stals and Inze, 2001). During G1, several growth factors, such as auxin, cytokinin, abscisic acid (ABA), gibberellin (GA), brassinosteroids (BR) and sugar regulate the expression of D-type cyclins (CycD) and their catalytic subunit, cyclin-dependent kinase A (CDKA). Activation of the CDKA–CycD complex requires the dissociation of the CDK inhibitory protein (ICK), the transcription of which is induced by the stress-responsive hormone ABA and phosphorylation of the Thr160 residue of CDKA by the CDK-activating kinase, CDKD;1, which is upregulated by GA. The active CDKA–CycD complex initiates the phosphorylation of retinoblastoma protein (RB) during late G1 phase, thereby releasing the E2F–DP complex that promotes the transcription necessary for progression into S phase. As mitotic activators auxin, cytokinin, and GA also regulate the kinase activity of A- and B-type CDKs by activating the transcription of CDKs and of A- and B-type cyclins. The G2–M transition is associated with an activating Thr160 phosphorylation of CDK by a CDK-activating kinase (CAK) and by dephosphorylation of the inhibitory Tyr phosphorylation that is induced by cytokinin. An ubiquitin-dependent degradation pathway targets B-type cyclins for proteolysis by the anaphase-promoting complex (APC) at the metaphase–anaphase transition, thereby activating the exit from mitosis.

The cell cycle is also regulated by cyclin-dependent kinase inhibitors (CKIs, KRPs-Kip-Related Proteins) that prevent cell cycle progression by binding and inhibiting CDKs (De Clercq and Inze, 2006; De Veylder et al, 2001; Morgan, 1997). KRPs interact with both CDKAs (but not CDKBs) and D-type cyclins (Wang et al, 1998; De Veylder et al, 2001). It has been shown that specific downregulation of *KRP2* gene expression precedes the re-entry of the auxin-responsive quiescent root pericycle cells into the cell cycle that is triggered by auxins (Himanen et al, 2002). *KRP1* was upregulated by abscisic acid, a plant hormone implicated in stress-induced cell cycle arrest (Wang et al, 1998).

For the G1/S transition, both animals and plants use the same RB/E2F/DP pathway. This suggests that this pathway evolved early in evolution, before the branching between animal and plant taxa. However plants do not contain retinoblastoma proteins (RB), but rather RB-related proteins (RBR). These control the activity of the adenovirus E2 promoter-binding factor (E2F) family of transcription factors that, in turn, control the expression of many genes required for entry into and execution of S phase and cell cycle progression (Attwooll et al., 2004; Blais and Dynlacht, 2004; Dimova and Dyson, 2005; Stevens and La Thangue, 2004). E2F binds DNA

as a heterodimer composed of two structurally related subunits, E2F and its heterodimerization partner (DP). Arabidopsis has six E2Fs and two DPs (Vandepoele et al., 2002). G1/S transition in plants is induced through transcriptional activation of D-type cyclins and their subsequent association with CDK4 or CDK6. This process is triggered by the continuous presence of certain growth factors (Fig 1.4). The CDK4/6–cyclin-D complexes that are activated via phosphorylation by a CDK-activating kinase (CAK) phosphorylate and inactivate the retinoblastoma protein (RB), thereby activating E2F-controlled genes, which are required for S phase progression (Fig 1.4). E2F sites are found in promoters of multiple plant and animal genes that are involved in cell-cycle progression and DNA replication (Ramirez-Parra et al, 2003; Vandepoele et al., 2005)

As can be seen in Figure 1.4, plant hormones play an important role in cell cycle progression, both in G1/S and G2/M transitions. Thus auxin affects cell division, expansion and differentiation in the following way: it increases both CDKA;1 and mitotic cyclin mRNA levels in roots in conjugation with cell division induction (Doerner et al., 1996; Ferreira et al., 1994; Hemerly et al., 1993). However, experimental data suggest that auxin requires cytokinins to stimulate cell division (Trehin et al., 1998; Zhang et al., 1996). Cytokinins are necessary, in concert with auxin, for cell division at the G1/S and G2/M transitions both in cultured plant cells and in planta (Meijer and Murray, 2000; Zhang et al., 1996). Brassinosteroids (BRs) regulate cell cycle progression through the upregulation of *CycD3* and *CDKB1;1* (Fig 1.4) (Hu et al., 2000; Yoshizumi et al., 1999). Gibberellic acid (GA) induces, by an unknown mechanism, A-type *CDK* and rice *CDKD;1* mRNAs at the G1/S transition. Furthermore, it modulates the expression of D-type cyclins so is thus involved in both G1/S and G2/M transitions (Inze, 2005; Inze and De Veylder, 2006; Stals and Inze, 2001). Interestingly, GA promotes endoreduplication cycles in developing trichomes (Perazza et al., 1998) (see below). The stress-responsive hormone abscisic acid (ABA) inhibits cell division in response to adverse environmental cues. This effect might be mediated by the induction of a CDK inhibitor, ICK1, which might, together with decreased CDKA;1 gene expression, result in the observed lower CDK activity (Fig 1.4) (Hemerly et al., 1993; Wang et al., 1998).

Endoreduplication (endocycling) is a cell cycle mode with cells undergoing iterative DNA replications without subsequent cytokinesis. It probably plays an important role in the differentiation process of postmitotic cells because the onset of the endocycle often characterizes the switch between cell proliferation and differentiation, as observed during hypocotyl elongation, trichome growth, and fruit and leaf development (Beemster et al., 2005; Boudolf et al., 2004; Joubes et al., 1999; Kondorosi et al., 2000; Larkins et al., 2001). The exit of the mitotic cycle in Arabidopsis correlates with the onset of endoreduplication, suggesting that this process

can be perceived as a continuum of the mitotic cell cycle in which mitosis, but not DNA replication, is inhibited. One of the possible regulators of the switch between mitosis and endocycling is the so-called mitosis-inducing factor (MIF), part of which is probably CDK B1;1 kinase that acts together with CYCA3;2, CYCA2;3, CYCD3;1 and CYCB1;2 (Dewitte et al., 2003; Imai et al., 2006; Schnittger et al., 2002b; Yu et al., 2003). Other factors involved in the regulation of the endoreduplication include ICK/KRP proteins, CCS52A protein, WEE1, DEL1 etc. (Inze and De Veylder, 2006). However, a large part of the mechanisms regulating this process still remains unknown.

1.1.3.2 Regulation of the switch between mitotic and endoreduplication cycles in developing trichomes

As mentioned above, after committing to the trichome developmental pathway, an epidermal cell exits mitosis and starts its endoreduplication cycles (Fig 1.5). It has been indicated that endoreduplication during trichome development is regulated by the plant hormone gibberellic acid (GA), which may also be a key regulator of trichome initiation (Perazza et al., 1998). Thus in a mutant that is incapable of gibberellin synthesis, (such as *ga1-3*), no trichomes are formed (Chien and Sussex, 1996; Telfer et al., 1997).

Another regulator of trichome endoreduplication is the *SIAMESE (SIM)* gene product. It suppresses the switch from mitotic divisions to endoreduplication cycles (Walker et al., 2000; Churchman et al., 2006). In *sim* mutants, trichomes are multicellular and contain between 2 and 15 cells. B-type and D-type cyclins could trigger the formation of multicellular trichomes. Expression of either CYCB1;2 or CYCD 3;1 cyclins under control of a trichome specific promoter caused emergence of multicellular trichomes (Schnittger et al., 2002a, 2002b). This finding is intriguing since D-type cyclins are thought to control the transition from the G1 to the S phase of the cell cycle in animals, but these results indicate that, in plants, D cyclins have an additional function in regulating the entry into mitosis. In *sim* mutants, CYCB1;2 is expressed in trichomes, which indicates that SIM inhibits the expression of mitotic cyclins.

Interestingly, cell-death mechanisms and plant pathogen response pathways are also involved in regulation of endoreduplication during trichome development (Schnittger et al., 2003; Kirik et al., 2001). It seems that cell cycle and the control of cell death are linked; the mechanisms of this link remain to be determined.

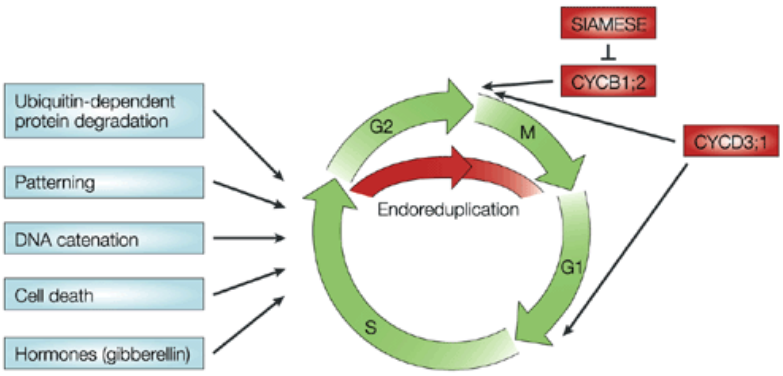

Figure 1.5 Endoreduplication in trichomes (*after* Hülskamp, 2004). Endocycling skips the G2 and M phases of the cell cycle. Processes that affect this process (blue) were identified by mutant analysis. The factors that are involved in the switch from mitosis to endoreduplication are indicated in red. For further explanation, see text

Trichome patterning genes *GLABRA 3 (GL3)* and *TRY* (Esch et al., 2003) (see above) function also as positive and negative regulators of endoreduplication cycles: trichomes of *try* mutants have a DNA content of 64C and different mutant *gl3* alleles exist that have either a reduced or an increased DNA content (Esch et al., 2003; Hülskamp et al., 1994). This dual function suggests that trichome cell fate is linked functionally with cell cycle regulation.

Ubiquitin-regulated protein degradation also controls the progression of endoreduplication: four trichome mutants, *kaktus* (*kak*), *rastafari* (*rfi*), *polychome* (*poc*) and *hirsute* (*hir*), show a similar phenotype: they all have a ploidy level of 64C. Subsequent cloning of the *KAK* gene revealed that it encodes a protein with sequence similarity to a UBIQUITIN E3 LIGASE, which marks proteins for degradation in the proteasome (Downes et al., 2003; El Refy et al., 2003; Perazza et al., 1999).

It has been reported that DNA catenation mechanisms influence endoreduplication in trichomes. ROOT HAIRLESS2 (RHL2) and HYPOCOTYL6 (HYP6) are positive regulators of endoreduplication cycles in trichomes and in other cell types. Both are plant homologues of the archaeal DNA topoisomerase VI complex and involved in decatenation (unwinding) of DNA. Incomplete decatenation of replicated DNA may result in progressively entangled chromosomes that either physically block further DNA replication or initiate a checkpoint mechanism to block further endocycles (Sugimoto-Shirasu et al., 2002).

1.2 Single cell analysis

In recent years, omics approaches have shifted away from sampling whole plants or organs, to sampling tissues, and now to sampling single cells, with the aim of dissecting more precisely processes involved in cell development, differentiation, cell function regulation etc. Gene transcript profiling data obtained from whole organisms, organs, or even specific tissue types represent averaged signals due to the mixing of different cell types. Thus, these data ignore the fact that each organ of a multicellular organism is unique at the level of its tissues, cells and

gene expression profiles. The same is true for other expression profiles, including proteins or metabolites. For these studies to provide meaningful information concerning cell state, it is necessary either that organs and tissues be separated into their constituent cell types prior to such analysis, or that alternative methods be designed that can deconvolute the contributions of specific cell types from the overall mixture (Galbraith and Birnbaum, 2006).

It should be taken into consideration that responses to environmental stimuli or developmental signals occur differentially at the single cell or tissue level (Lee et al., 2005). An investigation of the response of single cells to the plant hormone abscisic acid (ABA) provided substantial support for cell-specific gene regulation (Leonhardt et al., 2004). This study demonstrated that only 20% and 27% of genes induced by ABA in mesophyll and guard cells, respectively, had been detected on the whole plant level. These results suggest that regulatory networks deduced from whole plant profiling data could not be accurately projected onto the individual cell type, and vice versa. Thus, it would be more accurate to draw conclusions about gene regulation in response to hormones or other stimuli in the whole plant, based on an understanding of responses at the cellular level in various tissues and organs (Lee et al., 2005).

Another example is root cell profiling. It has been demonstrated that in total 54% of the genes expressed in roots are differentially expressed in root subzones (Birnbaum et al., 2003). In comparison, only 37% of genes were differentially expressed among seven organs in maize (Cho et al., 2002). Transcript profiling with more specific cell-type populations (i.e. protoxylem, pericycle, lateral root initials, etc.) in Arabidopsis revealed an even greater number of differentially expressed genes (Birnbaum and Benfey, 2004).

These examples underline the urgent need for increasing spatial resolution when performing expression profiling, preferably to the single cell level. This remains quite challenging technically, however; single cell transcript profiling relies on efficient and precise methods for cell sampling and requires special amplification technologies.

1.2.1 Methods of the single cell sampling

Several single cell sampling methods are used for cell-specific transcript profiling (Bligny and Douce, 2001; Kehr, 2001, 2003; Outlaw and Zhang, 2001; Tomos and Sharrock, 2001). According to Brandt, 2005 they could be classified by their interference with the overall plant metabolism into following groups: non- invasive, minimally invasive, and invasive sampling methods.

1.2.1.1 Non-invasive methods

Non-invasive methods of cell sampling do not interfere with the plant or at least do not cause any wounding. With respect to gene expression analysis, there is only one method available that could be classified as non-invasive: the generation of transgenic plants carrying promoter::reporter gene constructs, since no sampling per se is involved in this method.

1.2.1.2 Minimally invasive methods

Minimal invasive sampling can be performed using glass microcapillaries (Fig 1.6). This is one of the most direct methods for characterizing the molecular properties of specific cell types. This method is extremely accurate in terms of access to specific cell types, and has the advantage of minimal perturbation of the host tissue. Here glass microcapillaries are mounted on a micromanipulator allowing the researcher to visually monitor and physically control the penetration and aspiration of an individual cell. Microcapillary sampling has been used successfully for mRNA extraction from single epidermal, mesophyll and companion cells (Brandt et al., 1999). Repetitive sampling of individual cell types, followed by amplification, can provide sufficient RNA for array hybridization. Thus, extracts of 20 mesophyll and 50 epidermal cells sampled by microcapillaries have been successfully used for cDNA synthesis and microarray probe generation (Brandt et al., 2002). The method has also been used to investigate root hair cells (Jones and Grierson, 2003), plant-pathogen interactions at the single cell level (Mould et al., 2003), and to collect phloem-derived protoplasts via micromanipulation (Ivashikina et al., 2003). Typical volumes obtained using microcapillary sampling range from a few to few hundred picolitres, depending on the cell type and plant species. One drawback of the method is that it results in very small amounts of material for downstream analysis and therefore requires sufficient amplification procedures.

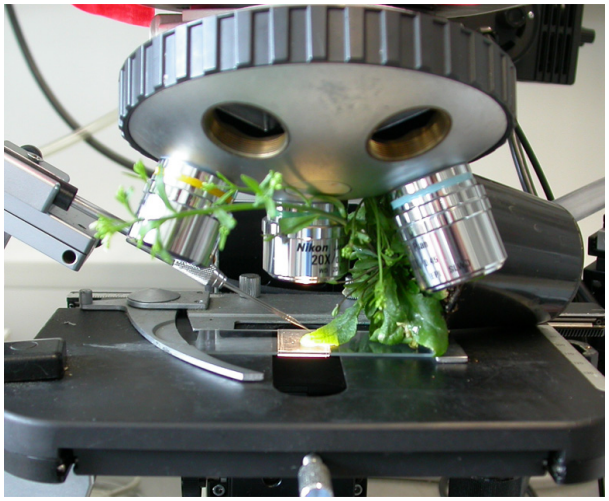

Figure 1.6 Single cell sampling procedure using glass microcapillary An intact Arabidopsis plant is mounted under the microscope. The rosette leaf is immobilized and it is possible to sample cells of interest using microcapillary that is mounted on a micromanipulator. After insertion, turgor pressure forces cell sap into the capillary. Extracted samples usually have volumes in the picolitre range

1.2.1.3 Invasive sampling methods

The goal of the more invasive sampling methods is to enrich greatly the cell type of interest. However, the cost of this enrichment is the physiological integrity of tissues and organs, which are destroyed. Separation and following accumulation of individual cell types from organized plant tissues requires the production of suspensions of protoplasts that have had their cell walls removed. Protoplasts can be produced by enzymatic digestion of organs. The resulting cells can be sorted based on properties such as size, viability, and chlorophyll content. Alternatively, protoplasts can be subjected to fluorescence-activated sorting (FAS) (Birnbaum et al., 2003; Lee et al., 2005). The development of the Green Fluorescent Protein (GFP) of *Aequorea victoria* (Chalfie et al., 1994), the prototypical Fluorescent Protein (FP), allows researches to identify individual cell types more specifically using FAS by placing transgenic FP expression under the control of appropriate regulatory sequences. Other invasive approaches include peeling off organ cell layers (Gaedeke et al., 2001) or clipping off surface localized cell types such as trichomes or root hairs (Wienkoop et al., 2004). Application of these techniques causes massive interference with physiology of the plant. Disruption to the plant system aside, enrichment protocols result in samples comprised of groups of similar cells, and the results gathered from these samples are averages among these cells. General differences between samples may be recognized, but the cell-to-cell differences between samples are lost (Gehwolf et al., 2002). Additionally, the disturbances to metabolism provoked by invasive sampling methods affect gene expression (Birnbaum et al., 2003; Grosset et al., 1990; Titarenko et al., 1997). However, these effects might be minimized by using transcription and RNA degradation inhibitors (Leonhardt et al., 2004). Other invasive methods require a fixation prior to sampling. Noteworthy, such fixation step reduces alterations in gene expression. After fixation and sectioning, cells of interest can be isolated from tissues by micromanipulation. This can be carried out mechanically using razor blade fragments (Outlaw and Zhang, 2001 and references therein) or by vibrating steel chisels (Brandt et al., 2003).

Laser- capture microdissection (LCM) applies a laser to physically dissect the cells within the regions of interest, which then can be captured either passively or actively by laser pressure catapulting using a single high-power pulse of laser irradiance. It was developed and used in gene expression profiling of animal cells (Emmert-Buck et al., 1996; Luzzi et al., 2003; Schütze and Lahr, 1998). However, for plant tissues and organs, LCM usually requires use of sectioned tissues, which therefore must be fixed or frozen.

Reports of the application of LCM to plants include production of cDNA libraries from RNA of captured rice phloem cells (Asano et al., 2002), array-based analysis of gene

expression in maize seedling epidermal and vascular tissues (Nakazono et al., 2003), evaluation of technical improvements for RNA isolation from miscellaneous plant tissues (Kerk et al., 2003), characterization of expression of individual genes within *Arabidopsis* phloem (Ivashikina et al., 2003), and tissue-specific protein and metabolite profiling of *Arabidopsis* (Schad et al., 2005 a, b). An improvement to the LCM methodology was proposed by Inada & Wildermuth (2005), who described the use of rapid microwave paraffin embedding without prior fixation to enhance the laser microdissection properties of Arabidopsis leaves.

The advantages of the LCM method are: minimization of the extensive manipulation of tissues that could change the RNA profile and reduction of the effects of collection time on experiments with important temporal components, such as the circadian clock (tissues are fixed simultaneously on a large scale). However, in most cases, LCM is very labour intensive during the dissection step and is tricky for the isolation of small cells or tissues with few cell layers. In particular, meristem cells are challenging for dissection since they are small and are made up of few cells. Even with tissue sections 6 μm thick or so, the probability of contamination with neighbouring cells could still be high (Lee et al., 2005). Regardless, LCM is subject to the same drawbacks as other highly invasive sampling methods (see above).

1.2.2 Amplification methods used for single cell transcript profiling

Due to the low amount of genetic material in single cells, special amplification technologies are necessary in order to proceed with transcript profiling. These technologies can be based on single transcript amplification (specifically primed RT-PCR, real-time RT-PCR, nucleic acid sequence based amplification (NASBA)); amplification of transcript subsets (differential display RT-PCR, multiplex RT-PCR, nested RT-PCR); or global transcript amplification (tailing, adaptor ligation, template switching and others).(See Table 1.1)

Some concerns related to low amount of genetic material in single cell samples still exist. For instance, the so-called “Monte Carlo Effect” described by Karrer et al (1995) can affect the reliability of results. The Monte Carlo Effect occurs when there is a very low amount of DNA template; the lower the abundance of a template, the less likely its true abundance will be maintained in the amplified product. This effect caused by small and random differences in amplification efficiency between PCR templates. Another factor is the size of amplified fragments: generally, the lower the amount of mRNA available, the shorter the amplified fragments would be (Glanzer and Eberwine, 2004; Feldman et al., 2002; Spiess et al., 2003). Another concern in single cell studies is related to the stochasticity of gene expression as a biological phenomenon. In this context, it is defined as variation in gene expression of

genetically identical cells in the same environmental and developmental context (Kaern et al., 2005).

Table 1.1 Amplification strategies used in single cell gene expression studies (*after* Brandt (2005) with minor changes and additions). References in italics indicate plant examples.

Method	Amplification strategy*	Reference
Single transcript amplification		
Specifically primed RT-PCR	Primers raised against a specific gene are used in the PCR reaction. Intron spanning primers allow the researcher to distinguish between genomic and cDNA origin of the products making DNase treatments prior to PCR obsolete.	*Richert et al., 1996; Brandt et al., 1999*
Real-time RT-PCR	The method was applied in our laboratory for quantification of gene expression in samples derived from single pavement, basal, trichome initial and mature trichome cells	He *et al.*, 2002; *Volkov et al., 2003 Lieckfeldt et al., 2007 Kryvych et al., 2007*
Nucleic acid sequence based amplification (NASBA)	cDNA is synthesized by a sequence specific 3'-primer harbouring a T7 promoter. Using a second (upstream) the complementary strand is produced. T7 RNA polymerase synthesis antisense RNA molecules which serve as templates for a second round of amplification.	Deiman *et al.*, 2002; *Vaskova et al., 2004*
Amplification of transcript subsets		
Differential display RT-PCR	In the PCR a $(dT)_{15}$-primer is used in combination with an arbitrary primer which binds statistically to the cDNA. Consequently, all cDNA molecules which are bound get amplified.	Liang and Pardee, 1992; Bauer *et al.*, 1993; *Brandt et al., 2002*
Multiplex RT-PCR	This method could be transferred to minute amounts of starting material with reasonable effort. In one reaction tube, primer pairs raised against different genes are combined. This reduces the number of samples as well as the work and time needed.	Recchi *et al.*, 1998; *Ponce et al., 2000*
Nested RT-PCR	In a first round of amplification, primers raised against conserved regions of, for example, a gene family are used to amplify all members. In a second round an aliquot of the first round is amplified by 'inner' primers specific for a single gene.	Massengill *et al.*, 1997; *Jones and Grierson, 2003*
Global transcript amplification		
Tailing	Terminal deoxynucleotidyltransferase synthesizes homomeric ends (tails) to the 3' end of any cDNA molecule. The PCR is performed with the complementary homomeric primer and a $(dT)_{15}$-primer	*Dresselhaus et al., 1994*; Klein *et al.*, 2002
Adaptor ligation	The first strand cDNA is converted into a double strand and adaptors are ligated to the unknown sequence end of the cDNA molecules. Its sequence as well as a $(dT)_{15}$-primer serve as primers in PCR.	*Karrer et al., 1995; Gallagher et al., 2001*
Template switching	Some reverse transcriptases exhibit a terminal deoxynucleotidyltransferase activity, which synthesizes some Cs at the 3' end of the nascent first strand. By adding a complementary G_n-primer, the transcriptase switches over to this new template elongating the cDNA first strand with its complementary known sequence. This primer in combination with a $(dT)_{15}$-primer can be used in a subsequent PCR.	Petalidis *et al.*, 2003; *Voelckel and Baldwin, 2003; Ivashikina et al., 2003 Lieckfeldt et al., 2007 Kryvych et al., 2007*
Linear antisense RNA amplification	The $(dT)_{15}$-primer for the reverse transcription also harbours a T7-RNA-polymerase-promoter region. After conversion into double stranded cDNA, antisense RNA is produced by *in vitro* transcription. The amplification is linear and thought to preserve the original transcript levels far better than exponential PCR amplification.	Van Gelder *et al.*, 1990; *Nakazono et al., 2003*
Terminal continuation	Terminal continuation is a mixture of template switching and linear antisense RNA amplification. During first strand cDNA synthesis either of the two primers can bear the RNA polymerase promoter. Consequently, either sense or antisense RNA is linearly amplified by subsequent *in vitro* transcription.	Ginsberg and Che, 2002
Multiple displacement amplification	Surprisingly, isothermal rolling circle amplification by use of random hexamer primers and φDNA polymerase also works with linear (genomic) DNA. However, the DNA is amplified in a cascading, strand displacement reaction.	Dean *et al.*, 2002

* Prior to the described strategies, the mRNA within the samples is reversibly transcribed into single-stranded cDNA.

1.3 Aims of this thesis

The general aim of this thesis was to discover novel pathways involved in trichome development and cell cycle regulation by identifying new candidate genes that are differentially expressed in subsequent stages of trichome development.

In order to achieve this goal, the following questions were addressed:

- How do gene expression profiles change during trichome development (what differences can be observed among pavement, trichome initial and mature trichome cells)?
- Which genes are highly expressed especially in the initial stages of trichome development (as compared to pavement cells and mature trichomes) and thus may be novel genes involved in trichome initiation/early development?
- What is the role of the upregulated genes that were selected as candidates in trichome development and cell cycle regulation?
- Do the data obtained coincide with existing models of cell cycle regulation and trichome patterning and development or how can these models be complemented with data obtained in this project? Is there any interaction between newly discovered genes and genes from traditional models? How do these genes interact with each other?

This work is a first report about application of the microcapillary sampling technique to sample initial stage of development of the certain cells (i.e. trichomes). Moreover, it is the first time that transcript profiling of trichome initial cells has been reported, and that comparisons among the transcriptomes of trichome developmental stages made. Expression of basic selected candidate genes in trichome initials was confirmed by independent methods, thus substantiating the reliability of the applied sampling and amplification techniques. Additional information about the functions of the genes of interest was obtained using reverse genetics. Furthermore, data mining using bioinformatic tools allowed identification of possible interactions of candidate genes with other compounds involved in trichome morphogenesis and cell cycle regulation.

The work performed allowed to propose functional implication of the three selected candidate genes in trichome morphogenesis and hence in cell cycle regulation in *Arabidopsis thaliana*.

2. MATERIALS AND METHODS

2.1 Commonly used equipment, kits, and consumables

2.1.1 Equipment

Amersham Pharmacia Biotech, Life Chalfont, UK: DynaQuant™ 200 fluorimeter.

Applied Biosystems, Forster City, USA: Primer Express software; SDS 7300 sequence detection system; SDS 2.1 software.

Bio-Rad, Richmond, USA: GenePulser II.

Eppendorf, Hamburg, Germany: Mastercycler Gradient system; Eppendorf BioPhotometer; remote controlled micromanipulator, model 5171; Microcentrifuge 5417C.

Imaging Research, St Catherine's, Canada: Array Vision software.

Leco, St Joseph, MI, USA: Pegasus III TOF-MS time-of-flight mass-spectrometer.

Leica Microsystems, Wetzlar, Germany: Leica MZ 12.5 stereo microscope; Leica Soft Imaging System IM 500 software.

List-Medical-Electronic, Darmstadt, Germany: L/M-3P-A Vertical Pipette Puller

Nikon, Duesseldorf, Germany: Optiphot 2 microscope

Raytest, Straubenhardt, Germany: Fuji BAS intensifying screens; Fuji BAS 1800 II phosphor imager; BAS cassettes.

Retsch, Haan, Germany: Retch-mill, model MM 200

World Precision Instruments, Sarasota, USA: Precision stereo zoom microscope

2.1.2 Consumables

AB Gene, Hamburg, Germany: 96 well PVR plates, adhesive PCR seals.

Affymetrix, Santa Clara, CA, USA: Affymetrix ATH1 GeneChip Array

Amersham biosciences, NJ, USA: Nick columns; Hybond N^+ nylon membranes

Applied Biosystems: SYBR™ Green Master Mix reagent.

Fermentas, Vilnius, Lithuania: RNA ladders.

Invitrogen, Karlsruhe, Germany: pDONR207 entry vector; SuperScript™ II reverse transcriptase; TRIzol reagent; 50 bp DNA ladder, BP Clonase™ Mix; LR Clonase™ Mix.

Merck, Darmstadt, Germany: other chemicals

MWG, Ebersberg, Germany: oligonucleotides

NEN, Zaventem Belgium: ^{33}P dCTP.

New England Biolabs, Ipswich, MA, USA: *Taq* DNA polymerase; restriction nucleases and restriction buffers

Peqlab, Erlangen, Germany: Peqlab1 kb ladder.

Promega, Heidelberg, Germany: RNAsin.

Restek GmbH, Bad Homburg, Germany: Rtx-5Sil capillary columns for GC-MS.

Qiagen, Hilden, Germany: Oligo dT primer.

Roche Applied Science, Mannheim, Germany: RNase A; restriction nucleases and restriction buffers, antibiotics

Sigma-Aldrich, Taufkirchen, Germany: Ethidiumbromide, Diethylpyrocarbonate (DEPC), other chemicals

Sigma, St. Louis, Missouri, USA: DNase I RNase free.

WPI, Berlin, Germany: borosilicate glass capillaries.

SERVA electrophoresis, Heidelberg, Germany: agarose.

Roth, Karlsruhe, Germany: other chemicals.

2.1.3 Kits

Affymetrix, Santa Clara, CA, USA: Affymetrix GeneChip® Two-Cycle cDNA Synthesis Kit

Clontech, Mountain View, USA: SuperSMART" cDNA synthesis kit

Invitrogen: pCR®8/GW/TOPO® TA cloning kit

Macherey-Nagel, Düren, Germany: NucleoSpin extract II kit; NucleoSpin plasmid Kit

Qiagen, Hilden, Germany: PCR Purification Kit

Roche: Random Primed Labelling Kit

2.2 Plant material

Arabidopsis thaliana (L.) ecotype Col-0

Arabidopsis thaliana (L.) ecotype Ler (*pGL2::GFP*)

2.3 Plant growth

Arabidopsis plants were grown in a greenhouse at an average photon flux density of 120µmol m^{-2} s^{-1}, at 60% relative humidity, and with a photoperiod of 16 h light (21°C) and 8 h darkness (17°C). Plants were grown in individual pots in a GS90 soil:vermiculite mixture (1:1 v/v) (Fritz Kausek GmbH & Co. KG, Mittenwalde, Germany) and watered daily. As necessary,

plants were harvested into paper bags and dried for 2 weeks to obtain seeds. Seeds were stored in 2 ml screw-cup glass vials at 14 °C and 10% relative humidity.

2.4 Single Cell Sampling

3-4 week-old plants were used for microsampling. Microcapillary sampling of single cell sap from pavement, trichome initial, and mature trichome cells in leaves was performed as described by Brand et al., 1999. Briefly, borosilicate glass capillaries (WPI) were pulled on a List pipette puller with a tip aperture of 1-10 µm and mounted on the micromanipulator. Young rosette leaves were detached from the plant using a stereo zoom microscope (World Precision Instruments) and immediately fixed under an Optiphot 2 microscope (Nikon). Pavement, trichome initial, and trichome cells were collected from the same rosette leaf. For sampling and pooling of pavement cells, protodermal cells from the same area of the leaf as trichome initials were used. A capillary was inserted into a single cell via the remote controlled micromanipulator (Eppendorf). Immediately after withdrawal, the content of the capillary was released into a sterile, 0.5 ml reaction vial containing 1 ml DEPC water with 5 U RNase inhibitor (RNAsin, Promega). Each capillary was used for only one sampling process. The same procedure was applied for harvesting mature trichome cells. Trichome initial cells expressing GFP in *pGL2::GFP* plants were visualized and localized using UV-light and the appropriate GFP filter (460-500nm/505-560 nm) and collected after switching to bright field conditions. A total of 10 cells of each cell type were collected per sample. Single cell sampling was performed in three biological replicates.

2.5 Single cell PCR amplification

Precautions to prevent contamination or degradation of RNA were taken as described by Brandt et al., 1999. In brief, sterile disposable microcapillaries, filter tips, and tubes were used. All RT-PCR reactions were prepared under a sterile UV hood without air circulation and all post-PCR work was done in a separate laboratory.

Reverse transcriptions were performed in the vials containing the extracted cell samples. cDNA synthesis was accomplished using the “SuperSMART” protocol (Clontech) according to the manufacturers instructions.

This protocol has been developed for small amounts of total RNA as a starting material. All commonly used cDNA synthesis methods rely on the ability of reverse transcriptase (RT) to transcribe mRNA into single-stranded (ss) DNA in the first-strand reaction.

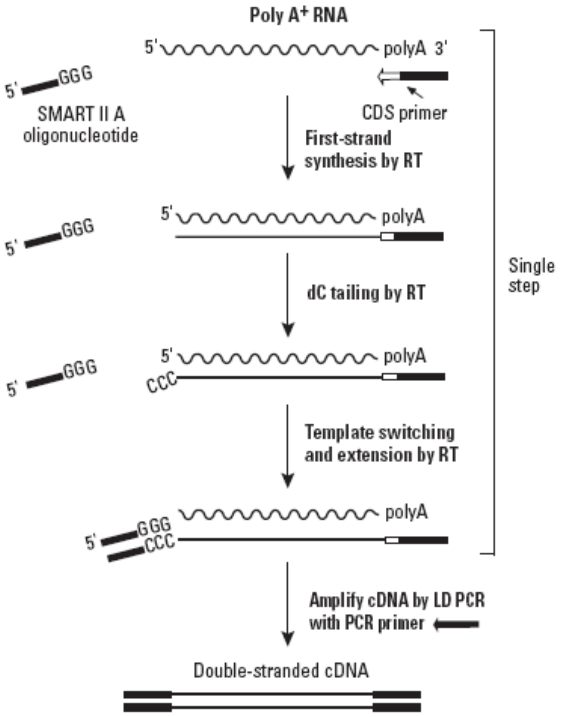

Figure 2.1 Principle of the SMART technology RT: reverse transcriptase. LD PCR: long distance PCR.

However, because RT cannot always transcribe the entire mRNA sequence, the 5' ends of genes tend to be underrepresented in cDNA populations. This is often the case for long mRNAs, especially if the first-strand synthesis is primed only with oligo(dT) primers, or if the mRNA has a persistent secondary structure. In the absence of RNA degradation, truncated cDNA molecules present in libraries are often due to the tendency of RT to pause before transcription is complete. In contrast, the SMART method is able to preferentially enrich for full-length cDNAs (see Fig. 2.1). A modified oligo(dT) primer (the 3' SMART CDS Primer II A) primes the first-strand synthesis reaction. When RT reaches the 5' end of the mRNA, the enzyme's terminal transferase activity adds a few additional nucleotides, primarily deoxycytidine, to the 3' end of the cDNA. Oligonucleotide, which has an oligo(G) sequence at its 3' end, base-pairs with the deoxycytidine stretch, creating an extended template. RT then switches templates and continues replicating to the end of the oligonucleotide (Chenchik et al, 1998). The resulting full-length, single-stranded (ss) cDNA contains the complete 5' end of the mRNA.

2.6 Single cell sampling control reactions

Control reactions related to microcapillary sampling were performed as described by Brandt et al., 2002. Briefly, the templates for all types of controls were handled in parallel by microcapillaries and expelled into sterile reaction vials as described for microsampling. To ensure the performance of all components of the RT-PCR reaction, RNA was used as a positive control. RNA was isolated from leaves of 3-4-week-old plants using the TRIzol reagent method (Invitrogen) (see below). Negative controls: to ensure amplification of RNA and not of genomic DNA, water was added to some samples instead of reverse transcriptase. Other cell extracts were treated for 30 min at 37°C with RNase A (Roche) prior to reverse transcription. To exclude false positive results caused by contamination, at least one mock experiment was performed in parallel

to every experiment using water instead of cell extracts. If one of the negative controls showed any PCR products as seen from results of agarose gel electrophoresis, the entire experiment was discarded. The elongation factor *EF-1αA4* (Axelos et al., 1989) was used as housekeeping gene for PCR to evaluate the equality of extraction volumes. In addition, direct determination of volumes collected from all three cell types was performed. Microcapillaries were filled with a pH sensitive fluorescent dye prior to sample collection. Entrance of cytoplasm into the capillary was demonstrated by detection of a fluorescent meniscus. Measuring the position of this meniscus under the microscope provided a precise volume determination (Brandt et al., 1999).

2.7 Probe generation for array hybridization

PCR products from single cell samples were purified using spin columns (PCR Purification Kit, Qiagen) and subsequently recovered in 50 µl EB buffer (see the manufacturers instructions). 20 µl of the products were denatured at 95°C for 10 min and labelled with 60 µCi ^{33}P dCTP (NEN, Zaventem) using the Random Primed Labeling Kit (Roche) according to the instructions of the manufacturer. After purification by Nick columns (Amersham biosciences) aliquots of the probes were counted for incorporation of the radioactive label into the products by a scintillation counter.

2.8 Filter array hybridization

Arabidopsis cDNA plasmid clones were obtained from the Arabidopsis Biological Resource Center (ABRC, Ohio, USA) where most of the clones were generated as part of the Michigan State University EST effort (Newman et al., 1994).

PCR amplification of cDNA inserts and array preparation were performed as described by Brandt et al., 2002.

2.8.1 Array hybridization and evaluation

2.8.1.1 Reference hybridization

Reference hybridization was performed on a shaker in 200 ml 1xSSarc (24% Sarcosyl NL30, 0.6 M NaCl, 0.06 M sodium citrate, 4 mM EDTA) at 5°C overnight using a ^{33}P end-labeled oligomer (5'-TTC CCA GTC ACG) unique to all PCR products. Membranes were washed for 30 min at

5°C in 0.5 l SSarc and exposed. Membrane regeneration was done by stripping twice in 0.1 l 0.1xSSarc at 65°C for 30 min.

2.8.1.2 Complex hybridization

Filters were permutated for different hybridizations. Prehybridization was done for at least 2 h at 65°C in a buffer consisting of 250 mM sodium phosphate at pH 7.2, 10 mM EDTA, 7% SDS, and 1% BSA. The hybridization was performed in the same buffer for 30 h at 65°C. The filters were washed for 20 min in 2x SSC, 0.5% SDS, 4 mM sodium phosphate (pH 7.2) at 65°C and for 20 min in 0.2x SSC, 0.5% SDS, 4 mM sodium phosphate (pH 7.2) at 65°C. Fuji BAS intensifying screens (Raytest) were exposed overnight and scanned at 50 µm resolution (16 bits per pixel) with a Fuji BAS 1800 II phosphor imager (Raytest). The image was analyzed and converted into a table of signal intensities using the Array Vision software (Imaging Research).

2.8.1.3 Data processing

The table of signal intensities was submitted to an in-house database (Haruspex). Within this database, the raw data were annotated, rearranged, and normalized. In the first normalization step, the local background was subtracted from each value, which was than divided by the average signal obtained for all spots on the filter. A second normalization step involved the values of each individual spot obtained by the reference hybridization based on the assumption that, under the chosen conditions, the signal from the complex hybridization is linearly proportional to the amount of bound PCR product (Thimm et al., 2001). The clone functions were determined by homology searches using the TAIR database (http://www. arabidopsis.org/).

2.9 Affymetrix GeneChip hybridization

First and second strand cDNA synthesis was performed with cell sap of ten sampled single cells using the SuperSMART method (see above). *In vitro* transcription (IVT), second cycle cDNA synthesis and biotin labeling of cRNA was performed using the Affymetrix GeneChip® Two-Cycle cDNA Synthesis Kit according to the manufacturer's instructions (Affymetrix). Afterwards, biotin-labeled cRNA was resolved on a 1% formaldehyde gel.

1% formaldehyde gel contained 10 ml 10X MOPS buffer, 87.5 ml H_2O and 1g agarose (SERVA electrophoresis). The agarose was melted and cooled down to 50-60°C followed by addition of 2.5 ml formaldehyde (37%). RNA samples and RNA ladders loading on

the gel was performed according to instructions of manufacturer of the ladders (Fermentas). Gels were run at 5 V cm^{-1}. Biotin-labeled cRNA analysis using Bioanalyzer 2100 (Agilent technologies) and Affymetrix test hybridization was performed by RZPD (German Resource Center for Genome Research; Berlin, Germany).

2.10 Real-time RT-PCR

cDNA synthesis was carried out with the cell sap of ten single cells per sample using SuperSMART (see above). Real-time RT-PCR primers were designed using Primer Express software (Applied Biosystems). Real-time RT-PCR reactions contained 12.5 µl 2X SYBR^{TM} Green Master Mix reagent (Applied Biosystems), 250-500 nM of each gene-specific forward and reverse primer, and cDNA template from the ten sampled single cells in a final volume of 25 µl. SDS 7300 sequence detection system (Applied Biosystems) was used for the quantification of mRNA transcripts by real-time RT-PCR. Reactions were performed in an optical 96-well plate and controlled by a dissociation protocol. Following thermal profile was used for all real-time RT-PCR reactions: denaturation for 10 min at 95°C followed by 40 cycles of 15 sec at 95°C and primer extension reaction at 60°C for 1 min. All PCR reactions and negative controls were run in triplicates. Data were analysed using SDS 2.1 software (Applied Biosystems). In order to compare amount of target in cDNA samples, the C_T (threshold cycle) values of genes of interest were normalized to the C_T value of the elongation factor 1 alpha housekeeping gene (Axelos et al., 1989), which was included in each PCR run. PCR efficiency was estimated as described previously (Ramakers et al., 2003). Expression of the gene of interest was normalized to that of *elongation factor 1 alpha* by subtracting the C_T value of *EF1 alpha* from the C_T value of gene of interest. Expression ratios of sample A to sample B were obtained from the equation $(1+E)^{-\Delta\Delta CT}$ where $\Delta\Delta C_T$ represents ΔC_{TA} minus ΔC_{TB}, and E is the PCR reaction efficiency. Dissociation curves of the PCR products were analyzed using SDS 2.1 software. All real-time RT-PCR products were resolved on 4% (w/v) agarose gels (agarose SERVA, SERVA electrophoresis) run at 4 V cm^{-1} in TAE buffer in parallel with a 50 bp DNA ladder (Invitrogen).

2.11 Genomic DNA isolation

For amplification of promoter regions of the genes of interest and for PCR-based screening of SALK knockout lines genomic DNA from whole plant material was extracted using CTAB protocol as described previously (Doyle and Doyle, 1987; Rogers, 1994) (CTAB buffer consists of 16.36g NaCl; 8ml 0.5M EDTA (pH 8.0); 20ml 1M Tris-HCl (pH 8.0); 4g CTAB;

H_2O to 200ml). RNase digestion of isolated DNA was carried out using RNase A (Roche) according to manufacturers instructions. Quantity and quality of DNA were evaluated spectrophotometrically (Eppendorf BioPhotometer) and using fluorimetry (DynaQuant™ 200 fluorimeter, Amersham).

2.12 RNA extraction using TRIzol protocol

Frozen plant material (100-200 mg) was homogenized in liquid nitrogen in a pre-cooled mortar and transferred to an Eppendorf tube. Afterwards TRIzol reagent (Invitrogen) was added and mixed well by vortexing. After a 5 min incubation at room temperature the homogenate was centrifuged at 13000 rpm for 5 min at 4°C in a pre-cooled centrifuge. The supernatant was removed and transferred to a fresh Eppendorf tube followed by addition of 400 µl chloroform and vortexing. The mixture was incubated for 5 min at RT. After a 10 min centrifugation at 13000 rpm at 4°C, the aqueous phase (~1ml) was transferred to a fresh Eppendorf tube. RNA was precipitated with 0.5 ml of isopropanol and 0.5 ml of HSS buffer (0.8 M Sodium Citrate and 1.2 M Sodium Chloride) per 1 ml of aqueous phase overnight at -20°C. The precipitate was pelleted by centrifugation at 13000 rpm for 30 min at 4°C. The supernatant was removed and the pellet was washed twice with 1 ml 70% EtOH, air dried and re-suspended in 50 µl sterile water. RNA quantity and quality was determined by photometric measurements using an Eppendorf BioPhotometer according to the instructions of the manufacturer. To eliminate possible DNA contamination, RNA samples were treated with DNase I RNase free (Sigma) according to the manufacturer's instructions.

2.13 Construction of promoter::β-glucuronidase fusions

Promoter regions of *At3g16980*, *At5g15230 (GASA4)* and *At4g27260* (*GH3.5*) were amplified by PCR using following primers: for *At3g16980*: 5'-ACTAAGAAAGCCACAA; 5'-CTCTTGAGAGAGAATTAGGTTCC; for *GASA4* (*At5g15230*): 5'-GATGGATCACATGCTTTCA; 5'- CCAAAGAACCAAACACTCCTCTAAATC, and for *GH3.5* (*At4g27260*): 5'- GGGGACAAGTTTGTACAAAAAAGCAGGCTCAAAC ATAATATACAACCATAGAGCC-3'; 5'- GGGGACCACTTTGTACAAGAAAG CTGGGTGTGTGAGGAAGAAAGAAAGAGAAAGGGT -3' (primers of the last primer pair contain *att*B sites necessary for GATEWAY™ BP-reaction - see below). In the case of *At3g16980*, a 420 bp region upstream of the start codon was amplified (from -12 to -431). For *GASA4* the length of the amplified promoter region was 2065 bp (from -23 to -2087) and for

GH3.5 1897 bp (from -89 to -1985). Amplification was carried out in a Mastercycler Gradient system (Eppendorf) using the following program: 5 min at 95°C followed by 35 cycles of 30 sec at 95°C, 60 sec annealing at 56°C, 120 sec at 72°C and finally 10 min at 72°C for the final extension. *Taq* DNA polymerase (New England Biolabs) was used for these PCR reactions according to the instructions of the manufacturer. After fractionation on agarose gel amplified promoter regions were extracted and purified using NucleoSpin extract II kit (Macherey-Nagel) according to the manufacturer's instructions.

Cloning of PCR- amplified promoter regions of the genes of interest was carried out using GATEWAY™ technology (Invitrogen) according to manufacturer's instructions.

This technology is based on the bacteriophage lambda site-specific recombination system which facilitates the integration of DNA of the virus into the *E. coli* chromosome (Ptashne, 1992). Lambda- based recombination involves two major components: the DNA recombination sequences (*att* sites) and the proteins that mediate the recombination reaction (i.e. Clonase™ enzyme mix). Lambda integration into the *E. coli* chromosome occurs via intermolecular DNA recombination that is mediated by a set of bacteriophage and *E. coli*-encoded recombination proteins (i.e. Clonase™ enzyme mix). Recombination occurs between specific *att* sites on the interacting DNA molecules. Recombination is conservative (there is no net gain or loss of nucleotides) and requires no DNA synthesis. The DNA segments flanking the recombination sites are switched, such that after recombination the *att* sites are hybrid sequences donated by each parental vector. For instance, *att*L sites are comprised of sequences from *att*B and *att*P sites. Two recombination reactions constitute the basis of GATEWAY™ technology:

BP reaction: facilitates recombination of an *att*B substrate (attB-PCR product or a linearised attB expression clone) with an *att*P substrate (i.e. donor vector) to create an *att*L-containing entry clone;

LR reaction: facilitates recombination of an *att*L substrate (entry clone) with an *att*R substrate (destination vector) to create an *att*B-containing expression clone.

An outline of how the GATEWAY™ cloning technology works is presented in Fig. 2.2.

Gel-purified PCR products (see above) were used for BP reaction with pDONR207 entry vector (Invitrogen, vector described in APPENDIX A).

Another way used to clone PCR products into a GATEWAY™ entry vector was TOPO® TA cloning system (Invitrogen). PCR products were cloned into the pCR®8/GW/TOPO® vector (description of the vector presented in APPENDIX A). The TOPO- reaction was performed according to manufacturer's instructions.

After production of GATEWAY™-compatible entry clones, LR clonase reactions were performed. In this way, DNA fragments were transferred from entry clones to destination vector pMDC162 containing GUS encoding sequence (Curtis and Grossniklaus, 2003). LR reactions were accomplished according to the manufacturer's instructions (Invitrogen).

a

b

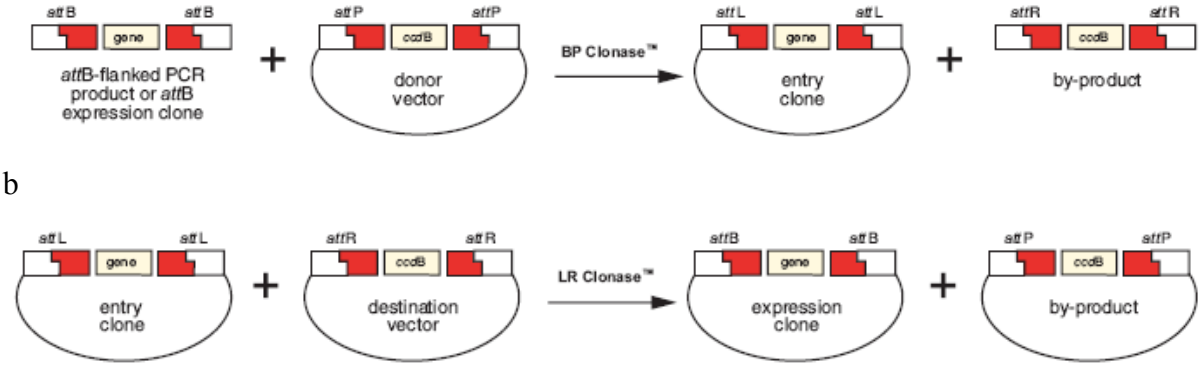

Figure 2.2 GATEWAY™ cloning technology a: production of entry clone using BP- reaction; **b.** LR reaction used for cloning a DNA fragment into a destination vector to produce an expression clone. attB, attP, attL, attR: recombination sites.

Transformed bacterial colonies were checked for the presence of the desired insert in the vector using PCR with gene specific primers (see above). For plasmid mini preparations the NucleoSpin plasmid Kit (Macherey-Nagel) was used and preparation was conducted according to the instructions of manufacturer.

Other standard DNA manipulations e.g. restriction digestions, gel electrophoresis etc. were performed as described in Sambrook et al., 1989. Positive entry clones were sequenced using M13 universal primers for pCR®8/GW/TOPO® and pDONRT207 primers for pDONR207 (see APPENDIX B). DNA sequencing was performed by AGOWA GmbH (Berlin, Germany) using Big Dye™ chemistry on a Perkin Elmer ABI 377 HT sequencer. Sequencing chromatograms were analysed using Chromas 1.45 software. Only those clones giving no sequence differences to the deposited in the TAIR database were chosen for the further cloning steps. Positive clones after LR reaction were digested with different combinations of restriction enzymes (depending on cloned sequence) to confirm that recombination events did not destroy the vector structure (vector structures are given in APPENDIX A). Only those clones showing a correct restriction pattern were used for transformation of *Agrobacterium tumefaciens* strain GV3101pMP90. Mini preparations of the *A. tumefaciens* plasmids were performed and the restriction pattern was checked again with the same sets of restriction enzymes as for positive *E. coli* clones after LR reaction (see above). Only *A. tumefaciens* clones giving the same pattern as the corresponding *E. coli* clones were used for plant transformation.

2.14 Bacteria transformation and growth

Transformation of *Escherichia coli* strain DH5α was conducted by a heat shock method described previously (Hanahan, 1983). *A. tumefaciens* strain GV3101pMP90 was transformed by electroporation with a GenePulser II (Bio-Rad) according to the manufacturer's instructions. *E. coli* strains were grown in LB medium (Sambrook et al., 1989) and *A. tumefaciens* strains in YEB medium (Vervilet et al., 1975). For growth on solid media 1.5% agar was added. Filter-sterilized antibiotics were added at following concentrations: Kanamycin- 50 µg/mL; Gentamycin- 25 µg/mL; Rifampicin- 100 µg/ml.

LB medium (autoclaved)
10g Bacto-tryptone
5g Bacto- yeast extract
10g NaCl
pH adjusted to 7.5 with 1M NaOH
dH_2O to 1 l

YEB medium (autoclaved)
5g Bacto-pepton
1g Yeast- extract
5g Beef- extract
5g sucrose
493 mg $MgSO_4$ x $7H_2O$
pH 7.2
dH_2O to 1 l

2.15 *Arabidopsis thaliana* transformation

A. thaliana (Ler and Col-0 ecotypes) plants were transformed using the floral dip method (Clough and Bent, 1998).

2.16 Histochemical analysis of plants transformed with promoter::GUS constructs

Transformants were selected by their ability to grow on the medium containing hygromycin. Histochemical assays for GUS activity of plant tissues and organs were conducted as described previously (Jefferson et al., 1987; Larkin et al., 1993; 1996). Histochemical GUS staining was performed on the T2 plants. Ten independent Arabidopsis transformants were assessed for each construct.

2.17 Promoter analysis

Promoter regions of the genes of interest were screened in silico for the presence of common cis-acting elements using the PlantPag tool (http://plantpag.mpimp-golm.mpg.de/). This is a web-based tool for the automated sequence analysis of plant promoter sequences, which

combines different databases, tools, and algorithms to analyze bigger sets of co-regulated genes. In particular, sets of all available plant promoter sequences can be searched for known cis-acting regulatory elements (using PlantCare, PLACE or AtcisDB databases). For this study, ActisDB (Davuluri et al., 2003) and PLACE (Higo et al., 1999) databases were used. Furthermore, PlantPag allows a genome-wide comparison for distribution of known cis-acting regulatory elements in promoter sequences of all Arabidopsis genes. As a result, genes that are enriched in specific regulatory elements in their promoters, as well as common regulatory motifs in sets of co-regulated genes can be identified.

Such enrichment analysis was performed for the candidate genes in this study. The enrichment score was calculated as

$$ES = Fq/Fg ,$$

where

- ES = enrichment score;
- Fq = frequency in query set:
- Fq = absolute number of a binding site in query set/ total number of binding sites in query set
- Fg = frequency in genomic set:
- Fg = absolute number of a binding site in genomic set/ total number of binding sites in genomic set.

However, the enrichment score could not be calculated for certain cis-acting elements since for these elements their frequency in the whole genome has not yet been calculated and hence was not available in PlantPag.

2.18 PCR-based screening for homozygous knockout (KO) plant lines

Two primer pairs were used to identify homozygous KO lines: two gene-specific primers that are unable to amplify product of expected size from homozygous KO line and primer pair consisting of gene specific primer plus T-DNA-specific primer that amplify DNA only from KO lines but not from the wild type plant material. Genomic DNA from WT plants grown in parallel was always used as a control for both PCR reactions. All gene- specific primers were designed using a web-based software tool (http://signal.salk.edu/tdnaprimers.html) with the following parameters: optimal primer size 21 bp; optimal T_m 65°C; and CG content between 20 and 80%. T-DNA-specific primers for the SALK lines (LBa1, LBb1) are available on the same webpage (see above). Sequences of all primers are presented in APPENDIX B.

PCR was performed on DNA prepared by CTAB protocol as described above, using the combination of two gene-specific primers or one gene-specific primer and LBa1/ LBb1 primer. PCR products were visualized by ethidiumbromide staining following agarose gel electrophoresis.

The most commonly used PCR program for screening was:

- 1 cycle of 95°C for 5 min
- 35 cycles of 95°C for 30 s, 56°C for 1 min, 72°C for 2 min
- 1 cycle of 72°C for 10 min

Some parameters of the program were modified according to T_m differences of the primers, length of the desired product etc.

For checking expression of the targeted genes in KO-lines, RNA was isolated using the TRIzol method (see above) followed by cDNA synthesis. Reverse transcription reactions were carried out using 5 µg of total RNA with SuperScript^{TM} II reverse transcriptase (Invitrogen) according to the instructions of the manufacturer. Subsequently, semi quantitative PCR with gene-specific primers was performed using PCR program described above. After a certain amount of cycles, 10 µl aliquots were taken and electrophoretically analyzed. Sequences of the primers are presented in APPENDIX B.

2.19 Microscopic analysis of the knockout plant lines

Microscopy of the leaves was performed using a Leica MZ 12.5 stereo microscope (Leica Microsystems). Trichome amount and leaf area were measured with the help of Leica Soft Imaging System IM 500 software. For calculations of trichome density, the numbers of trichomes per leaf were divided by the corresponding leaf area.

2.20 Gas chromatography-mass spectrometry (GC-MS)

For GC-MS analysis, *gh3.5* plants (SALK_151766 line) and WT control plants were used. Plant material was shock frozen in liquid nitrogen and ground to fine powder. 120 ± 5 mg of frozen material was homogenized with a Retsch-mill (Retsch) set to $15s^{-1}$ for 3 min and extracted with 300 µl pre-cooled (−20°C) absolute methanol. To each sample, 30 µl of a methylnonadecanoate stock solution (2 mg ml^{-1} methanol) (Sigma-Aldrich) and 30 µl of a ribitol stock solution (0.2 mg ml^{-1} methanol) (Sigma-Aldrich) were added. After shaking at 70°C for 15 min, 200 µl chloroform was added to the samples, which were shaken at 37°C for an

additional 5 min following by centrifugation for 5 min at 14000 rpm in a microfuge. Then 400 µl H_2O was added. The protocol was downscaled to 10 µl of the final methanol/water phase, which was dried in a SpeedVac concentrator (Concentrator 5301; Eppendorf) overnight. Chemical derivatization (Roessner et al., 2000; Fiehn et al., 2000) and GC-TOF-MS metabolite profiling analysis (Wagner et al., 2003; Weckwerth et al., 2006) was performed essentially as described previously.

Chromatograms were acquired, deconvoluted and processed with ChromaTOF™ software (Leco). For each metabolite, at least five expected mass fragments were quantified. The quantitative results were tested using Pearson's correlation analysis to ensure the lack of unexpected, co-eluting compounds that might form identical mass fragments. Only those mass fragments that exhibited significant correlations ($P < 0.01$) were accepted. Statistical analysis of the quantitative response of each metabolite was conducted using baseline corrected peak height and normalization for sample fresh weight and intensity of the internal standard ribitol. *gh3.5* plants were compared to the WT controls using fifteen biologically independent replicas each.

Response ratios of mutant over control samples were calculated independently for each of the multiple selected mass fragments and checked for identical numerical values and statistical significance and then averaged for each sample. Standard deviation of the response ratio was calculated among the independent biological samples, each representing a separate, individual plant. Response ratios were considered to differ significantly with a 0.05% error threshold. Metabolites were identified with the GMD library (Golm Metabolome Database, http://csbdb.mpimp-golm.mpg.de/csbdb/gmd/gmd.html; Kopka et al., 2005; Schauer et al., 2005) and commercially available authentic reference substances. Mass spectral and RI comparison was performed using NIST02 (National Institute of Standards and Technology, Gaithersburg, MD, USA) mass spectral search and comparison software, accepting mass spectral matches > 650 on a scale of 1000 and retention time index matches ± 5.0 RI units. Metabolites were characterized using chemical abstracts system (CAS) identifiers and compound codes issued by the Kyoto Encyclopedia of Genes and Genomes (KEGG; Kanehisa *et al.*, 2004).

3. RESULTS

3.1 Workflow

After sampling single trichome initials, mature trichomes, and pavement cells, I amplified the extracted mRNA, radioactively labeled it, and proceeded with filter array hybridization. Three biological replicates of each cell type were used for hybridization. Candidate genes were selected based on ratios of differential gene expression within pairs of compared cell types. The expression pattern of selected candidate genes was investigated further and confirmed using real-time RT-PCR and/or histochemical GUS assays. To evaluate the possible roles of the candidate genes in trichome development and cell cycle regulation, knockout (KO) as well as RNAi plant lines were analyzed. Metabolic profiling of one of the KO plant lines was performed. To gain additional information on the possible interactions between candidate genes and the cell cycle machinery I analyzed the promoter regions of selected candidate genes in silico.

3.2 Single cell sampling and array hybridization

To label trichome initial cells I used transgenic Arabidopsis plants that expressed GFP under the control of the *GLABRA 2 (GL2)* promoter (*pGL2::GFP*) (a gift from Prof. Martin Hülskamp, University of Cologne). It has been demonstrated that *GL2* is expressed during early stages of trichome development when there are still no visible signs of trichome formation (Hülskamp 2004; Marks 1994; Szymanski et al., 1998, 2000; Fig3.1). Furthermore, *GL2* is required for normal trichome morphogenesis. The GFP signal localized to the nucleus since the *pGL2::GFP* construct contained a nuclear localization sequence (NLS, Grebenok et al., 1997; Fig 3.1).

GFP labeling enabled the detection and sampling of incipient trichomes at the initial stage of their development. Samples of single trichome initial cells, mature trichomes, and pavement cells contained an average volume of 5 pl. Fig 3.2 depicts the sampling procedure for single Arabidopsis leaf epidermal cells. 10 single cell extracts were combined, radioactively labeled and hybridized on array filters. In total, 9 filters were hybridized (3 filters per cell type using three biological replicates).

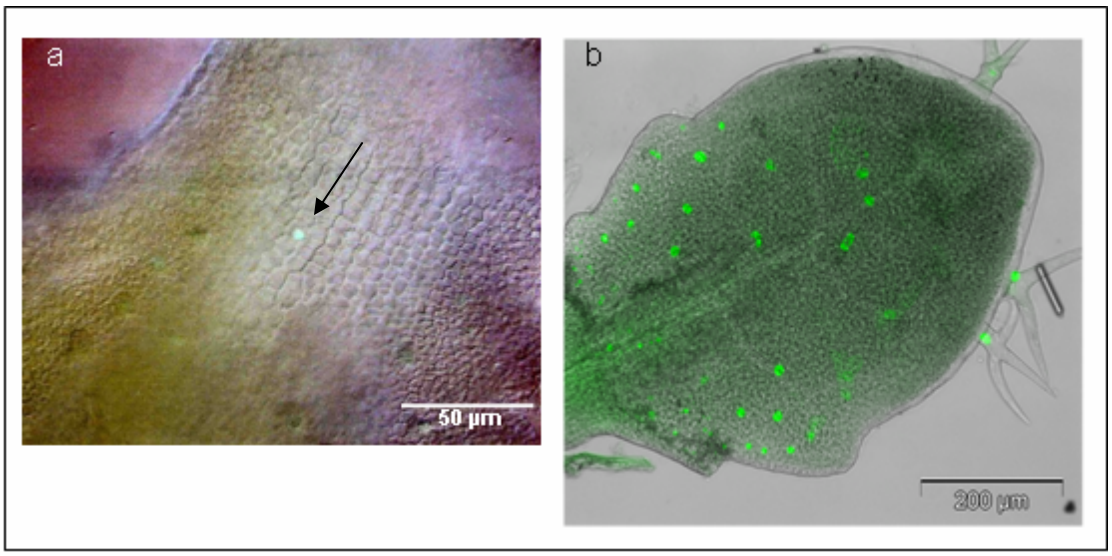

Figure 3.1 Visualization of trichome initial cells using the *pGL2::GFP* localization Pictures were obtained by overlaying the UV-image and the bright field image. Green dots- nuclei of GFP-positive cells; **a:** trichome initial cells (one marked by an arrow); **b:** latter stages of trichome development (including mature trichomes).

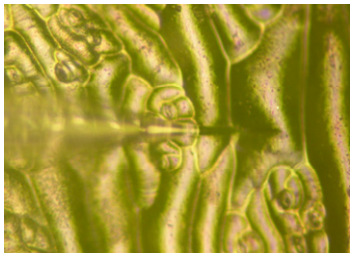

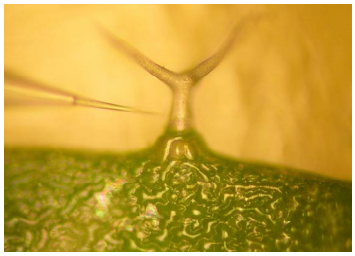

Figure 3.2 Sampling of single leaf epidermal cells
Left: A microcapillary approaching a pavement cell. Right: A mature trichome has been sampled; the cell sap is visible inside in the microcapillary. (Daniela Zöller)

Genes identified in extracts from trichome initial cells, mature trichomes, and pavement cells were subsequently grouped into functional clusters (separately for each cell type) using Gene Ontology annotation available at the TAIR database (www.arabidopsis.org; GO Biological Process). Comparisons among pavement, trichome initial, and mature trichome cells revealed only small differences in distribution of functional categories (Fig 3.3). Interestingly, when compared to the whole genome functional categorization, values for some categories were found to be remarkably higher in cells of interest than in the entire genome. These categories are "response to abiotic or biotic stimuli" (2.9% in whole genome and 4.7%. 5% .4.5 % in single cells) and "response to stress" (2.2% in the whole genome and 4.1%. 4.5 %. 4.1 % in single cells). It should be noted that this functional categorization did not take the degrees of gene expression into account.

The degree of differential gene expression between pairs of the selected cell types was visualized using MAPMAN (Fig 3.4, Thimm et al., 2004). In order to identify genes that were specifically upregulated at very early stages of trichome development, I compared trichome initials and pavement cells in the same region of the leaf (Fig 3.4a). In addition, mature trichomes

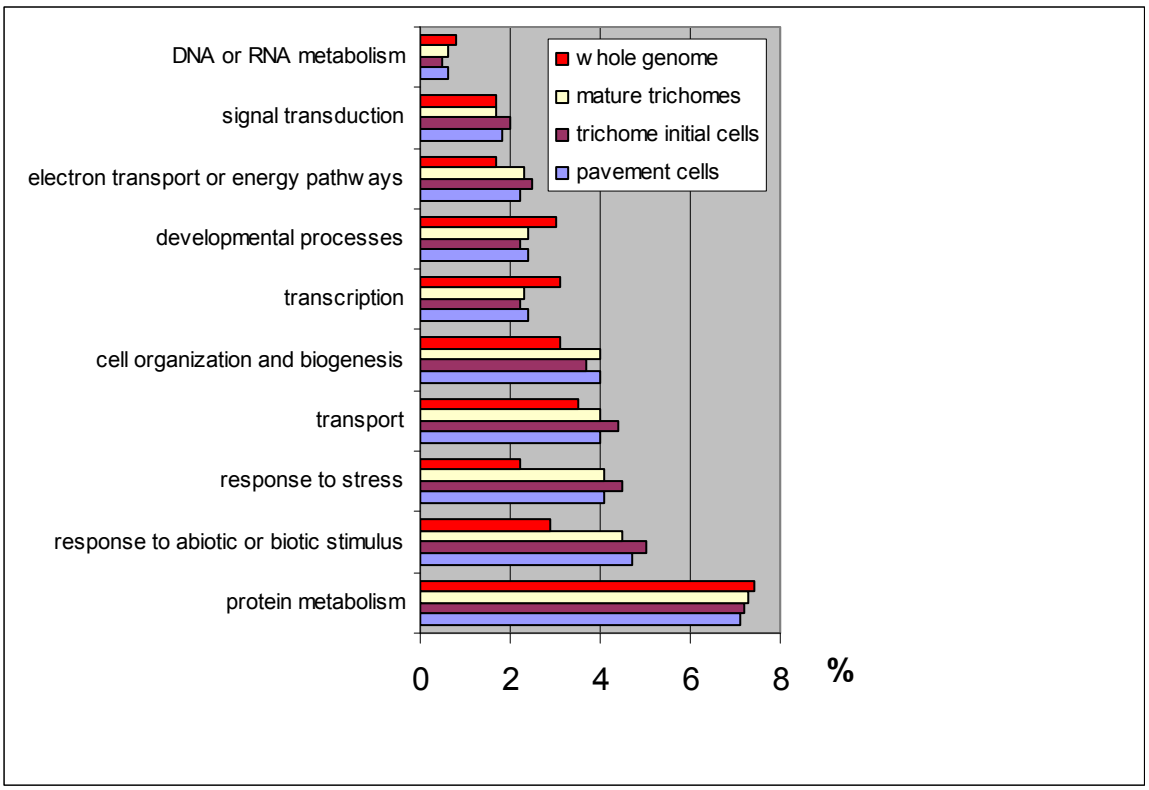

Figure 3.3 Functional categorization of genes expressed in pavement, trichome initial, and mature trichome cells Transcripts identified by array filter hybridization were clustered into functional groups (GO annotation). In comparison, a high degree of similarity in functions of genes expressed in pavement, trichome initial cells, and mature trichomes was observed. When compared to the functional categorization of the whole genome, the sets "response to stress" and "response to abiotic or biotic stimulus" are over-represented in cells of epidermal origin.

and pavement cells were compared (Fig 3.4 b). 1804 out of 1929 transcripts modified in expression in comparison trichome initials / pavements cells and 1139 out of 1926 transcripts within the comparison mature trichomes vs. pavement cells are still unknown or not yet annotated (Fig 3.4 a, b). Therefore, applied single cell analysis provides initial clues to assign spatial or functional attributes to these transcripts. Noteworthy is that the amount of upregulated genes increases during trichome development. White bars (Fig 3.4b) denote greater similarity between mature trichomes and pavement cells than between trichome initials and pavement cells (Fig 3.4a). Furthermore, in comparison to pavement cells, trichome initials exhibit increase in transcripts related to DNA synthesis and cell cycle progression.

Genes with a differential expression ratio >2 and P-value ≤ 0.05 were considered as differentially expressed between compared cell types. In total, 38 genes were found to be more highly expressed in trichome initials than in pavement cells, 31 were more highly expressed in mature trichomes than in pavement cells, and, surprisingly, 509 genes were more

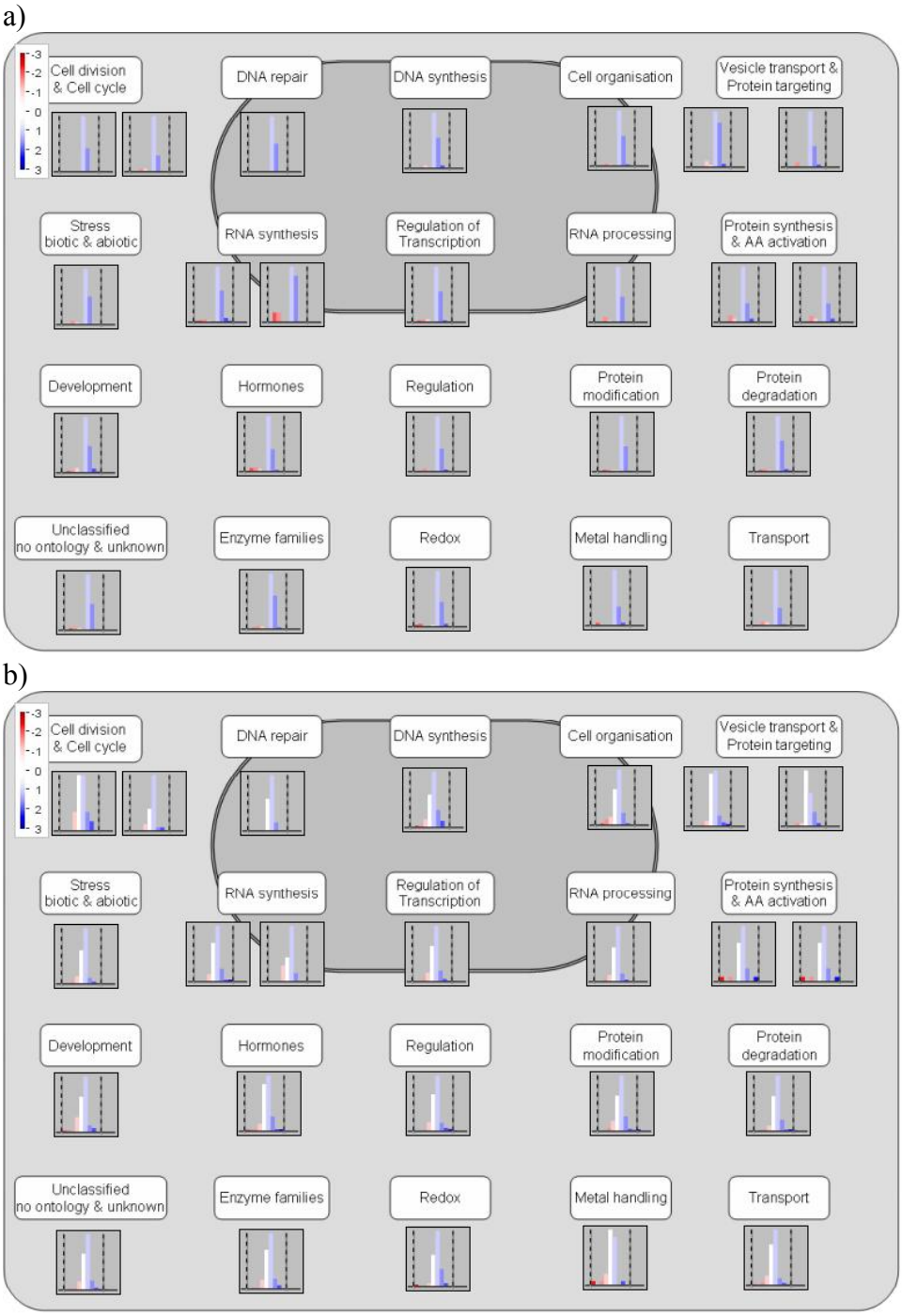

Figure 3.4 Visualization of differential expression of the genes between two cell types using MAPMAN
a) Trichome initial cells vs. pavement cells. Blue bars represent genes preferentially expressed in trichome initial cells; red bars, genes more highly expressed in pavement cells. **b)** Mature trichomes vs. pavement cells. Blue bars corresponding to genes preferentially expressed in mature trichomes; red bars, genes more highly expressed in pavement cells. Log2 of the ratio of differential gene expression between trichome initial/pavement cells for a) and mature trichomes/pavement cells for b) was used as an input for MAPMAN software. Blue bars indicate positive values of ratios (up regulation of the genes in cell type placed in numerator when calculating the ratio); red bars indicate negative value of ratio (up regulation of the genes in cell type placed in denominator). White bars correspond to genes showing no differential expression between the two cell types. a) A greater number of genes is preferentially expressed in trichome initials as compared to pavement cells; b) More genes with higher expression levels occur in mature trichomes than in pavement cells. Several categories are labeled by two histograms. Several reasons can account for this subdivision (compare: Thimm et al. 2004). In most cases: the gene annotation is too diverse to be represented in one diagram.

highly expressed in mature trichomes than in trichome initial cells. A complete list of differentially expressed genes is presented in APPENDIX C.

Table 3.1 summarizes a set of selected candidate genes that were differentially expressed within trichome initials/pavement cells and mature trichomes/pavement cells. Among these are genes with unknown function, transcription factors, and genes involved in hormonal responses. Furthermore, several genes were expressed in only one cell type or the other; *At3g16980*, *At3g53420*, *At5g11730*, *At5g44790* were observed exclusively in trichome initial cells and *At5g45820*, *At1g48750*, *At2g47980* exclusively in mature trichome cells. The expression of At3g22440 was particularly interesting; it was expressed at progressively higher levels as trichomes matured.

Table 3.1 Selected candidate genes highly expressed in trichome initial cells compared to pavement cells
EST: expressed sequence tag

Gene ID	MSU EST ID	Ratio	P-value	Gene Function
AT3G16980	MSU01-E1H12T7-0	2.2	0.04	putative DNA-directed RNA polymerase II,
AT5G15230	MSU01-E2A1T7-0	2.3	0.05	gibberellin-regulated protein GASA 4
AT4G27260	MSU01-H5F4T7-1	7.9	0.02	auxin-responsive GH3 family protein GH3.5
AT3G53420	MSU01-G9D9T7-1	7.3	0.01	PIP2.1; plasma membrane intrinsic protein
AT5G11730	MSU01-G5H7T7-1	5.2	0.03	expressed protein
AT1G64720	MSU01-E6H3T7-1	5.2	0.03	expressed protein
AT5G44790	MSU01-G5G1T7-1	2.3	0.02	Cu Transporter
AT3G22440	MSU01-G11D8T7-1	4.5	0.02	hydroxyproline-rich glycoprotein family protein
AT5G13240	MSU01-E6G2T7-1	4.5	0.03	expressed protein

Selected candidate genes highly expressed in mature trichomes compared to pavement cells

Gene ID	MSU EST ID	Ratio	P-value	Gene Functionn
AT5G13240	MSU01-E6G2T7-1	2.6	0.09	expressed protein
AT3G22440	MSU01-221N3T7-0	14.3	0.04	hydroxyproline-rich glycoprotein family protein
AT2G47980	MSU01-98B4T7-0	2.3	0.1	expressed protein
AT5G45820	MSU01-92F7T7-0	2.8	0.06	serine threonine protein kinase
AT1G48750	MSU01-124N17T7-0	4.1	0.08	protease inhibitor/seed storage/lipid transfer protein (LTP) family protein

3.3 Affymetrix GeneChip hybridization

An attempt to hybridize the amplified transcriptome of 10 single pavement cells to an Affymetrix ATH1 GeneChip representing approximately 24000 Arabidopsis genes was made. However, in vitro transcription of cDNA derived from single cells yielded short cRNA fragments (ranging from about 150 to 550 median size (nt)). Such short cRNAs are inadequate for successful Affymetrix hybridization. Therefore, this experiment was aborted (Fig 3.5).

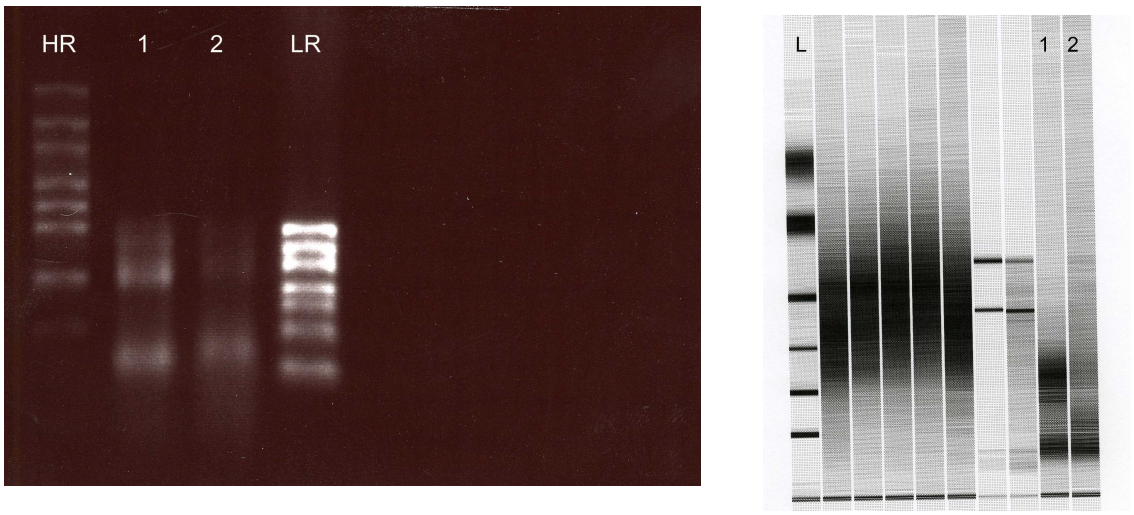

Figure 3.5 Biotin-labeled cRNA derived from 10 single pavement cells
Left: formaldehyde gel: 1, 2: samples; HR, HL: RNA-ladders. HR, band sizes (from bottom): 200, 500, 1000, 1500, 2000, 3000, 4000, 6000 nt; LR, band sizes (from bottom): 100, 200, 300, 400, 600, 800, 1000 nt. Right: Agilent Bioanalyser RNA assay: 1, 2- samples, L: RNA ladder. Band sizes (from bottom): 25, 200, 500, 1000, 2000, 4000, 6000 nt.

3.4 Candidate gene selection and validation of single cell gene expression profiling

During trichome development the DNA content of the nucleus increases through several rounds of endoreduplication (Hülskamp et al., 1994; Hülskamp, 2004; Traas et al., 1998). This process is controlled by several plant hormones, such as auxins, cytokinins, abscisic acid, gibberellins, etc. (Stals and Inze, 2001, see Introduction). Genes involved in cell cycle regulation and hormonal responses that were found to be expressed in trichome initial cells are presented in Table 3.2 (note that the degree of gene expression was not taken into account). Due to the already known predominant role of hormones in trichome development, I subsequently focused on two transcripts related to hormonal signalling: the auxin responsive *At4g27260* (*GH3.5*) gene and gibberellin regulated *At5g15230* (*GASA4*) gene (Table 3.1). *GH3.5* exhibited a high ratio of differential expression when trichome and pavement cells were compared (7.9), whereas the ratio of differential expression was low for GASA4 (2.3; Table 3.1), thus providing an ultimate challenge in terms of confirming the reliability of applied single cell expression profiling approach.

Interestingly, a putative DNA-directed RNA polymerase II (*At3g16980*) was differentially expressed in pavement and trichome initial cells (Table 3.1). Upon a gene expression database query (Genevestigator, AtGenExpress), *At3g16980* showed high expression levels in

Table 3.2 Genes involved in cell cycle regulation and plant hormonal response expressed in trichome initial cells

Note that degree of gene expression was not taken into account. ORF: open reading frame

ORF name	Gene description
Cell cycle	
AT5G08290	yellow-leaf-specific protein 8 (YLS8) / mitosis protein DIM1, putative
AT3G14290	20S proteasome alpha subunit E2 (PAE2)
AT5G58290	26S proteasome AAA-ATPase subunit (RPT3)
AT1G14320	60S ribosomal protein L10 (RPL10A) / Wilm's tumor suppressor protein-related
AT1G66580	60S ribosomal protein L10 (RPL10C)
AT4G37010	caltractin, putative / centrin, putative
AT3G48750	cell division control protein 2 homolog A (CDC2A)
AT3G09840	cell division cycle protein 48 (CDC48A) (CDC48)
AT5G46210	cullin, putative
AT2G27960	cyclin-dependent kinase / CDK (CKS1)
AT1G75950	E3 ubiquitin ligase SCF complex subunit SKP1/ASK1 (At1)
AT3G51800	metallopeptidase M24 family protein
AT5G20010	Ras-related GTP-binding nuclear protein (RAN-1) /// Ras-related GTP-binding nuclear protein (RAN-2)
AT1G04820	tubulin alpha-2/alpha-4 chain (TUA2) /// tubulin alpha-2/alpha-4 chain (TUA4) /// tubulin alpha-6 chain (TUA6)
AT5G41700	ubiquitin-conjugating enzyme 8 (UBC8)
AT1G64230	ubiquitin-conjugating enzyme, putative
Hormonal regulation	
AT2G38120	amino acid permease, putative (AUX1)
AT5G11740	arabinogalactan-protein (AGP15)
AT1G30330	auxin-responsive factor (ARF6)
AT5G20730	auxin-responsive factor (ARF7)
AT1G28130	auxin-responsive GH3 family protein
AT4G27260	auxin-responsive GH3 family protein
AT4G09610	gibberellin-regulated protein 2 (GASA2)
AT4G09600	gibberellin-regulated protein 3 (GASA3)
AT5G15230	gibberellin-regulated protein 4 (GASA4)
AT5G58710	peptidyl-prolyl cis-trans isomerase, putative
AT3G62980	transport inhibitor response 1 (TIR1) (FBL1)

meristematic, flower tissues, cell culture, and seeds. Since this gene was more highly expressed in trichome initials than in pavement cells, it might be involved in cell division and/or early stages of differentiation. Therefore, I endeavored to confirm its differential expression in developing tissue using an alternative method. Together, *At4g27260* (*GH3.5*), *At3g16980* and *At5g15230* (*GASA4)* (Table 3.1) were selected to substantiate microcapillary approach applied in this work by a second set of experiments. Furthermore, confirmation of expression of these candidates in trichome initials will contribute to a more precise elucidation of processes that are involved in trichome development and thus aid in assigning functions to still unknown genes.

3.4.1 Real-time RT-PCR

In order to substantiate the reliability of the microarray data, a real-time RT-PCR protocol developed in our group for single leaf epidermal cell samples was applied. cDNA synthesized from 10 single pavement and trichome initial cells per cell type per sample were used as a template for a real-time RT-PCR.

For the auxin-responsive *GH3.5* gene increased expression in trichome initials was confirmed using this method. The primer pair designed for *GH3.5* cDNA produced a single DNA product of the expected size (96 bp), as shown on Fig 3.6a. Ratios of differential expression of *GH3.5* were calculated for two replicates using the equation described in Materials and Methods. The values of these ratios were 56.72 and 52.14 (Fig 3.6b).

However, due to technical difficulties associated with the low degree of differential expression (Table 3.1) I could not confirm differential expression of *At3g16980* (putative DNA-directed RNA polymerase II) and *At5g15230 (GASA4)* by this method. Therefore, I used promoter::GUS fusions to substantiate the microarray-derived expression profiles of these two candidate genes.

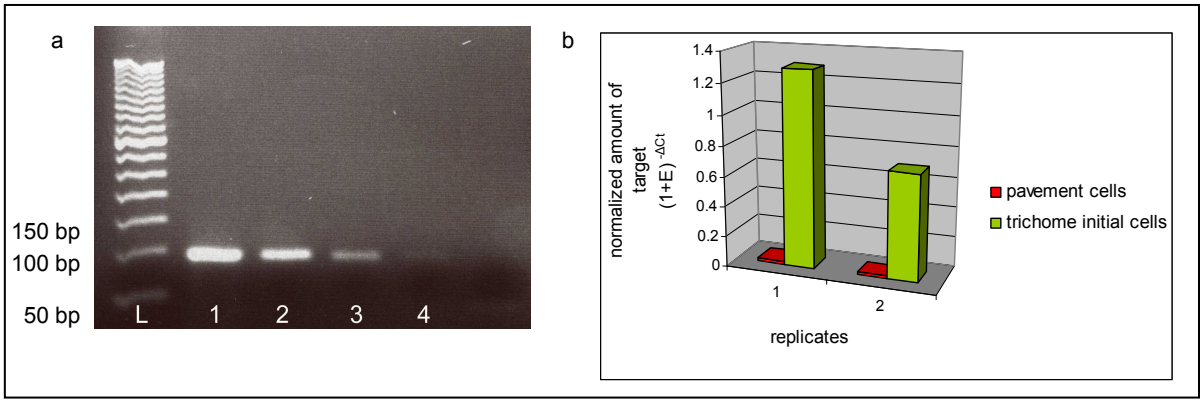

Figure 3.6 Results of the single cell real-time RT PCR
a) separation of RT-PCR products on 4% (w/v) agarose gel. The primer pair for GH3.5 yields the single product of the expected size (96 bp). L: ladder (size standards in base pairs (bp) are indicated at the left); 1: whole leaf cDNA and 2: whole leaf cDNA diluted 1:10 were used as a positive control; 3: PCR product derived from 10 single trichome initial cells; 4- PCR product derived from 10 single pavement cells. **b**) expression of *GH3.5* in pavement and trichome initial cells as measured by RT-PCR in two replicates.

3.4.2. The construction of promoter::*GUS* plant lines

The expression pattern of *GASA 4* has been already characterized by Aubert et al. (1998). However, these authors performed their analyses using the almost glabrous C24 ecotype of Arabidopsis. Therefore, I decided to complement their work by looking at the potential involvement of *GASA4* in trichome development. For production of the *GASA4* promoter::*GUS* construct, I fused a larger region of the promoter than was used in the previous study (2065 bp upstream of the start codon instead of 890 bp) which potentially allowed the inclusion of more regulatory elements.

To examine the expression pattern of the putative RNA polymerase II (*At3g16980*) and *GH3.5* (*At4g27260*) in detail, transgenic promoter::*GUS* lines were produced. GUS expression was tested by histochemical staining of the T2 progeny of plants transformed with p*At3g16980*::*GUS*, p*At5g15230 (GASA4)*::*GUS* and p*At4g27260 (GH3.5)*::*GUS* constructs in the course of their development (from 6-day-old seedlings up to 28-day-old mature flowering plants, see Table 3.3 and Fig 3.7- 3.11).

In 6-day-old seedlings, GUS-staining was localized in the vegetative meristem of all transformants (Table 3.3, Fig 3.7, Fig 3.8). Basal regions of hypocotyls exhibited stronger staining in *GH3.5* plants than p*GASA4*::GUS transformants. *At3g16980* plants showed the weakest hypocotyl staining. Promoter activity was observed in lateral roots of *pAt3g16980::GUS* and in the entire root of *pGASA4::GUS* and *pGH3.5::GUS* plants (Fig 3.7, Fig 3.8). Roots of *GH3.5* transformants showed more intensive GUS-staining (Table 3.3). Furthermore, I detected GUS-staining in trichomes on the first two leaves of all plant lines (Fig 3.7 g, h; Fig 3.8, d). Staining was slightly more intense in *GH3.5* and *pGASA4::GUS* plants than in *At3g16980* plants.

On day 9 staining of hypocotyls became less pronounced (to a smaller extent in *pGH3.5::GUS* plant lines). In contrast, promoter activity remained almost unchanged in the vegetative meristematic region in *GASA4* and *At3g16980* plant lines.

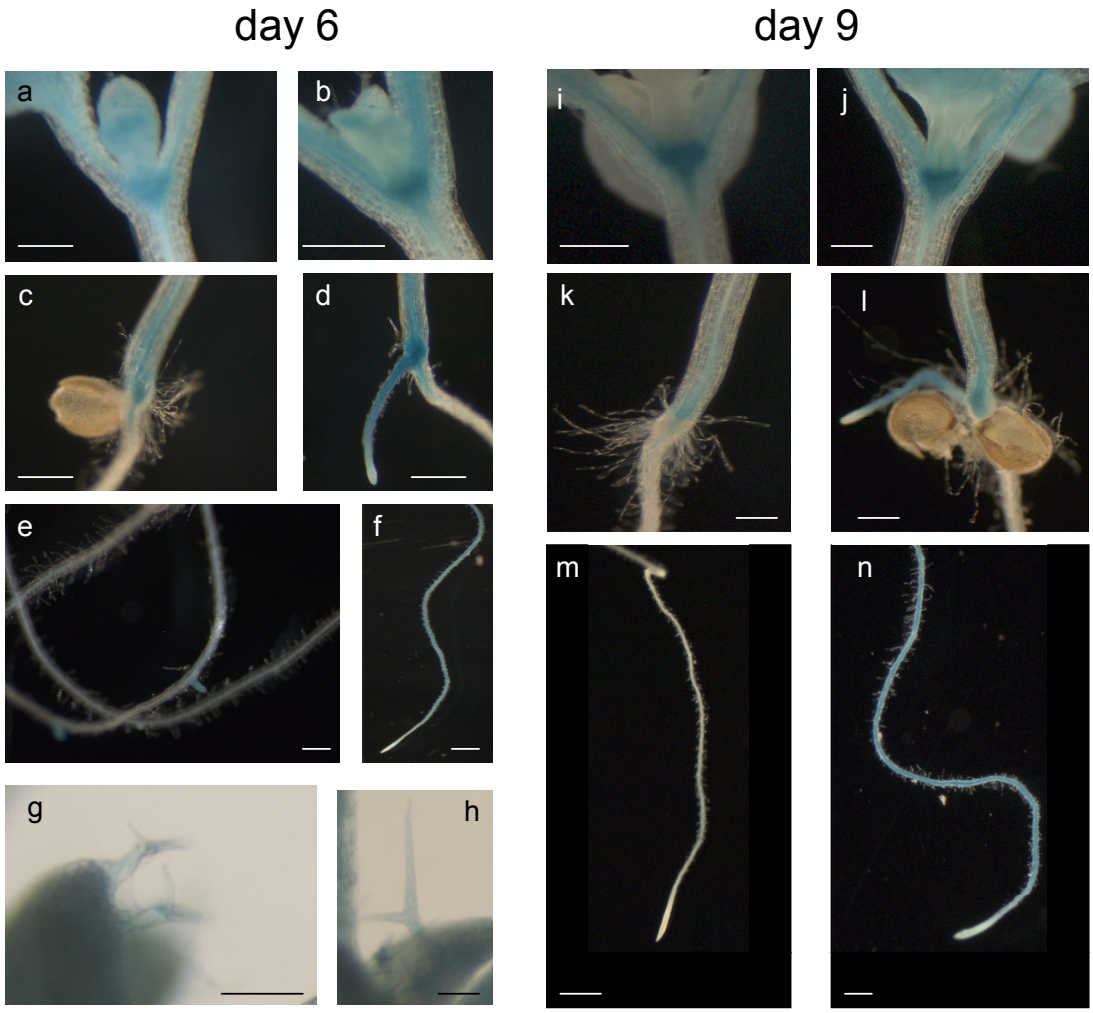

Figure 3.7 GUS staining in p*At3g16980::GUS* and p*GASA4::GUS* transformants at day 6 and day 9
a, c, e, g, i, k, m: *pAt3g16980::GUS*; b, d, f, h, j, l, n- *pGASA4::GUS*;
a, b, i, j- vegetative meristem; c, d, k, l: root-shoot boundary at the base of hypocotyl; e, f, m, n: roots; g, h: trichomes. Scale bars 200 µm.

In turn, in *GH3.5* transformants at this stage of development, GUS-staining appeared to be detectable also in young leaf primordia (Fig 3.8 e, f). Furthermore, the GUS signal was hardly detectable in roots of *pAt3g16980::GUS*, but was still intense in *GASA4* lines and became only slightly lesser pronounced in the roots of *pGH3.5::GUS* plants (Fig 3.7 m, n; Fig 3.8 g; Table 3.3). At this developmental stage staining was still detectable in leaf trichomes of all plant lines.

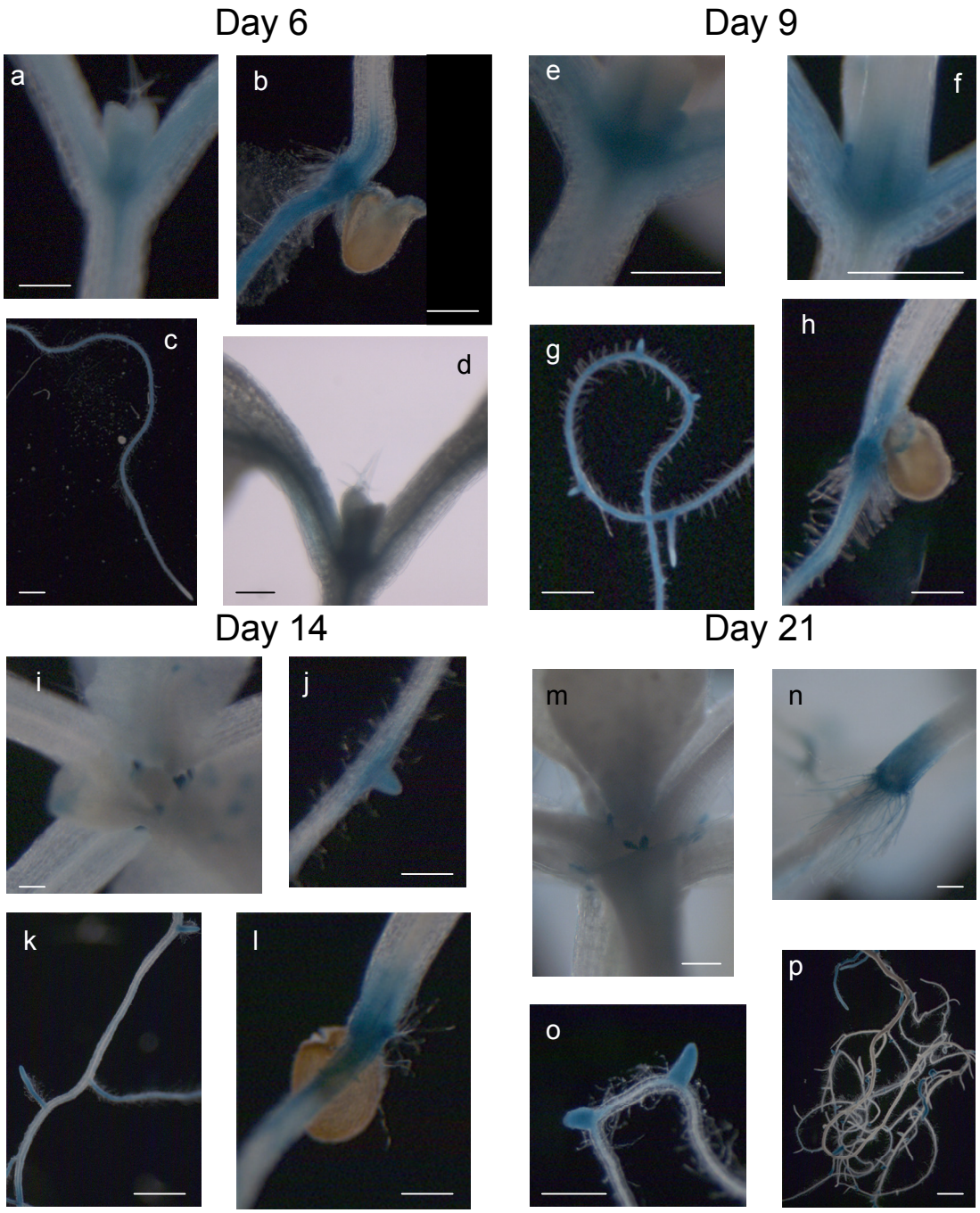

Figure 3.8 GUS staining in *pGH3.5::GUS* transformants at days 6 to 21
a, e, f, i, m: vegetative meristem and leaf primordia; b, h, l, n: root-shoot boundary at the base of hypocotyl; c, g, k, p: roots; j, o: lateral roots; d: trichomes on the first pair of true leaves. Scale bars: 200 µm, except of k, p: 1000 µm.

On day 14 staining was again still active in the vegetative shoot meristem of *GASA4* and *At3g16980* lines. However, in *GH3.5* plants the GUS signal in this region was localized solely to rosette leaf primordia (Fig 3.8 i). At this stage, GUS staining almost disappeared at the root-shoot boundary of *pAt3g16980::GUS* whereas it remained unchanged in *pGASA4::GUS* and *pGH3.5::GUS* transformed plants (Fig 3.8 l; Fig 3.9 a, b; Table 3.3). At this time GUS expression was no longer detectable in the roots of *pAt3g16980::GUS* plants, but became limited

to lateral roots in *GASA4* and *GH3.5* lines. In *GH3.5* plant lines GUS staining in this and following stages was especially intense in incipient and developing lateral roots (Fig 3.8 k, o, p). In later stages of development (days 21 through 28) the GUS expression pattern did not change significantly with one exception: it completely disappeared from the root-shoot boundary of *pAt3g16980::GUS* plants, became less pronounced in *pGH3.5::GUS* plants, and was only slightly visible in this area in the *pGASA4::GUS* lines (Fig 3.8 n; 3.9 e, f; Table 3.3).

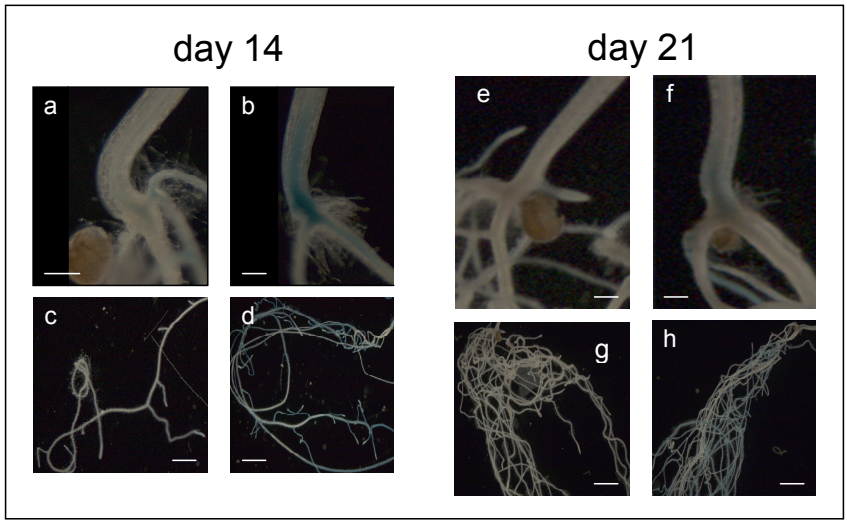

Figure 3.9 GUS staining in *pAt3g16980::GUS* and *pGASA4::GUS* transformants at day 14 and day 21
a, c, e, g: *pAt3g16980::GUS*; b, d, f, h: *pGASA4::GUS*; a, b, e, f: root-shoot boundary at the base of hypocotyl; c, d, g, h: roots. Scale bars a, b: 200 µm; c, d: 1000 µm; e, f: 250 µm; g , h: 1000 µm.

During reproductive development I detected GUS activity in the style of unopened buds in *At3g16980* and *GASA4* plants, as well as in this area in later stages of flower development in all three lines (this activity was intensively pronounced in *pAt3g16980::GUS* plants and, to a lesser extent, in *GASA4* and *GH3.5* plants). Furthermore, GUS staining was detected in anthers of plants in the *GH3.5* and *GASA4* lines (Fig 3.10). Staining of the stigmatic papillae was less intensive in *pGASA4::GUS* and *pGH3.5::GUS* plants when compared to *At3g16980* plant lines. I also observed GUS-staining on the top and at the base of the siliques of all plant lines (Fig 3.10 e, f, i).

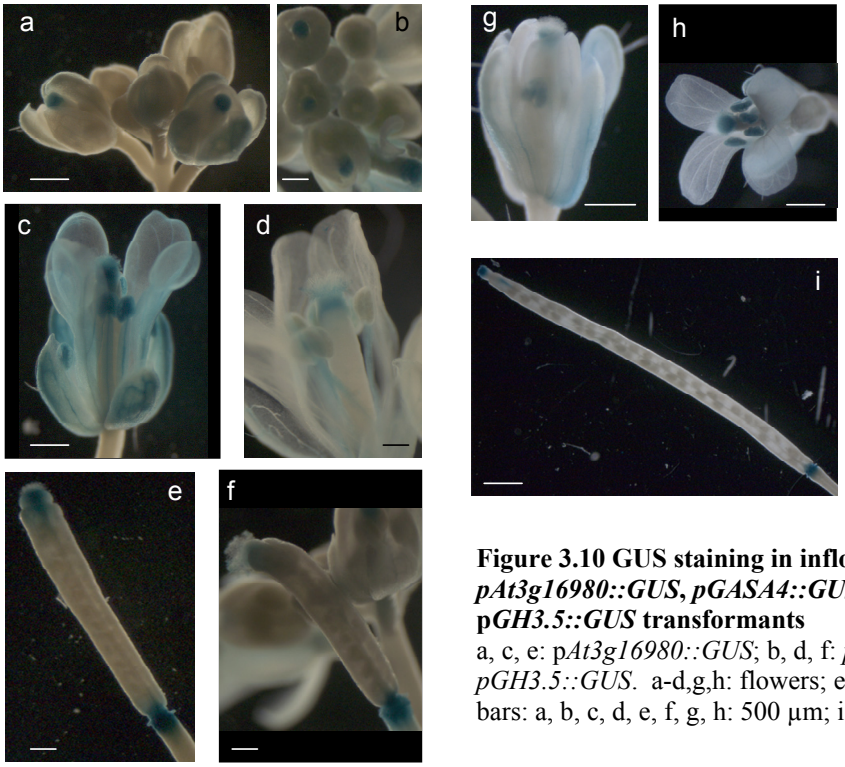

Figure 3.10 GUS staining in inflorescence of *pAt3g16980::GUS*, *pGASA4::GUS*, and p*GH3.5::GUS* transformants
a, c, e: p*At3g16980::GUS*; b, d, f: *pGASA4::GUS*; g,h,i- *pGH3.5::GUS*. a-d,g,h: flowers; e, f,i: siliques. Scale bars: a, b, c, d, e, f, g, h: 500 µm; i: 1000 µm

Table 3.3 GUS staining patterns in the vegetative meristem, root-shoot boundary at the base of hypocotyl and roots of p*At3g16980*::*GUS*, p*GASA4*::*GUS* and *pGH3.5*::*GUS* transformants

	Vegetative meristem			Root- shoot boundary (base of hypocotyl)			Roots		
	At3g16980	*GASA4*	*GH3.5*	*At3g16980*	*GASA4*	*GH3.5*	*At3g16980*	*GASA4*	*GH3.5*
Day 6	++	++	++	+	++	+++	++ (lateral)	++	+++
Day 9	++	++	++*	+	+	+	+	++	++
Day 14	++	++	-*	+/-	+	+	-	++ (lateral)	++ (lateral)
Day 21	++	++	-*	-	+/-	+	-	++ (lateral)	++ (lateral)

*- GUS staining shifted to the rosette leaf primordia

On day 11 of plant development, rosette leaves were detached and stained for GUS expression (Fig 3.11). In these leaves, GUS-staining was localized in developing trichomes in the bulging stage of their development as well as in mature trichomes. The signal was slightly more intensive in trichomes of *pGASA4::GUS* and *pGH3.5::GUS* plants. Weak staining was also

observed in certain regions of underlying tissues. In the leaves in later stages of development, staining was still detectable during the early stages of trichome development of all plant lines. However, in mature trichomes it was observed in *pGASA4::GUS* lines whereas was not detectable in *pAt3g16980::GUS* and *pGH3.5::GUS* plants (Fig 3.11 f-k).

It is noteworthy that the localization of GUS staining to early stages of trichome development in all plant lines confirmed the reliability of the microarray data. Furthermore, it is consistent with *GL2* expression in the *pGL2::GFP* transgenic plants that were used for single cell sampling (Fig 3.1, Fig 3.11). To this end, promoter::*GUS* expression studies and real-time RT-PCR confirm the applicability, usefulness, and reliability of applied single cell transcript profiling and suggest that the selected candidate genes are involved in trichome development.

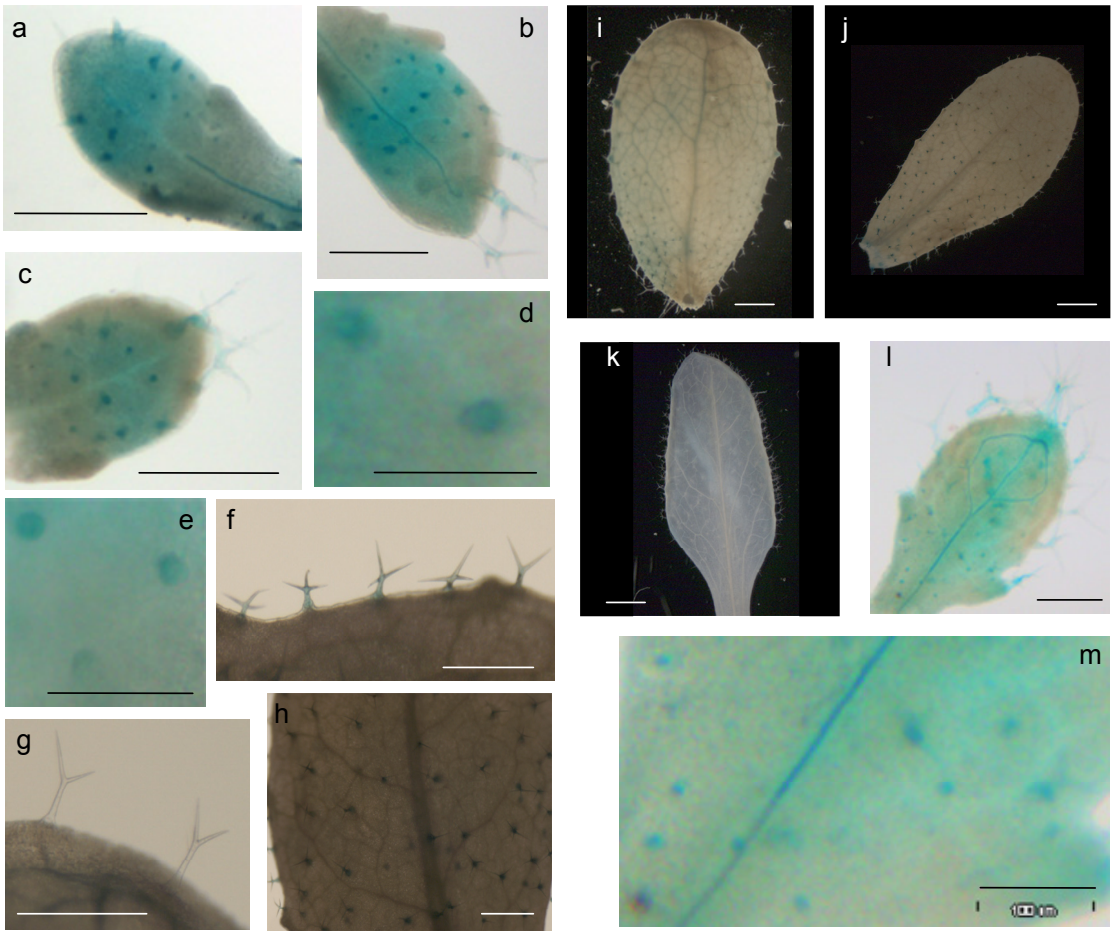

Figure 3.11 GUS staining in leaf trichomes of pAt3g16980::*GUS*, p*GASA4*::*GUS* and p*GH3.5*::*GUS* transformants
a, c, e, g, i: pAt3g16980::*GUS*; b, d, f, h, j: p*GASA4*::*GUS*; k, l, m: p*GH3.5*::*GUS*. a-e, l, m: rosette leaves on day 11; f- k: mature leaves. Scale bars: a-c: 250 µm; d,e- 100 µm; f, g:500 µm, h, i, j, k: 1 mm; l-250 µm; m: 100 µm.

3.5 Knockout and RNAi plant lines

To determine the possible roles of three selected candidate genes may play in trichome development and cell cycle regulation, KO plant lines were ordered from publicly available stocks (see Materials and Methods). In addition RNAi constructs available in the Agrikola collection (www.agrikola.org; Hilson et al., 2004) were used to create transgenic plant lines with altered transcription activity for these genes.

The presence of a T-DNA insert in the genome of SALK_151766 plants was verified using PCR (Fig 3.12; 3.13). The insert was localized to the third exon of *At4g27260*.
The absence of *GH3.5* expression in this plant line was also confirmed using RT-PCR (Fig 3.13) – no gene transcript could be detected. The *At3g16980* T-DNA insertion plant line was analyzed in the same ways.

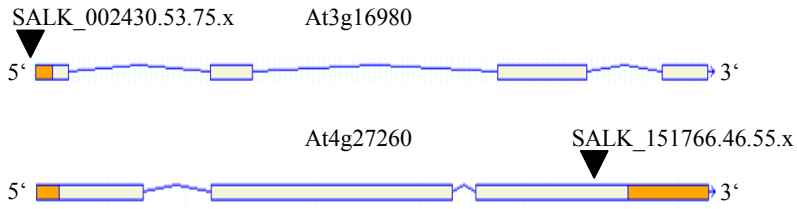

Figure 3.12 T-DNA insertion sites in *At3g16980* and *At4g27260* (*GH3.5*) - indicated by arrowheads. In *At3g16980* insertion is localized to the promoter region, in *GH3.5*- to the third exon.
Yellowish boxes: exons, arcs: introns, orange boxes- UTRs (www.atidb.org)

However, while PCR performed using genomic DNA as a template verified the presence of the insert in the desired location (the promoter region), the gene was nevertheless expressed. Moreover, the transcript was produced at even higher levels than in wild type plants (Fig 3.13 d).

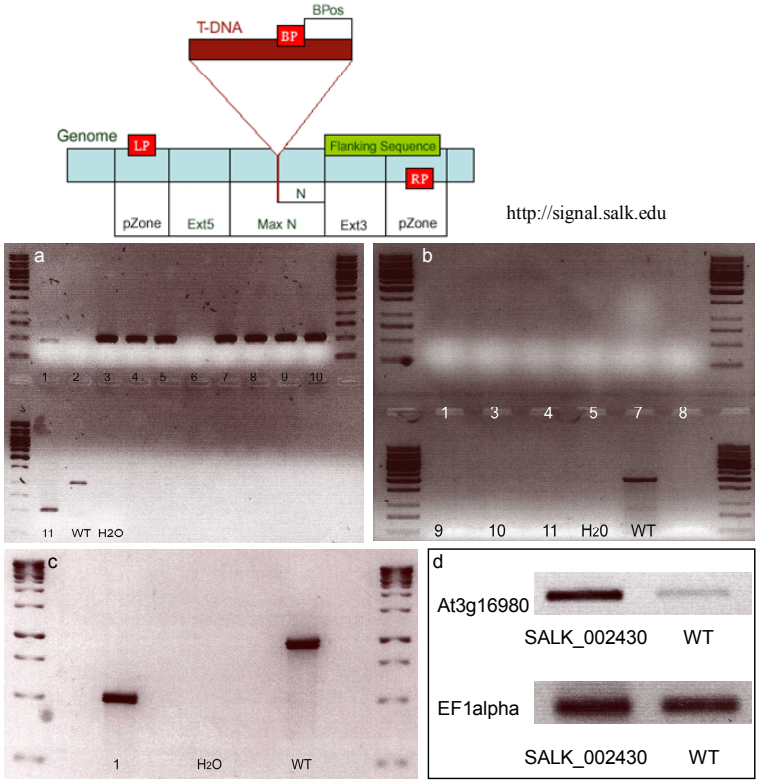

Figure 3.13 Verification of the T-DNA insertion position in the genomes of SALK_151766 (*gh3.5*) and SALK_002430 (*At3g16980*) plant lines using PCR 1% (a-c) and 4% (d) (w/v) agarose gels.
a: PCR performed with genomic DNA of SALK_151766 plants as a template. Combination of primers flanking insert position and primer, specific for insertion is used (see scheme above). All samples (except of N2 and N6) showing product of desired length (508 bp, amplified between BP and RP primer positions) and absence of wild type product (LP+RP primers), confirming correct T-DNA insertion position and homozygozity of the line. DNA of the wild type plant included as a control. **b:** *GH3.5* expression examined in SALK_151766 plants. Whole plant total RNA was used for RT PCR. All plants show absence of *GH3.5* expression. RNA of the wild type plant is included as a control. **c:** genomic DNA of one of the SALK_002430 plants was used for verifying the position of T-DNA insert. Reaction setup like in a. Plant N1 is homozygous, WT gDNA included as a control. **d:** higher expression of *At3g16980* in SALK_002430 plant N1 comparing to the wild type. Total RNA used as a template for the semi- quantitative PCR, *EF1α* used as a loading control
Band sizes (from bottom): 250, 500, 750bp; 1; 1,5; 2; 2,5; 3; 3,5; 4; 5; 6; 8; 10kb

Other plant lines with insertions in *GH3.5* and *At3g16980* (GT_5_92613 and SALK_032670, respectively) were also ordered and examined for T-DNA and transposon insertions and homozygosity. However, attempts to determine the insertion positions in the genome of these plant lines failed and all of the plants examined have been shown to express the targeted genes. This was also the case for knockout plant lines targeting *GASA4* gene. These were the lines GT_5_20762, SALK_042431 and GABI_218B05. Interestingly, SALK_042431 line was later characterized by Roxrud et al. (2007). I contacted the corresponding author, Prof Hilde-Gunn Opsahl-Sorteberg from the Norwegian University of Life Sciences, and asked for the seeds of homozygous plants of the SALK_042431 line.

In order to obtain more information about the possible functions of the selected candidate genes in trichome development I decided to apply a gene silencing approach,

specifically, post-transcriptional gene silencing (PTGS- in plants or RNA interference in other organisms) (Hannon, 2002; Waterhouse and Helliwell, 2002). The advantage of this method is the possibility to more precisely target a single gene of interest and study the function of duplicated or highly homologous genes, which could be members of one gene family (see Discussion). Two of candidate genes are in fact members of gene families. *GH3.5* is a member of the GH3 family (Nakazawa et al., 2001; Sorin et al., 2006; Staswick et al., 2002, 2005) and *GASA4* is one of the fourteen members of the GASA family (Roxrud et al., 2007).

RNAi constructs with gene-specific tags (GST) for *GH3.5* (CATMA4a28840) and *GASA4* (CATMA5a13515) were obtained from the Agrikola collection. Unfortunately, no RNAi construct for *At3g16980* was available in this collection. For unknown reasons the propagation of bacteria from one of the glycerol stocks from the Agrikola collection, (the CATMA5a13515 GST construct) failed. Therefore I wasn't able to analyze the effects of *GASA4* PTGS. In order to find other possible targets for GST that were specific for *GH3.5* among GH3 gene family, a BLAST search was performed with appropriate GST. The *GH3.5*-specific GST (CATMA4a28840) showed, as expected, 100% identity with the *GH3.5* sequence and 70% identity with the *GH3.6 (DFL1)*, a close relative of *GH3.5* (Staswick et al., 2002; 2005). However, it is unclear if *GH3.6* could be another target of this GST, because 70% identity is the threshold above which cross-hybridization is detected in microarray experiments, hence interaction of siRNA and mRNA could take place (Girke et al., 2000; Hilson et al., 2004; Richmond et al., 1999)

Plants transformed with a vector containing GST for *GH3.5* were checked for the presence of GST in the genome (Fig 3.14). The presence of both strands of the GST was confirmed by PCR using appropriate vector-specific primers (see Materials and Methods). However, due to the time constraints it was not possible to quantify the level of *GH3.5* silencing in these plant lines.

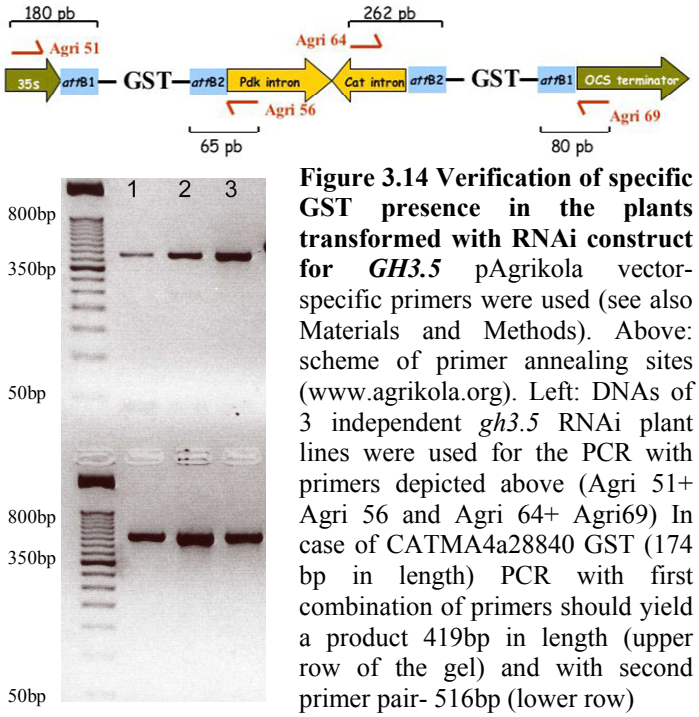

Figure 3.14 Verification of specific GST presence in the plants transformed with RNAi construct for *GH3.5* pAgrikola vector-specific primers were used (see also Materials and Methods). Above: scheme of primer annealing sites (www.agrikola.org). Left: DNAs of 3 independent *gh3.5* RNAi plant lines were used for the PCR with primers depicted above (Agri 51+ Agri 56 and Agri 64+ Agri69) In case of CATMA4a28840 GST (174 bp in length) PCR with first combination of primers should yield a product 419bp in length (upper row of the gel) and with second primer pair- 516bp (lower row)

3.5.1 Phenotypic analysis of knockout and RNAi plant lines

As a next step, I tried to estimate the influence of knockout or silencing of the candidate genes on trichome development and general plant performance. In order to achieve this goal, morphological analysis was performed on both macro- and microscopic levels during the course of plant development. During microscopic investigation of the leaf trichomes, special attention was paid to the morphology of the trichomes and trichome density on the leaf. One general observation emerging from this analysis was that mutations in the genes of interest do not strikingly affect either trichome morphology or leaf trichomes spacing (density) (see below).

The phenotype of SALK_042431 plants (*gasa4*) was described by Roxrud et al. (2007, see above). These investigators reported an increase in the number of axillary inflorescence shoots produced prior to flower formation. Plants carrying a T-DNA insertion in *At3g16980* (SALK_002430) showed no obvious phenotypic changes when compared to the wild type plants in the same stage of development (Fig 3.15a). In contrast, *gh3.5* plants (SALK_151766 T-DNA insertion line) showed an obvious dwarf phenotype (Fig 3.15b). Phenotypes of the plants of both mutant lines didn't change significantly during development. In contrast, plants transformed with RNAi construct for *GH3.5* showed slight changes during development (Fig 3.16). Five-week-old plants were obviously smaller when compared to the wild type plants (Fig 3.16a). This was also the case for these plants when they were six and

seven weeks old (Fig 3.16 b, c). However, at week 8, the difference in size of the plants between wild type and mutants was no longer as striking as before (Fig 3.16d).

Figure 3.15 Phenotype of the plants carrying T-DNA insertion in *At3g16980* gene (SALK_002430) and *gh3.5* plants (SALK_151766) a: SALK_002430: the plants are 8 weeks old. 1- wild type plant; 2- mutant plant; **b:** SALK_151766: 7 week old plants. 1, 2, 3- wild type plants, 4, 5, 6- *gh3.5* plants

Figure 3.16 Phenotype of the *gh3.5 RNAi* plants during their course of development
Left side: three wild type control plants; right side: mutant plants
a- 5; b- 6; c- 7; d- 8 weeks of development

I counted trichomes on the adaxial surface of the rosette leaves of the plants of all four mutant lines at 4 weeks post germination. The amount of trichomes per leaf was normalized

to total leaf area thus indicating leaf trichome density. I observed no significant alterations in leaf trichome density of any plant lines when compared to wild type (Table 3.4).

In addition, I explored leaf trichome morphology microscopically in mutant plants. For instance alteration of endoreduplication in growing trichomes guides to changes in trichome branches amount. It is known that changes in trichome ploidy level positively correlate with the number of trichome branches (Hülskamp et al., 1994; Jacobsen et al., 1996; Perazza et al., 1999). However, no alterations in trichome morphology were observed in mutant plants.

Table 3.4 Rosette leaf trichome density (per mm^2 of adaxial surface) in mutant plant lines in comparison to the wild type control plants; ns- not significant

Plant line	Average amount of the trichomes on the adaxial side of the rosette leaf per mm^2	P- value
WT Col-0	1.11	-
SALK_002430 (*at3g16980*)	1.013	ns
SALK_151766 (*gh3.5*)	1.041	ns
SALK_042431 (*gasa4*)	0,76	ns
RNAi (*gh3.5*)	1.12	ns

3.6 Metabolite profiling of *gh3.5* mutants (SALK_151766 T-DNA insertion line)

GH3.5 is a member of the GH3 gene family and is involved in maintaining auxin homeostasis in plants (Nakazawa et al., 2001; Sorin et al., 2006; Staswick et al., 2002, 2005; see Discussion). Since *gh3.5* plants exhibited a dwarf phenotype (or delay in growth in case of RNAi PTGS), I decided to investigate the effects of KO of this gene on plant metabolism using metabolic profiling via gas chromatography-mass spectrometry (GC-MS). However, only minor differences in metabolite profiles of SALK_151766 plants were detected when compared to wild type plants. The resulting data are presented in Table 3.5 and Fig 3.17. It is noteworthy that none of the metabolites were present at levels higher than three-fold, even when statistically significant (P- value ≤ 0.05) differences between mutant and wild type were evident. The highest value detected was 2.6-fold (Table 3.5). This suggests only minor (if any) influence of *GH3.5* alone on plant metabolism (see Discussion).

Table 3.5 Fold changes of the metabolite content between *gh3.5* plant line and wild type control plants

P≤ 0.05; average fold change values ± s.d. for 15 replicates are presented

Metabolite	Fold change (gh3.5 vs. WT)
beta-D-Glucopyranose	2.58± 0.26
Threonine	1.81± 0.17
Serine	1.75± 0.18
Trehalose	1.74± 0.18
Succinic anhydride	1.60± 0.15
N/A	1.59± 0.09
Phenylalanine	1.56± 0.13
Glycine	1.45± 0.13
Galactonic acid	1.38± 0.10
Sucrose	1.36± 0.08
N/A	0.73± 0.12
N/A	0.57± 0.24
1-(3,7-Dimethyl-1,2,3,4-tetrahydro-2-naphthalenyl)-4-methylpiperazine	0.54± 0.13

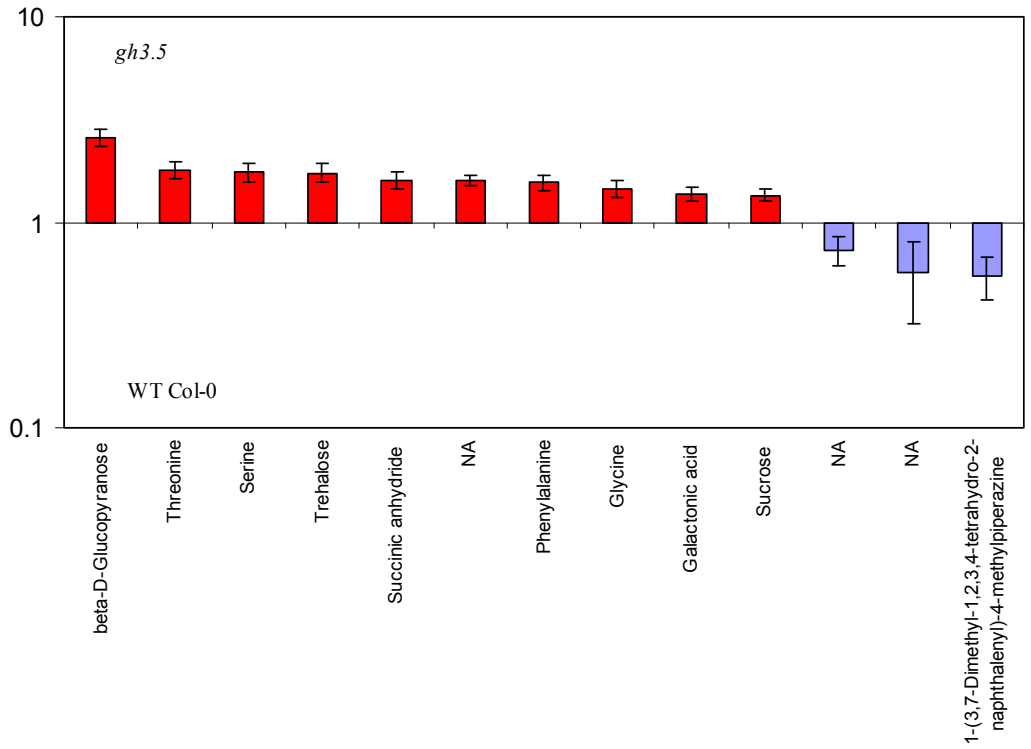

Figure 3.17 Changes in metabolite content in *gh3.5* (SALK_151766) when compared to wild type control plants GC-MS data are presented as average fold change on a logarithmic scale; red bars- higher content in *gh3.5* plants; lilac bars- lower content in mutant plant line compared with wild type plants. P≤ 0.05

3.7 In silico analysis of promoter cis-regulatory elements of candidate genes

To analyze the gene expression profiling data further I searched for common cis-acting elements (transcription factor binding sites) among the promoter regions of the genes preferentially expressed in trichome initial cells in silico. This promoter query was preformed using the PlantPag tool (http://plantpag.mpimp-golm.mpg.de/). This web-based tool allows information about the presence and frequency of cis-acting elements in the promoter regions of genes of interest to be retrieved from external databases. Initially, I screened the promoter regions of the candidate genes *At3g16980*, *At5g15230 (GASA4)* and *At4g27260 (GH3.5)* for common cis-elements. Several elements were found in the promoters of all three genes (see below).

Several genes involved in trichome patterning and negative regulators of trichome development exhibit transcription factor activity. Among them, *GL1* and *WER* belong to the *MYB* gene family, whereas *GL3* and *EGL3* encode BHLH factors and TTG1 is a member of the WD-40 protein family. The negative regulators TRY, CPC and ETC1 all belong to single-repeat MYB proteins that have no obvious transcription activation domain (Hülskamp, 2004; Schellmann and Hülskamp, 2005). Based on this information, I specifically searched for MYB and BHLH factors binding sites in the promoter regions of the 38 genes I found to be preferentially expressed in trichome initials, including *At3g16980*, *At5g15230 (GASA4)* and *At4g27260 (GH3.5)*. No transcription factor binding sites for BHLH could be identified. However, I discovered various MYB-binding sites with high abundance in the promoter regions of genes preferentially expressed in trichome initial cells (Table 3.6; 3.8).

One of these MYB binding sites was identical to one found in the promoter of the *Arabidopsis thaliana cyclin B1:1* gene (MYBCOREATCYCB1, Planchais et al., 2002). Interestingly, binding sites for MYB transcription factors involved in abscisic acid signalling and drought response were also present within the promoter regions of the 38 genes preferentially expressed in trichome initial cells (MYB1AT, MYB2AT, MYB2CONSENSUSAT, see Table 3.6). Another MYB binding site (MYBGAHV) identified in the promoter regions of 17 of the 38 genes (including *GASA4* and *GH3.5*) was described as a gibberellin responsive element in barley and rice (Gubler et al., 1995; Morita et al., 1998). The distribution of MYB binding elements within the promoters of *At3g16980*, *GASA4*, *GH3.5* and all 38 genes more highly expressed in trichome initials is shown in Table 3.6.

Table 3.6 Distribution of MYB binding sites in promoter regions of 3 (*At3g16980*, GASA4, GH3.5) and 38 candidate genes preferentially expressed in trichome initial cells

	At3g16980	GH3.5	GASA4	Absolute number of this binding site in the query set of 38 genes	Number of promoter sequences in query set of 38 genes containing this binding site
MYB1AT	1	8	9	93	27/38
MYB1LEPR	0	1	0	10	9/38
MYB2AT	0	2	0	13	11/38
MYB2CONSENSUSAT	0	4	5	42	23/38
MYBATRD22	0	1	1	4	4/38
MYBCORE	1	11	7	74	28/38
MYBCOREATCYCB1	0	2	2	37	19/38
MYBGAHV	0	2	3	25	17/38
MYBPLANT	0	1	1	20	16/38
MYBPZM	0	0	0	27	17/38
MYBST1	0	2	3	55	25/38

Interestingly, promoter regions of both *GASA4* and *GH3.5* contained the E2FCONSENSUS binding site described for promoters of potential E2F-DP target genes. Further cis-acting elements involved in hormone perception, metal homeostasis, sulfur response and cell cycle regulation were also identified in the promoters of the 38 genes preferentially expressed in trichome initial cells. These elements are listed in Table 3.7.

Frequencies of a given cis-acting element in the promoter regions of the 38 candidate genes were compared to their occurrence in promoters of the whole genome by applying the automated enrichment analysis function of PlantPag. This function scores the relative abundance of a given cis-acting element within one promoter or set of promoters in comparison to all promoters within the entire genome (for details see Materials and Methods). For instance, the MYBPLANT motif was contained in 16 promoters of the 38 selected candidate genes. Within these 16 promoters it occurred 20 times. Compared to its presence within all promoters of the entire genome this represents a 1.7-fold enrichment of this element in the set of 38 candidate genes (Table 3.8).

Table 3.7 Cis-acting elements found in promoter regions of the 38 genes preferentially expressed in trichome initial cells

The elements are involved in hormonal, metal, sulfur response and cell-cycle regulation (not including MYB elements).

Binding site	Absolute number of this binding site in the query set	Number of promoter sequences in query set containing this binding site	Description; organism
ARFAT	13	9/38	ARF (auxin response factor) binding site found in the promoters of primary/early auxin response genes of Arabidopsis thaliana
ASF1MOTIFCAMV	39	24/38	Involved in transcriptional activation by auxin and/or salicylic acid; Cauliflower mosaic virus, tobacco, Arabidopsis
CATATGGMSAUR	25	18/38	Involved in auxin responsiveness; soybean
CURECORECR	155	30/38	Copper-response element; Chlamydomonas
DPBFCOREDCDC3	41	23/38	bZIP transcription factors, ABA response; carrot, A. thaliana
E2FCONSENSUS	11	10/38	"E2F consensus sequence" of all different E2F-DP-binding motifs in plants; A. thaliana, tobacco,rice, Nicotiana benthamiana
GAREAT	34	20/38	GA-responsive element; Arabidopsis
NTBBF1ARROLB	47	25/38	Required for tissue-specific expression and auxin induction; Agrobacterium rhizogenes
PYRIMIDINEBOXOSRAMY1A	40	24/38	Found in the promoter of barley alpha-amylase gene which is induced in the aleurone layers in response to GA; barley, rice
SEBFCONSSTPR10A	17	14/38	Similar to the auxin response element; Solanum tuberosum
SURECOREATSULTR11	50	24/38	Core of sulfur-responsive element (SURE) found in the promoter of SULTR1;1-high-affinity sulfate transporter gene in Arabidopsis, SURE contains auxin response factor (ARF) binding sequence; this core seq is involved in -S response; Arabidopsis
TATCCAOSAMY	32	18/38	Involved in mediation of sugar and hormone (GA) regulation of alpha-amylase gene expression in rice; rice

Table 3.8 Enrichment of promoter regions of 38candidate genes by most abundant MYB-binding sites and cis- acting elements involved in hormonal, metal, sulfur response and cell-cycle regulation in comparison with whole genome data

Binding site	Absolute number of this binding site in the query set	Number of promoter sequences in query set containing this binding site	Enrichment score (enrichment analysis) in comparison to whole genome (ratio)	P-value
ASF1MOTIFCAMV	39	24/38	1.6140	0.003
CATATGGMSAUR	25	18/38	1.3283	0.1
CURECORECR	155	30/38	N/A	
DPBFCOREDCDC3	41	23/38	1.2506	0.1
E2FCONSENSUS	11	10/38	N/A	
GAREAT	34	20/38	1.1772	0.23
MYB1AT	93	27/38	1.0519	0.4
MYB1LEPR	10	9/38	1.8506	0.04
MYB2AT	13	11/38	1.2479	0.27
MYB2CONSENSUSAT	42	23/38	1.2949	0.07
MYBATRD22	4	4/38	1.2070	0.42
MYBCORE	74	28/38	1.0684	0.35
MYBCOREATCYCB1	37	19/38	N/A	
MYBGAHV	25	17/38	1.2408	0.18
MYBPLANT	20	16/38	1.7641	0.01
MYBPZM	27	17/38	1.6767	0.02
MYBST1	55	25/38	1.1693	0.18
NTBBF1ARROLB	47	25/38	1.3294	0.04
PYRIMIDINEBOXOSRAMY1A	40	24/38	1.2563	0.09
SEBFCONSSTPR10A	17	14/38	1.2235	0.24
SURECOREATSULTR11	50	24/38	N/A	
TATCCAOSAMY	32	18/38	1.4196	0.05

4. DISCUSSION

Trichome development is a model system for studying cell morphogenesis in plants. To the best of my knowledge, this work represents the first attempt at expression profiling at the single cell level during the earliest stage of trichome development. Molecular, genetic, and bioinformatic methods were applied to garner information about the function of candidate genes detected through applied approach.

This work held several major challenges. The first lay in developing a protocol for sampling trichome initial cells, a feat in itself since these cells are morphologically indistinct from pavement cells. Another challenge was the extremely small amount of material to be sampled; samples contained cell sap from as few as ten cells. Finally, established protocol had to be applied for accomplishment of the general task of the project: getting more insight into growth and differentiation of an individual cell, especially at the initial stage of its development.

4.1 Single cell sampling and array hybridization

This study aimed at identifying candidate genes that are differentially expressed during stages of trichome development, especially in trichome initial cells. To achieve this goal, a single cell sampling approach was applied that significantly increases spatial resolution for the study of cell morphogenesis, especially in the context of cell cycle control; this is a vast improvement over studies at the tissue, organ, or organism level. Furthermore, contamination by genetic material of neighboring cell types is excluded completely. Thus, the single cell technique provides a valuable foil for mutant complementation studies, which to date have yielded most of the data concerning cell cycle regulation and trichome development (Hülskamp, 2004; Inze and De Veylder, 2006; Schellmann and Hulskamp, 2005).

To avoid background contamination, trichome initial cells (GFP labeled protodermal cells) were sampled directly using glass microcapillaries (Fig 3.1; 3.2). The method was previously described and proven to yield reproducible and reliable results (Brandt et al., 1999; 2002; Jones and Grierson, 2003; Karrer et al., 1995; Mould et al., 2003). This method is the most suitable for the purposes of this study, since it is fast, accurate, and can be used for intact tissues. Furthermore, it was previously used for collecting samples from leaf tissues (Brandt et al., 1999, 2002).

One of the most significant and novel results of this work was the adaptation of the microcapillary sampling method to the collection of single GFP-labeled trichome initial cells (Fig 3.1). Furthermore, in a manner enabled by early GFP expression, a protocol to harvest a

single cell type at two progressive developmental stages was established. Therefore, a new dimension in cell developmental biology was introduced. It is noteworthy that all previous expression profiling approaches at single cell level have been applied exclusively to mature, finally differentiated cells.

Certain difficulties occur and some general concerns must be taken into account when exploring gene expression at the single cell level (see Introduction). For instance, a limitation in the size of amplified RNA fragments can limit the applicability of some gene expression profiling techniques. It is known that the lower the amount of available mRNA, the shorter the resulting amplified fragments (Feldman et al., 2002; Glanzer and Eberwine, 2004; Spiess et al., 2003). It is likely that the attempt to perform Affymetrix GeneChip hybridization failed for this reason; the size of the fragments obtained didn't reach the threshold for successful hybridization to the Affymetrix ATH1 chip (Fig 3.5). An additional concern is that due to the comparably low signal intensities seen on microarrays when working with single cell extracts, minor differences in transcript levels can lead to relatively high variation in signal intensities as compared to experiments with larger amount of starting material (Brandt et al., 2002 and references therein). However, the method was proven reliable and additional support of its robustness came from the results of real-time RT-PCR and promoter-GUS studies that were performed in order to confirm microarray-derived data. Thus, the challenge of applying an enhanced sampling protocol to answer biological questions was met.

I compared functional categorization of the genes expressed in cells of interest (Fig 3.3) with other results from studies of trichome and pavement cells (Lieckfeldt et al., 2007). This comparison showed a similar distribution of genes expressed in these cells between the functional categories. Therefore, it confirmed the reliability of the single cell profiling approach applied in this work and provided valuable information about functional features of leaf epidermal cells. High numbers of transcripts within the selected epidermal cell types were identified (Fig 3.3), including those participating in cell cycle regulation and plant hormonal responses (Table 3.2). The increases seen in the transcription of genes within the functional abiotic or biotic stimuli and/or stress response category reflects the protective role of the epidermal cells. In particular, trichomes are active in plant defense against herbivores, UV light, reduction of transpiration, freezing tolerance, heavy metal detoxification, etc (Garcia-Hernandez et al., 1998; Gutierrez-Alcala et al., 2000; Hülskamp, 2004 and references therein; Wienkoop et al., 2004). These defense and stress-associated functions are supported by reported here in silico detection of cis-acting elements mediating abscisic acid signaling, drought response, copper homeostasis, and sulfur metabolism (Table 3.6; 3.7).

Visualization of global differences in gene expression of a single cell type at different stages of development provides unprecedented insights into processes of cell differentiation. Using MAPMAN (Thimm et al., 2004) I compared differential gene expression in pavement, trichome initial, and mature trichome cells. In particular, it became evident that the amount of upregulated genes strongly increased during trichome maturation (Fig 3.4). This increase provides a scale for the degree of change in gene expression that occurs during cell expansion and specification. In conclusion, the protocol applied in this work enabled the comparison of adaptations in progressive gene expression profiles during the life cycle of a selected single cell type that is embedded within a multicellular organism. Furthermore, MAPMAN allowed the visualization of differential gene expression within defined functional categories (Fig 3.4). The greater degree of similarity that exists between mature trichomes and pavement cells than between trichome initials and pavement cells is reflected by the increased amount of white bars in the MAPMAN histograms (Fig 3.4 a, b). This elevation in gene expression distance could be due to the initiation of the developmental program associated with trichome initiation in incipient trichomes. However, these histograms clearly document that pavement and mature trichome cells exhibit characteristic specifications in their gene expression profiles.

More specifically, trichome initials exhibit a significant increase in transcripts associated with DNA synthesis and cell cycle propagation relative to pavement cells (Fig 3.4 a). From this result, one can conclude that the cell cycle moves to a new phase within trichome precursors. Moreover, induction of genes associated with DNA synthesis suggests the onset of endocycling. Control of these processes by plant hormones is indicated by the up-regulation of transcripts depicted in the respective category (Fig 3.4 a). In summary, this work documents the specificity in transcript expression associated with individual cell types within the same layer of leaf tissue.

4.2 Candidate gene selection and validation of single cell gene expression profiling

Of the genes that exhibit higher expression levels in trichome initials, three candidates for further analysis were selected: the gibberellin-regulated *At5g15230 (GASA4)* gene, the auxin-responsive element *At4g27260 (GH3.5, WES1),* and a putative DNA-directed RNA polymerase II (*At3g16980*) (Table 3.1).

I used real-time RT-PCR for confirmation of results obtained via microarrays, especially to confirm the higher expression level of the selected candidate genes upregulated in trichome initial cells. While it was possible to verify the higher expression of *GH3.5* in incipient trichomes using this method (Fig 3.6), it failed to do the same for other candidate genes (*GASA4*

and *At3g16980*). This likely occurred due to the low degree of differential expression of both these genes in cell types of interest (Table 3.1). A two-fold difference in gene expression levels is the detection limit for real-time RT-PCR due to random PCR variation. Since this is an amplification-based method, small fluctuations in the starting conditions of a PCR assay will lead to large fluctuation of the product amount, which is expressed in Ct values. Thus seemingly small standard deviations of Ct values are amplified in the analysis because a Ct difference of one represents a two-fold difference in starting amount (Bubner et al., 2004). Additional difficulty with applying real-time RT-PCR to single cell research is a selection of appropriate housekeeping genes, which seems to be a general problem not only of this method, but of many studies which require reference genes usage (Czechowski et al., 2005; Radonić et al., 2004). Low differential expression levels are also hard to quantify using real-time RT-PCR due in part to the binding properties of SYBR Green (Lieckfeldt et al., 2007; Vitzthum et al., 1999), which binds to any double-stranded DNA in the reaction mix, including primer dimers and other non-specific reaction products. This may result in an overestimation of the target concentration.

4.2.1 *GASA4*

Since it has been demonstrated that gibberellin promotes endoreduplication and trichome development, the gibberellin-regulated *At5g15230 (GASA4)* gene could be involved in regulation of endoreduplication within trichomes (Table 3.1; Chien and Sussex, 1996; Jacobsen et al., 1996; Perazza et al., 1998; Telfer et al., 1997). Gibberellins play a pivotal role in trichome development via up-regulation of *GL1* and possibly *TTG*. Both are central genes of the trichome-promoting complex (see Introduction) (Perazza et al., 1998). Several rounds of endoreduplication occur during trichome development (Hülskamp et al., 1994; Inze and De Veylder, 2006; Melaragno et al., 1993). Remarkably, gibberellins promote endoreduplication themselves. In particular, it was demonstrated that in *spindly (spy)* mutants, which exhibit a constitutive gibberellin response, trichomes have a higher than normal DNA content of 64C (Jacobsen et al., 1996; Perazza et al., 1998). On the other hand, in a mutant that is incapable of gibberellin synthesis, *ga1-3*, no trichomes are formed at all (see Introduction).

Taken together with the data above, the localization of *GASA4* to trichome initial cells and its continued expression throughout the stages of trichome development suggests that this gene could be involved in regulation of endoreduplication (Table 3.3, Fig 3.7; 3.11). Localization of *GASA4* expression to meristematic regions was reported previously by Aubert et al. (1998). Interestingly, it was found that in a *ga1-3* (GA-deficient) mutant background, addition of exogenous GAs inhibits *GASA4* expression in expanding cotyledons and leaves,

indicating that *GASA4* is down-regulated in these organs. Additionally, *GASA4* expression in meristematic regions suggests preferential involvement of this gene in processes of cell division rather than cell elongation. Here I detected expression of *GASA4* in trichomes, which have ceased mitotic activity but are undergoing several rounds of endoreduplication (Fig 3.7 h; Fig 3.11 b, d, f, h, j). In concert with data from Aubert et al. (1998), obtained results suggest that *GASA4* plays a dual role both in regulating cell division in meristems and endoreduplication during trichome development. Additional support for this hypothesis emerges from promoter element analysis. In silico screening for cis-elements in the promoter region of *GASA4* revealed the presence of MYB binding sites (see Table 3.6), including one that had been previously annotated as central element of the GA response of several genes in barley and rice (MYBGAHV, Gubler et al., 1995; Morita et al., 1998). This element is present in triplicate in the promoter region of *GASA4*. Taking into account that the central trichome promoting gene GL1 encodes a MYB transcription factor (see above), this finding triggered the idea that GASA4 might play a role in trichome initiation and endoreduplication onset being upregulated by gibberellic acid and/or probably by GL1 in incipient trichomes.

Another interesting finding from the analysis of the *GASA4* promoter is that it contains an E2FCONSENSUS cis-acting element (Table 3.7) thus being a potential E2F-DP target and hence one of the genes required for S-phase entry (De Veylder et al., 2002; Ramirez-Parra et al., 2003; Stals and Inze, 2001; Vandepoele et al., 2005). This supports the involvement of *GASA4* in endoreduplication onset/regulation during trichome development. However, the exact role of *GASA4* (one of the fourteen members of the *GASA* gene family, Roxrud et al., 2007) in cell cycle regulation and trichome development still requires further investigation.

4.2.2 *At3g16980*

The expression of the second candidate gene, *At3g16980*, annotated in the TAIR database as a putative DNA-directed RNA polymerase II, was localized to trichome initial cells (Fig 3.11 a, c, e). This suggests the involvement of *At3g16980* in trichome development, especially in its early stages. Furthermore, expression of this gene was observed in meristematic regions as well as in roots and at the root-shoot boundary region at the base of the hypocotyl in early stages of plant development (until day 14, see Fig 3.7; 3.9) and during inflorescence (Fig 3.10). Due to this expression pattern, I suggest that this gene is involved in cell growth, differentiation, and/or cell cycle regulation in fast growing tissues, in particular at early stages of their development.

Since this putative polymerase had not been functionally characterized, I searched for its expression pattern in public databases. Genevestigator Gene Atlas data indicates a high expression level of *At3g16980* in cell suspensions, seeds, and inflorescence organs. Expression in seeds and inflorescence is also reported by the AtGenExpress Visualization Tool. Moreover, AtGenExpress indicates high expression levels of *At3g16980* in the shoot apex. These data are consistent with the results from promoter::GUS study of the expression of this putative polymerase and support involvement of this gene in early stage developmental processes.

In silico analysis of cis-acting elements in the promoter region of *At3g16980* revealed several transcription factor binding sites that are involved in hormonal responses and cell cycle regulation: these are ARFAT, SEBFCONSSTPR10A (response to auxin), GARE1OSREP1 (gibberellin responsive element), MYB1AT and MYBCORE (Table 3.6; 3.7). Taken together these data suggest that *At3g16980* might be involved in cell development and differentiation: it may target for transcription certain specific genes required for cell growth and differentiation. Presence of the above mentioned transcription factor binding sites in the promoter region of *At3g16980* hints at a possible involvement of this gene in mediating hormonal signals. This certainly may be the case for developing trichomes. Furthermore, this putative polymerase could participate in the regulation of the GH3 gene family (see below) and the gibberellin response via microRNAs.

It is possible that *At3g16980* is involved in microRNA genes transcription since it is known that they are transcribed by RNA polymerase II (Lee et al., 2004). Thus *At3g16980* may be involved in regulation of transcription of *miR160*, which down-regulates *AUXIN RESPONSE FACTOR17* (*ARF17*). ARF17 is a regulator of GH3 genes; it inhibits expression of *GH3.5*, one of the candidate genes explored in this study (Mallory et al., 2005). *At3g16980* can also be a part of GAMYB expression feedback loop. GAMYB is GA- responsive transcriptional regulator that binds specifically to GARE elements in promoters of GA-activated genes (Gubler et al., 1995). GAMYB can up-regulate *At3g16980* to activate the transcription of *miR 159* (microRNA 159), which down-regulates GAMYB (Achard et al., 2004). However, these suggestions about the possible involvement of putative RNA polymerase II (At3g16980) in microRNA pathways are highly speculative and require experimental confirmation. Unfortunately it was not possible to estimate effects of the absence of *At3g16980* expression; however it was serendipitously revealed that overexpression of this gene does not cause any remarkable changes of the phenotype of the plant and doesn't affect trichome development (see Results).

4.2.3 *GH3.5*

Expression of the third candidate gene *At4g27260 (GH3.5, WES1)* in trichome initial cells suggests involvement of this gene in regulation of trichome development. *GH3.5* belongs to the GH3 family of early auxin inducible Arabidopsis genes (Nakazawa et al., 2001; Sorin et al., 2006; Staswick et al., 2002, 2005) that first was described in *Glycine max* by Hagen et al. in 1984. The function of the proteins encoded by phylogenetically related members of this family involves conjugation of auxin to amino acids thus regulating auxin homeostasis. IAA-amino acid conjugates are inactive forms of auxin that are either subsequently degraded or used as a temporary storage reservoir of auxin.

Interestingly, *GH3.5* and its close relative *GH3.6/DFL1* (*Dwarf In Light 1*; Nakazawa et al. 2001) respond to auxin application slightly differently than other GH3 family members (while after auxin addition *GH3.1*, *GH3.2*, *GH3.3*, and *GH3.4* were elevated >10-fold in seedlings, *GH3.5* and *GH3.6* were induced 2.5-fold to 8-fold; Staswick et al., 2005). The protein encoded by *GH3.5* among products of other GH3 family members was identified as highly expressed in auxin-overproducing mutants that caused development of adventitious roots in Arabidopsis (Sorin et al., 2006). Moreover, *GH3.5* was shown to be involved in a stress adaptation response and hypocotyl growth in Arabidopsis (Park et al., 2007 a, b). The latter observation was reinforced by finding concerning *GH3.5* expression in the hypocotyl reported here (Fig 3.8). However, until this work, no reports have been made concerning *GH3.5* performance on the single cell level.

In respect to trichome development, I suggest a similar participation of *GH3.5* in auxin signaling. Auxin-amido synthase encoded by *GH3.5* might temporarily bind auxin to amino acids to create a reservoir of this hormone for subsequent usage in the developing trichome. This hypothesis is consistent with the finding that auxin is required for cell cycle progression and hence might be involved in regulation of endoreduplication (Inze 2005; Inze and De Veylder, 2006; Stals and Inze, 2001; Trehin et al, 1998). Alternatively, auxin could be blocked (at least to some extent) to avoid its mitosis-promoting action. It is known that the highest levels of auxin are normally found in young leaves (which are undergoing high rates of cell division) in comparison to expanding leaves, where cell division has ceased and growth depends solely on cell expansion (Ljung et al., 2001; 2002). This is consistent with the finding that *GH3.5* is actively transcribed in young leaf primordia (Fig 3.8). Performed promoter::GUS studies have shown that from day 9 of plant development on, this gene is expressed in these developing organs (see Results; Fig 3.8 e, f, i, m). Moreover, expression of *GH3.5* in incipient

and developing lateral roots also supports such role of this gene in auxin homeostasis (Fig 3.8 o, p; Table 3.3).

Another possible role of GH3.5 (auxin-amido synthase) in the developing trichome is the transformation of auxin to an inactive form to avoid toxic effect of auxin excess in growing trichome through activation of ethylene biosynthesis (Woeste et al., 1999; Yu and Yang, 1979). It is known that high concentrations of auxin may have a growth inhibiting effect (Foster et al., 1952.) In this scenario, significantly lower concentrations of auxin may cause ethylene production on the single cell level. However, this suggestion is highly speculative because, to date, there have been no reports about the specific role of ethylene in either single cells or in cell cycle regulation. Furthermore, ethylene is thought to depress the polar transport of auxin, thus causing growth inhibition and senescence in tissues and organs (Polevoy, 1989).

In summary, *GH3.5* may provide "fine tuning" of auxin concentrations in trichome initial cells in order to regulate its action during the progression towards endoreduplication cycles. It could also be related to stress responses in trichomes since it is known that they are involved in certain stress reactions (see above). In turn, *GH3.5* was shown to participate in both abiotic and biotic stress responses through regulation of auxin homeostasis (Park et al., 2007 a, b). Furthermore, expression of this gene is induced not only by auxin but also by salicylic and abscisic acids (Park et al., 2007 a). The latter is consistent with the promoter analysis data obtained here (cis-acting elements involved in SA and ABA response were detected in promoters of certain candidate genes, including *GH3.5* (see above; Table 3.6; 3.7; partially not shown)).

In a manner similar to the promoter of *GASA4,* the promoter region of *GH3.5* contains E2FCONSENSUS sequence (see above) and additionally an E2FAT element-binding site found in many potential E2F target genes (Ramirez-Parra et al., 2003) (Table 3.7; 3.8). This finding also suggests involvement of this gene in regulation of cell cycle progression. In this scenario, expression of *GH3.5* switches on in S-phase of cell cycle and *GH3.5* encoded amido synthase blocks auxin eliminating its mitosis-promoting action thus allowing the cell to omit mitosis. However, a more precise estimation of *GH3.5* function is difficult because of the overlapping and redundancy of functions within the GH3 gene family in Arabidopsis (Nakazawa et al., 2001). This is true not only for this gene family, but for the whole Arabidopsis genome as well as for many other eukaryotic genomes (Bouché and Bouchez, 2001). Latter statement is supported by the analysis of *GH3.5* knockout and RNAi lines as well as by performed metabolite profiling (see below).

4.3 Analysis of knockout and RNAi plant lines

Reverse genetic approaches seek to find the possible phenotypes that may derive from a specific gene. These approaches are a subset of functional genomics methods devised to interfere with normal gene activity, in particular by abolishing gene function, e.g. by knockout or gene silencing (Alonso et al., 2003; Hannon, 2002; Hilson et al., 2004; Waterhouse and Helliwell, 2003).

Gene knockouts are a major reverse genetics tool aimed at revealing the function of genes discovered through large-scale sequencing programs. The method of production for loss-of-function mutations by T-DNA or transposon mutagenesis has several advantages (Parinov and Sundaresan, 2000). These are high probability of the complete inactivation of a gene and possibility for identification of the plants carrying an insertion by means of PCR screening or sequencing of the DNA flanking an insertion. Moreover, T-DNA directly generates stable insertions into genomic DNA and does not require additional steps to stabilize the insert. In turn, a transposon can be excised from the disrupted gene in the presence of transposase, with the resulting reversion of the mutation. This provides a simple means to confirm that an observed mutation is tagged by the transposon. Disadvantages of T-DNA mutagenesis include the complex patterns of insertion integration, including transfer of vector sequences adjacent to T-DNA borders and a high frequency of concatemeric T-DNA insertions. This can complicate further PCR analysis for reverse genetics. Additionally, small and major chromosomal rearrangements induced by T-DNA integration could lead to difficulties in the genetic analysis of the insertion, such as mutant phenotypes that are not correlated with the T-DNA insertion (Laufs et al., 1999; Nacry et al., 1998).

Many Arabidopsis genes demonstrate different levels of functional redundancy, whereas others are only needed for survival in specific conditions, such as resistance to specific biological or environmental stresses. As a result, most of the insertion lines do not demonstrate clear morphological phenotypes when grown and examined under standard conditions. Therefore, relatively few informative knockouts have been reported in the literature to date. The problem of redundancy can be solved by combining the knockouts of closely related genes. However, this might be a tough task. For example, for a family of five genes there are 31 combinations of single, double, and multiple knockouts (Bouché and Bouchez, 2001). Significantly, two-thirds of Arabidopsis nuclear genes belong to gene families and, out of these, one-third to families with more than five members (The Arabidopsis Genome Initiative 2000; Simillion et al., 2002).

An alternative to the T-DNA/transposon knockouts production is gene silencing, in particular PTGS- post transciptional gene silencing (RNA interference) (Hannon, 2002; Hilson et al., 2004; Waterhouse and Helliwell, 2003). This method is based on the delivery of double-stranded RNA (dsRNA) into an organism or cell, to induce a sequence-specific RNA degradation mechanism that effectively silences a targeted gene. RNAi silencing can target whole gene families whose sequences diverge by up to 30% (see Results). The clear advantage of this method is the possibility of silencing whole gene families or several, unrelated genes by either targeting conserved regions of nucleic acid sequence or including several target sequences in the same RNAi-inducing construct, respectively (Waterhouse and Helliwell, 2003). A drawback of PTGS is the possible presence of residual gene activity. Thus, in many RNAi experiments levels, the transcripts of targeted genes have ranged between wild type and undetectable levels (Helliwell et al., 2002; Stoutjesdijk et al., 2002).

I used both of the above approaches (T-DNA/transposon knockout lines and RNAi) for studying the function of genes of interest. While evaluation of some of the available knockout and RNAi lines failed (see Results), some of them were successfully investigated. Thus homozygous KO plant line for *At3g16980* didn't show any deviations in the outward phenotype (Fig 3.15 a) yet revealed a significantly higher level of expression than the wild type (see above) (Fig 3.13). This can be explained by the location of insertion (the promoter region of the gene, see Results; Fig 3.12). It is likely that the T-DNA disrupts one of functional elements in the promoter that is normally involved in negative regulation of *At3g16980* expression. I suggest that changing the expression level of this gene alone is not sufficient to cause any remarkable deviations in plant growth phenotype and/or trichome development since it might have many interaction partners and genes sharing functions with it (e.g. putative RNA polymerase II *At4g16265*).

Plants carrying a T-DNA insertion in the *GH3.5* gene proved to be homozygous and did not express this gene. These plants showed a dwarf phenotype (Fig 3.15 b). However, the same knockout plant line (SALK_151766) was characterized in a paper published later (Park et al., 2007 a). In contrast to results presented here, these authors showed that under normal conditions these mutants are phenotypically indistinguishable from wild type plants except that they have slightly larger leaves. They also report that *gh3.5* mutant plants are extremely sensitive to various abiotic and biotic stresses. Taking these findings into account, I suggest that the investigated SALK_151766 plants were for some reason exposed to certain stress conditions (e.g. insects, light or water regime disturbance etc.). Therefore, these mutants showed the dwarf phenotype.

From this point of view, it is more complicated to explain the growth delay observed in RNAi plants carrying the specific GST for *GH3.5* (Fig 3.14, 3.16). However, it is possible that in this plant line both *GH3.5* and its close relative *GH3.6/DFL1* are silenced (see Results) and therefore auxin homeostasis is disturbed. This can lead to observed phenotype abnormalities, which may be caused by excess of auxin (see above) governed by contemporary silencing of both the auxin binding genes *GH3.5* and *GH3.6/DFL1*. In the case of the simultaneous silencing of both genes, the observed delay in growth might also be provoked by certain deviations from the normal plant growth conditions, as in case with *gh3.5* T-DNA mutants. It is worth mentioning that GH3.6 is involved in hypocotyl growth (Nakazawa et al., 2001). Interestingly, during plant development, phenotypic changes of *gh3.5* RNAi plants became less pronounced in comparison to wild type control plants (Fig 3.16). This seems to indicate a decrease in RNAi silencing efficiency. As the activity of transcription decreases during the life span of the organism, less dsRNA is produced. Furthermore, unlike insertional mutagenesis, PTGS requires additional functional elements for proper performance (like DCL (Dicer-like) proteins, RISC (RNA-induced Silencing Complex) protein complex etc.; Hannon, 2002; Waterhouse and Helliwell, 2002). In older organisms, protein biosynthesis generally becomes less precise in comparison to young ones (Finch and Schneider, 1985). This can affect the expression of proteins required for RNAi silencing, making silencing less efficient.

Knockout or silencing of *GH3.5* does not affect number, spacing, or morphology of the leaf trichomes of Arabidopsis (Table 3.4). This is likely due to functional redundancy within the GH3 Arabidopsis gene family (see above). The same is probably true for *gasa4* mutants. Plants of the homozygous *GASA4* T-DNA knockout line also display unaltered leaf trichome phenotypes (Table 3.4). I suggest that other member(s) of GASA family (Roxrud et al., 2007) take over the missing functions of this gene in GA signaling during trichome development.

Performed metabolite profiling of *gh3.5* plants (SALK_151766 plant line) showed no remarkable changes in metabolite composition of the plants with knocked-out *At4g27260* (*GH3.5*) gene (Table 3.5; Fig 3.17). It is obvious that changing the expression of *GH3.5* alone is not sufficient to cause alterations of plant performance (at least under normal conditions, Park et al., 2007 a). The results obtained serve as additional evidence of overlapping and redundancy of functions between members of GH3 gene family (Nakazawa et al., 2001) as well as underlining the problem of gene functional redundancy in general (see above; Bouché and Bouchez, 2001).

4.4 In silico analysis of promoter cis-regulatory elements of candidate genes

In silico promoter analysis can provide novel clues about cell cycle progression during trichome development. In particular, the presence of cis-acting elements involved in hormonal response and cell cycle regulation (see Tables 3.6- 3.8) enable conclusions on novel interactions between trichome initiating and cell cycle regulating factors during trichome development to be made. Therefore, in addition to the analysis of the three selected candidate genes, I analyzed the promoter sequences of other genes found to be preferentially expressed in trichome initials. I detected multiple putative MYB-binding sites within the promoters of the 38 genes found to be preferentially expressed in trichome initial cells, including some genes with currently unknown functions (Table 3.6, 3.8). This finding suggests the presence of potential targets for trichome promoting factors like GL1 among these genes or, perhaps, possible mechanisms of trichome development inhibition in the surrounding basal cells. The mechanism by which trichome inhibiting factors transfer information to arrest trichome development in neighboring cells is not well understood. It has been hypothesized that members of trichome inhibiting complex (i.e. TRY, CPC, ETC1 and ETC2) themselves move to the trichome surrounding cells to arrest trichome development in these cells (see Introduction, Fig 1.3). However, the in silico promoter analysis performed here provides additional clues about possible lateral inhibition mechanisms during trichome development. Being MYB proteins, members of inhibiting complex may activate expression of some MYB binding site-containing genes in the developing trichome. These in turn may serve as signals (or activate some yet unknown signaling mechanisms) that are transferred to the neighboring cells to arrest trichome development there.

Interestingly, more than half of the 38 genes preferentially expressed in trichome initial cells contained the MYBCOREATCYCB1 cis-acting element (Table 3.6; 3.8). This sequence has been identified in the promoter of the Arabidopsis *thaliana cyclin B1:1* gene (Planchais et al., 2002), which is required for the proper timing of entry into mitosis. However, once committed to the trichome fate, epidermal cells exit the mitotic pathway. Therefore, I suggest an alternative function of promoters containing the MYBCOREATCYCB1 motif: similar signals that regulate *cycB1;1* expression (or *cycB1;1* itself) may be required in developing trichomes to push the cell cycle towards endoreduplication. It was found that persistence of cycB1;1 after termination of mitosis leads to additional endoreduplication events (Weingartner et al., 2004). Furthermore, ectopic expression of cycB1;1 in trichomes does not cause induction of mitotic cycles unlike such expression of cycB1;2 (Schnittger et al., 2002 b). Unfortunately, it was not possible to estimate the behavior of *cycB1;1* itself in early stages of

trichome development because of the absence of appropriate ESTs in the collection spotted on the nylon filters that were used in this work.

Further cis-acting elements, CURECORECR and SURECOREATSULTR11 (Table 3.7), were found to be present in many genes highly expressed in trichome initials (including those with currently unknown functions). These elements are involved in processes of copper metabolism and sulfur response respectively. The presence of these elements could be related to the function of trichomes in the processes of sulfur metabolism, heavy metal detoxification, and reaction to other stress conditions (Garcia-Hernandez et al., 1998; Gutierrez-Alcala et al., 2000; Wienkoop et al., 2004). In particular, *RAN1* (AT5G44790), which encodes an ATP dependent copper transporter, was found among the 38 genes more highly expressed in trichome initial cells in comparison to pavement cells. Furthermore, several promoters of genes with unknown function in the set of 38 candidate genes contain different amounts of the CURECORECR and SURECOREATSULTR11 cis-acting elements. Therefore, a role for these genes in sulfur metabolism and detoxification is possible.

Some of the cis-acting elements identified within the promoter regions of the 38 candidate genes are consistently enriched in this set (Table 3.8). However, for certain elements an enrichment score could not be calculated (see Materials and Methods). In summary the derived bioinformatic data should be considered with appropriate caution, since it can only provide information about comparative frequencies of given cis-acting elements in the promoter regions of selected genes.

4.5 Investigating potential functions for candidate genes in developing trichomes

In summarizing the data presented in this work, I include possible functions for the genes implicated in trichome morphogenesis (Fig 4.1). Three of the candidate genes investigated are likely to be involved in mediating hormone signaling in developing trichomes. Specifically, *At3g16980* regulates cell differentiation in early stages of development at the transcriptional level, and possibly has a role in the microRNA pathway. *GASA4* is downstream of *GL1*. Both *GASA4* and *GH3.5* are potential E2F-DP targets and therefore required for S-phase entry. *GH3.5* regulates auxin homeostasis in developing trichomes. Genes containing MYB cis-acting elements can mediate *GL1* effects and are probably involved in a lateral inhibition mechanism.

As the major outcome of this work, I propose the scheme of action of the candidate genes in developing trichomes. This scheme could complement recent models of cell cycle progression and trichome development (Inze, 2005; Inze and De Veylder, 2006 Schellmann and Hülskamp, 2005).

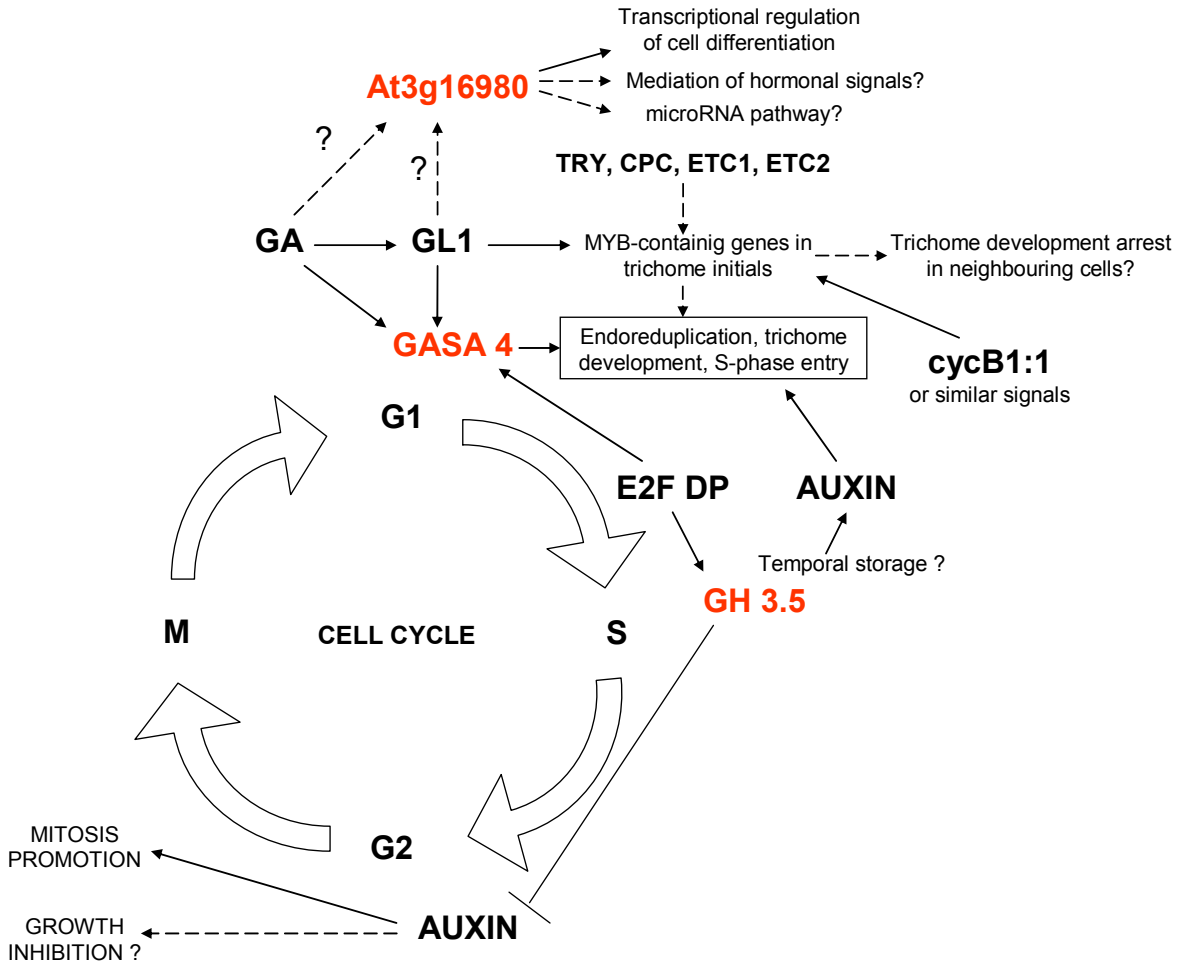

Figure 4.1 Possible roles of candidate genes in trichome development and cell cycle regulation in developing trichomes

These suggestions are based mostly on expression pattern data in silico promoter analysis of the genes of interest (for more details see text). The three candidate genes are depicted in red; highly speculative interactions and effects are shown by dashed arrows and/or marked by question marks.

5. SUMMARY AND CONCLUSIONS

Importance of the studies on the level of individual cells for biology today is hard to overestimate. Major advantage of single cell approach is that it provides higher spatial resolution in comparison to whole organ or organism investigation. This allows obtaining data on principally new level of accuracy. Furthermore, single cell studies allow identification of cell-specific markers.

Although recently large amount of data concerning different aspects of single cell performance is accumulated, our knowledge about development and differentiation of individual cell within specialized tissue are still far from being complete.

In order to get more insight into processes that occur in certain individual cell during its development and differentiation changes in gene expression during life cycle of *A. thaliana* leaf trichome were explored. Microcapillary sampling technique was applied for assessment of transcriptome of leaf pavement cells, trichome initial cells and mature trichomes- final state of trichome differentiation. Noteworthy, such approach was for the first time used for trichome development investigation and plant cell cycle studies. During this work microcapillary sampling procedure was improved allowing sampling trichome cells at the earliest stage of their development. These cells are incipient trichomes that do not possess any visible hallmarks of commitment to trichome pathway. Trichome initials were marked by GFP and sampled by microcapillaries under UV-light. This enhanced sampling method allowed to gather samples from as few as 10 individual trichome initial cells. Subsequent microarray hybridization of genetic material derived from single cells allowed to evaluate differences in gene expression of different stages of trichome development. Furthermore candidate genes involved in hormone signalling, cell cycle regulation and detoxification were picked up for further analysis.

Three candidate genes, namely *At3g16980*, *At5g15230 (GASA4)* and *At4g27260 (GH3.5)*) were selected for detailed expression studies by means of real-time RT-PCR and/or promoter::reporter studies. The expression pattern of these genes confirmed the reliability and applicability of applied single cell approach. Phenotypic analysis of available knockout and RNAi lines for genes of interest as well as metabolite profiling of *gh3.5* plants underlined the problem of gene functional redundancy in reverse genetics studies. Therefore effects of loss- and gain-of-function mutations targeting selected here candidate genes have to be further studied with higher precision. In silico performed promoter analysis allowed identification of common regulatory elements in the set of candidate genes thus giving the possibility to discover new common regulatory pathways and interactions in cell cycle control, in particular during trichome development. Furthermore conducted studies allowed to suggest possible roles for the candidate

genes in trichome initiation, development and cell cycle regulation. In particular, analysed genes of interest are probably involved in onset of trichome development, trichome differentiation and regulation of endocycling during trichome development. These effects of candidate genes are likely governed by plant hormones- this gives additional insight into hormonal influence on trichome development and cell cycle regulation in particular in developing trichome. Possible involvement of some genes more highly expressed in trichome initial cells in lateral inhibition of trichome development is intriguing, but require further analysis since such conclusion is based solely on in silico performed promoter analysis.

As an outcome of this work novel components in the sophisticated machinery of trichome development and cell cycle progression were identified. These factors could integrate hormone stimuli and network interactions between characterized and as yet unknown members of this machinery. However, exact modes of action of selected candidate genes as well as mechanisms of trichome development and cell cycle regulation require further investigation.

I expect findings presented in this work to enhance and complement our current knowledge about cell cycle progression and trichome development, as well as about cell fate determination and cell differentiation in general.

6. OUTLOOK

Selected candidate genes have to be further investigated by means of reverse genetics. Phenomenon of functional redundancy within gene families has to be taken into account while performing this analysis. Thus construction of multiple knockouts and/or creating RNAi lines targeting large part of appropriate gene family would be reasonable in the future. Proposed interactions of trichome patterning factors encoding MYB proteins (i. e. GL1, TRY, CPC, ETC1 and ETC2, see above) with candidate genes containing MYB cis-acting elements in their promoters have to be confirmed experimentally (e.g by chromatin immunoprecipitation or electrophoretic mobility shift assay (EMSA)). Investigation of other genes from the set of those preferentially expressed in trichome initials (total 38) is also of a big interest. Some of them like, for example, *At4g20150*, *At5g11730* and *At5g13240* encode unknown proteins. Others can provide additional information about trichome functions (e.g. *RAN1* (*At5g44790*), which encodes copper transporter- see Discussion). Expression pattern of these genes should be investigated using promoter::reporter studies. Such analysis together with assessment of function of unknown genes will definitely shed some light on processes occurring at initial stage of trichome development.

Further confirmation of expression pattern of the genes expressed solely in one cell type as revealed by microarray analysis would be interesting in terms of determination of novel cell-specific marker genes. Thus *At3g16980*, *At3g53420*, *At5g11730*, *At5g44790* were found to be expressed only in trichome initial cells and *At5g45820*, *At1g48750*, *At2g47980*- in mature trichome cells (see Results). Exploration of spatial expression pattern of these genes (e. g. *in vivo* via construction of promoter::*GFP* plant lines) will provide valuable information about their cell specificity.

In order to obtain more data on changes of gene expression during trichome development it is also worth to repeat single cell microarray experiment using hybridization platform which covers larger portion of the *Arabidopsis* genome (e. g. Affymetrix ATH1 GeneChip). As performed already experiment was not successful (see Results), hybridization protocol for such microarray study needs to be improved.

Furthermore, it makes sense to include more stages of trichome development in gene expression profiling experiments. Trichomes in bulging stage of development, stalk formation and initial stages of branching could be sampled by microcapillaries. Since these stages are visible, there is no need for usage of trichome-specific markers (e. g. GFP). Data obtained in such experiment will definitely provide more insight in trichome development and differentiation, in particular in mechanisms of cell expansion, regulation of endoreduplication, trichome branching etc.

REFERENCES

(2000) Analysis of the genome sequence of the flowering plant Arabidopsis thaliana. *Nature*, **408**, 796-815.

Achard, P., Herr, A., Baulcombe, D.C. and Harberd, N.P. (2004) Modulation of floral development by a gibberellin-regulated microRNA. *Development*, **131**, 3357-3365.

Alonso, J.M., Stepanova, A.N., Leisse, T.J., Kim, C.J., Chen, H., Shinn, P., Stevenson, D.K., Zimmerman, J., Barajas, P., Cheuk, R et al (2003) Genome-wide insertional mutagenesis of Arabidopsis thaliana. *Science*, **301**, 653-657.

Asano, T., Masumura, T., Kusano, H., Kikuchi, S., Kurita, A., Shimada, H. and Kadowaki, K. (2002) Construction of a specialized cDNA library from plant cells isolated by laser capture microdissection: toward comprehensive analysis of the genes expressed in the rice phloem. *Plant J*, **32**, 401-408.

Attwooll, C., Lazzerini Denchi, E. and Helin, K. (2004) The E2F family: specific functions and overlapping interests. *Embo J*, **23**, 4709-4716.

Aubert, D., Chevillard, M., Dorne, A.M., Arlaud, G. and Herzog, M. (1998) Expression patterns of GASA genes in Arabidopsis thaliana: the GASA4 gene is up-regulated by gibberellins in meristematic regions. *Plant Mol Biol*, **36**, 871-883.

Axelos, M., Bardet, C., Liboz, T., Le Van Thai, A., Curie, C. and Lescure, B. (1989) The gene family encoding the Arabidopsis thaliana translation elongation factor EF-1 alpha: molecular cloning, characterization and expression. *Mol Gen Genet*, **219**, 106-112.

Bauer, D., Muller, H., Reich, J., Riedel, H., Ahrenkiel, V., Warthoe, P. and Strauss, M. (1993) Identification of differentially expressed mRNA species by an improved display technique (DDRT-PCR). *Nucleic Acids Res*, **21**, 4272-4280.

Beemster, G.T., De Veylder, L., Vercruysse, S., West, G., Rombaut, D., Van Hummelen, P., Galichet, A., Gruissem, W., Inze, D. and Vuylsteke, M. (2005) Genome-wide analysis of gene expression profiles associated with cell cycle transitions in growing organs of Arabidopsis. *Plant Physiol*, **138**, 734-743.

Birnbaum, K. and Benfey, P.N. (2004) Network building: transcriptional circuits in the root. *Curr Opin Plant Biol*, **7**, 582-588.

Birnbaum, K., Shasha, D.E., Wang, J.Y., Jung, J.W., Lambert, G.M., Galbraith, D.W. and Benfey, P.N. (2003) A gene expression map of the Arabidopsis root. *Science*, **302**, 1956-1960.

Blais, A. and Dynlacht, B.D. (2004) Hitting their targets: an emerging picture of E2F and cell cycle control. *Curr Opin Genet Dev*, **14**, 527-532.

Bligny, R. and Douce, R. (2001) NMR and plant metabolism. *Curr Opin Plant Biol*, **4**, 191-196.

Bouche, N. and Bouchez, D. (2001) Arabidopsis gene knockout: phenotypes wanted. *Curr Opin Plant Biol*, **4**, 111-117.

Boudolf, V., Vlieghe, K., Beemster, G.T., Magyar, Z., Torres Acosta, J.A., Maes, S., Van Der Schueren, E., Inze, D. and De Veylder, L. (2004) The plant-specific cyclin-dependent kinase CDKB1;1 and transcription factor E2Fa-DPa control the balance of mitotically dividing and endoreduplicating cells in Arabidopsis. *Plant Cell*, **16**, 2683-2692.

Brandt, S., Kehr, J., Walz, C., Imlau, A., Willmitzer, L. and Fisahn, J. (1999) Technical Advance: A rapid method for detection of plant gene transcripts from single epidermal, mesophyll and companion cells of intact leaves. *Plant J*, **20**, 245-250.

Brandt, S., Kloska, S., Altmann, T. and Kehr, J. (2002) Using array hybridization to monitor gene expression at the single cell level. *J Exp Bot*, **53**, 2315-2323.

Brandt S, Walz C, Schad M, Pavlovic N, Kehr J. (2003). A simple, chisel assisted mechanical microdissection system for harvesting homogenous plant tissue suitable for the analysis of

nucleic acids and proteins. *Plant Mol Biol Rep,* **21,** 417–427

Brandt, S.P. (2005) Microgenomics: gene expression analysis at the tissue-specific and single-cell levels. *J Exp Bot*, **56**, 495-505.

Bubner, B., Gase, K. and Baldwin, I.T. (2004) Two-fold differences are the detection limit for determining transgene copy numbers in plants by real-time PCR. *BMC Biotechnol*, **4**, 14.

Chalfie, M., Tu, Y., Euskirchen, G., Ward, W.W. and Prasher, D.C. (1994) Green fluorescent protein as a marker for gene expression. *Science*, **263**, 802-805.

Chenchik A., Moqadam, F. and Siebert, P. (January 1995) Marathon cDNA amplification: A new method for cloning full-length cDNAs. *Clontechniques* **X**(1):5–8.

Chien, J.C. and Sussex, I.M. (1996) Differential regulation of trichome formation on the adaxial and abaxial leaf surfaces by gibberellins and photoperiod in Arabidopsis thaliana (L.) Heynh. *Plant Physiol*, **111**, 1321-1328.

Cho, Y., Fernandes, J., Kim, S.H. and Walbot, V. (2002) Gene-expression profile comparisons distinguish seven organs of maize. *Genome Biol*, **3**, research0045.

Churchman, M.L., Brown, M.L., Kato, N., Kirik, V., Hulskamp, M., Inze, D., De Veylder, L., Walker, J.D., Zheng, Z., Oppenheimer, D.G et al (2006) SIAMESE, a Plant-Specific Cell Cycle Regulator, Controls Endoreplication Onset in Arabidopsis thaliana. *Plant Cell*.

Clough, S.J. and Bent, A.F. (1998) Floral dip: a simplified method for Agrobacterium-mediated transformation of Arabidopsis thaliana. *Plant J*, **16**, 735-743.

Cockcroft, C.E., den Boer, B.G., Healy, J.M. and Murray, J.A. (2000) Cyclin D control of growth rate in plants. *Nature*, **405**, 575-579.

Curtis, M.D. and Grossniklaus, U. (2003) A gateway cloning vector set for high-throughput functional analysis of genes in planta. *Plant Physiol*, **133**, 462-469.

Czechowski, T., Stitt, M., Altmann, T., Udvardi, M.K. and Scheible, W.R. (2005) Genome-wide identification and testing of superior reference genes for transcript normalization in Arabidopsis. *Plant Physiol*, **139**, 5-17.

Davuluri, R.V., Sun, H., Palaniswamy, S.K., Matthews, N., Molina, C., Kurtz, M. and Grotewold, E. (2003) AGRIS: Arabidopsis gene regulatory information server, an information resource of Arabidopsis cis-regulatory elements and transcription factors. *BMC Bioinformatics*, **4**, 25.

De Clercq, A. and Inze, D. (2006) Cyclin-dependent kinase inhibitors in yeast, animals, and plants: a functional comparison. *Crit Rev Biochem Mol Biol*, **41**, 293-313.

De Veylder, L., Beeckman, T., Beemster, G.T., de Almeida Engler, J., Ormenese, S., Maes, S., Naudts, M., Van Der Schueren, E., Jacqmard, A., Engler, G. and Inze, D. (2002) Control of proliferation, endoreduplication and differentiation by the Arabidopsis E2Fa-DPa transcription factor. *Embo J*, **21**, 1360-1368.

De Veylder, L., Beeckman, T., Beemster, G.T., Krols, L., Terras, F., Landrieu, I., van der Schueren, E., Maes, S., Naudts, M. and Inze, D. (2001) Functional analysis of cyclin-dependent kinase inhibitors of Arabidopsis. *Plant Cell*, **13**, 1653-1668.

Dean, F.B., Hosono, S., Fang, L., Wu, X., Faruqi, A.F., Bray-Ward, P., Sun, Z., Zong, Q., Du, Y., Du, J., Driscoll, M et al (2002) Comprehensive human genome amplification using multiple displacement amplification. *Proc Natl Acad Sci U S A*, **99**, 5261-5266.

Deiman, B., van Aarle, P. and Sillekens, P. (2002) Characteristics and applications of nucleic acid sequence-based amplification (NASBA). *Mol Biotechnol*, **20**, 163-179.

Dewitte, W., Riou-Khamlichi, C., Scofield, S., Healy, J.M., Jacqmard, A., Kilby, N.J. and Murray, J.A. (2003) Altered cell cycle distribution, hyperplasia, and inhibited differentiation in Arabidopsis caused by the D-type cyclin CYCD3. *Plant Cell*, **15**, 79-92.

Dimova, D.K. and Dyson, N.J. (2005) The E2F transcriptional network: old acquaintances with new faces. *Oncogene*, **24**, 2810-2826.

Doerner, P., Jorgensen, J.E., You, R., Steppuhn, J. and Lamb, C. (1996) Control of root growth and development by cyclin expression. *Nature*, **380**, 520-523.

Downes, B.P., Stupar, R.M., Gingerich, D.J. and Vierstra, R.D. (2003) The HECT ubiquitin-protein ligase (UPL) family in Arabidopsis: UPL3 has a specific role in trichome development. *Plant J*, **35**, 729-742.

Doyle, J.J.and Doyle.J.L., (1987) A rapid DNA isolation procedure for small quantities of fresh leaf tissue. *Phytochemistry Bulletin 19:11-15*, **19**, 11-15.

Dresselhaus, T., Lorz, H. and Kranz, E. (1994) Representative cDNA libraries from few plant cells. *Plant J*, **5**, 605-610.

El Refy, A., Perazza, D., Zekraoui, L., Valay, J.G., Bechtold, N., Brown, S., Hulskamp, M., Herzog, M. and Bonneville, J.M. (2003) The Arabidopsis KAKTUS gene encodes a HECT protein and controls the number of endoreduplication cycles. *Mol Genet Genomics*, **270**, 403-414.

Emmert-Buck, M.R., Bonner, R.F., Smith, P.D., Chuaqui, R.F., Zhuang, Z., Goldstein, S.R., Weiss, R.A. and Liotta, L.A. (1996) Laser capture microdissection. *Science*, **274**, 998-1001.

Esch, J.J., Chen, M., Sanders, M., Hillestad, M., Ndkium, S., Idelkope, B., Neizer, J. and Marks, M.D. (2003) A contradictory GLABRA3 allele helps define gene interactions controlling trichome development in Arabidopsis. *Development*, **130**, 5885-5894.

Feldman, A.L., Costouros, N.G., Wang, E., Qian, M., Marincola, F.M., Alexander, H.R. and Libutti, S.K. (2002) Advantages of mRNA amplification for microarray analysis. *Biotechniques*, **33**, 906-912, 914.

Ferreira, P.C., Hemerly, A.S., Engler, J.D., van Montagu, M., Engler, G. and Inze, D. (1994) Developmental expression of the arabidopsis cyclin gene cyc1At. *Plant Cell*, **6**, 1763-1774.

Finch C., Schneider E. (editors) (1985) Handbook of the biology of aging, New York: *VAN NOSTRAND REINHOLD COMPANY*.

Foster, R.J., McRae, D.H. and Bonner, J. (1952) Auxin-Induced Growth Inhibition a Natural Consequence of Two-Point Attachment. *Proc Natl Acad Sci U S A*, **38**, 1014-1022.

Gaedeke, N., Klein, M., Kolukisaoglu, U., Forestier, C., Muller, A., Ansorge, M., Becker, D., Mamnun, Y., Kuchler, K., Schulz, B., Mueller-Roeber, B. and Martinoia, E. (2001) The Arabidopsis thaliana ABC transporter AtMRP5 controls root development and stomata movement. *Embo J*, **20**, 1875-1887.

Fiehn, O., Kopka, J., Dormann, P., Altmann, T., Trethewey, R.N. and Willmitzer, L. (2000) Metabolite profiling for plant functional genomics. *Nat Biotechnol*, **18**, 1157-1161.

Gad-el-Hak, M., (2004) Publish or perish- an ailing enterprise? *Physics today*, March, 61

Galbraith, D.W. and Birnbaum, K. (2006) Global Studies of Cell Type-Specific Gene Expression in Plants. *Annu Rev Plant Biol*, **57**, 451-475.

Gallagher JA, Koroleva OA, Tomos AD, Farrar JF, Pollock CJ. (2001) Single cell analysis technique for comparison of specific mRNA abundance in plant cells. *J Plant Physiol,* **158,** 1089–1092

Garcia-Hernandez, M., Murphy, A. and Taiz, L. (1998) Metallothioneins 1 and 2 have distinct but overlapping expression patterns in Arabidopsis. *Plant Physiol*, **118**, 387-397.

Gehwolf, R., Griessner, M., Pertl, H. and Obermeyer, G. (2002) First patch, then catch: measuring the activity and the mRNA transcripts of a proton pump in individual Lilium pollen protoplasts. *FEBS Lett*, **512**, 152-156.

Ginsberg SD, Che SL. (2002) RNA amplification in brain tissues, *Neurochem Res,* **27,** 981–992.

Girke, T., Todd, J., Ruuska, S., White, J., Benning, C. and Ohlrogge, J. (2000) Microarray analysis of developing Arabidopsis seeds. *Plant Physiol*, **124**, 1570-1581.

Glanzer, J.G. and Eberwine, J.H. (2004) Expression profiling of small cellular samples in cancer: less is more. *Br J Cancer*, **90**, 1111-1114.

Grebenok, R.J., Pierson, E., Lambert, G.M., Gong, F.C., Afonso, C.L., Haldeman-Cahill, R., Carrington, J.C. and Galbraith, D.W. (1997) Green-fluorescent protein fusions for efficient characterization of nuclear targeting. *Plant J*, **11**, 573-586.

Grosset, J., Marty, I., Chartier, Y. and Meyer, Y. (1990) mRNAs newly synthesized by tobacco mesophyll protoplasts are wound-inducible. *Plant Mol Biol*, **15**, 485-496.

Gubler, F., Kalla, R., Roberts, J.K. and Jacobsen, J.V. (1995) Gibberellin-regulated expression of a myb gene in barley aleurone cells: evidence for Myb transactivation of a high-pI alpha-amylase gene promoter. *Plant Cell*, **7**, 1879-1891.

Gutierrez-Alcala, G., Gotor, C., Meyer, A.J., Fricker, M., Vega, J.M. and Romero, L.C. (2000) Glutathione biosynthesis in Arabidopsis trichome cells. *Proc Natl Acad Sci U S A*, **97**, 11108-11113.

Hagen, G., A. Kleinschmidt, and T. Guilfoyle. (1984). Auxin-regulated gene expression in intact soybean hypocotyl and excised hypocotyl sections. *Planta* **162**,147-153.

Hanahan, D. (1983) Studies on transformation of Escherichia coli with plasmids. *Journal of molecular biology*, **166**, 557-580.

Hannon, G.J. (2002) RNA interference. *Nature*, **418**, 244-251.

Hanson, V.D. and Heath, J., (1998) Who Killed Homer? The Demise of Classical Education and the Recovery of Greek Wisdom. New York: *The Free Press*.

He, L., Chinnery, P.F., Durham, S.E., Blakely, E.L., Wardell, T.M., Borthwick, G.M., Taylor, R.W. and Turnbull, D.M. (2002) Detection and quantification of mitochondrial DNA deletions in individual cells by real-time PCR. *Nucleic Acids Res*, **30**, e68.

Helliwell, C. A., Wesley, S. V., Wielopolska, A. J. and Waterhouse, P. M. (2002) High throughput vectors for efficient gene silencing in plants. *Funct Plant Biol* **29**, 1217-1225

Hemerly, A.S., Ferreira, P., de Almeida Engler, J., Van Montagu, M., Engler, G. and Inze, D. (1993) cdc2a expression in Arabidopsis is linked with competence for cell division. *Plant Cell*, **5**, 1711-1723.

Higo, K., Ugawa, Y., Iwamoto, M. and Korenaga, T. (1999) Plant cis-acting regulatory DNA elements (PLACE) database: 1999. *Nucleic Acids Res*, **27**, 297-300.

Hilson, P., Allemeersch, J., Altmann, T., Aubourg, S., Avon, A., Beynon, J., Bhalerao, R.P., Bitton, F., Caboche, M., Cannoot, B et al (2004) Versatile gene-specific sequence tags for Arabidopsis functional genomics: transcript profiling and reverse genetics applications. *Genome Res*, **14**, 2176-2189.

Himanen, K., Boucheron, E., Vanneste, S., de Almeida Engler, J., Inze, D. and Beeckman, T. (2002) Auxin-mediated cell cycle activation during early lateral root initiation. *Plant Cell*, **14**, 2339-2351.

Hu, Y., Bao, F. and Li, J. (2000) Promotive effect of brassinosteroids on cell division involves a distinct CycD3-induction pathway in Arabidopsis. *Plant J*, **24**, 693-701.

Huala, E., Dickerman, A.W., Garcia-Hernandez, M., Weems, D., Reiser, L., LaFond, F., Hanley, D., Kiphart, D., Zhuang, M., Huang, W et al (2001) The Arabidopsis Information Resource (TAIR): a comprehensive database and web-based information retrieval, analysis, and visualization system for a model plant. *Nucleic Acids Res*, **29**, 102-105.

Hulskamp, M. (2004) Plant trichomes: a model for cell differentiation. *Nat Rev Mol Cell Biol*, **5**, 471-480.

Hulskamp, M., Misra, S. and Jurgens, G. (1994) Genetic dissection of trichome cell development in Arabidopsis. *Cell*, **76**, 555-566.

Hulskamp, M. and Schnittger, A. (1998) Spatial regulation of trichome formation in Arabidopsis

thaliana. *Semin Cell Dev Biol*, **9**, 213-220.

Imai, K.K., Ohashi, Y., Tsuge, T., Yoshizumi, T., Matsui, M., Oka, A. and Aoyama, T. (2006) The A-type cyclin CYCA2;3 is a key regulator of ploidy levels in Arabidopsis endoreduplication. *Plant Cell*, **18**, 382-396.

Inada, N. and Wildermuth, M.C. (2005) Novel tissue preparation method and cell-specific marker for laser microdissection of Arabidopsis mature leaf. *Planta*, **221**, 9-16.

Inze, D. (2005) Green light for the cell cycle. *Embo J*, **24**, 657-662.

Inze, D. and De Veylder, L. (2006) Cell cycle regulation in plant development (1). *Annu Rev Genet*, **40**, 77-105.

Ivashikina, N., Deeken, R., Ache, P., Kranz, E., Pommerrenig, B., Sauer, N. and Hedrich, R. (2003) Isolation of AtSUC2 promoter-GFP-marked companion cells for patch-clamp studies and expression profiling. *Plant J*, **36**, 931-945.

Jacobsen, S.E., Binkowski, K.A. and Olszewski, N.E. (1996) SPINDLY, a tetratricopeptide repeat protein involved in gibberellin signal transduction in Arabidopsis. *Proc Natl Acad Sci U S A*, **93**, 9292-9296.

Jefferson, R.A., Kavanagh, T.A. and Bevan, M.W. (1987) GUS fusions: beta-glucuronidase as a sensitive and versatile gene fusion marker in higher plants. *Embo J*, **6**, 3901-3907.

Jones, M.A. and Grierson, C.S. (2003) A simple method for obtaining cell-specific cDNA from small numbers of growing root-hair cells in Arabidopsis thaliana. *J Exp Bot*, **54**, 1373-1378.

Joubes, J., Phan, T.H., Just, D., Rothan, C., Bergounioux, C., Raymond, P. and Chevalier, C. (1999) Molecular and biochemical characterization of the involvement of cyclin-dependent kinase A during the early development of tomato fruit. *Plant Physiol*, **121**, 857-869.

Kaern, M., Elston, T.C., Blake, W.J. and Collins, J.J. (2005) Stochasticity in gene expression: from theories to phenotypes. *Nat Rev Genet*, **6**, 451-464.

Kanehisa, M., Goto, S., Kawashima, S., Okuno, Y. and Hattori, M. (2004) The KEGG resource for deciphering the genome. *Nucleic Acids Res*, **32**, D277-280.

Karrer, E.E., Lincoln, J.E., Hogenhout, S., Bennett, A.B., Bostock, R.M., Martineau, B., Lucas, W.J., Gilchrist, D.G. and Alexander, D. (1995) In situ isolation of mRNA from individual plant cells: creation of cell-specific cDNA libraries. *Proc Natl Acad Sci U S A*, **92**, 3814-3818.

Kehr, J. (2001) High resolution spatial analysis of plant systems. *Curr Opin Plant Biol*, **4**, 197-201.

Kehr, J. (2003) Single cell technology. *Curr Opin Plant Biol*, **6**, 617-621.

Kerk, N.M., Ceserani, T., Tausta, S.L., Sussex, I.M. and Nelson, T.M. (2003) Laser capture microdissection of cells from plant tissues. *Plant Physiol*, **132**, 27-35.

Kirik, V., Bouyer, D., Schobinger, U., Bechtold, N., Herzog, M., Bonneville, J.M. and Hulskamp, M. (2001) CPR5 is involved in cell proliferation and cell death control and encodes a novel transmembrane protein. *Curr Biol*, **11**, 1891-1895.

Klein, C.A., Seidl, S., Petat-Dutter, K., Offner, S., Geigl, J.B., Schmidt-Kittler, O., Wendler, N., Passlick, B., Huber, R.M., Schlimok et al (2002) Combined transcriptome and genome analysis of single micrometastatic cells. *Nat Biotechnol*, **20**, 387-392.

Kondorosi, E., Roudier, F. and Gendreau, E. (2000) Plant cell-size control: growing by ploidy? *Curr Opin Plant Biol*, **3**, 488-492.

Kopka, J., Schauer, N., Krueger, S., Birkemeyer, C., Usadel, B., Bergmuller, E., Dormann, P., Weckwerth, W., Gibon, Y., Stitt, M., Willmitzer, L., Fernie, A.R. and Steinhauser, D. (2005) GMD@CSB.DB: the Golm Metabolome Database. *Bioinformatics (Oxford, England)*, **21**, 1635-1638.

Kryvych S., Nikiforova V., Herzog M., Perazza D., and Fisahn J. (2007) Gene expression profiling of the different stages of *Arabidopsis thaliana* trichome development on the single cell level. *Funct Plant Biol, Submitted*

Landrieu, I., da Costa, M., De Veylder, L., Dewitte, F., Vandepoele, K., Hassan, S., Wieruszeski, J.M., Corellou, F., Faure, J.D., Van Montagu, M., Inze, D. and Lippens, G. (2004) A small CDC25 dual-specificity tyrosine-phosphatase isoform in Arabidopsis thaliana. *Proc Natl Acad Sci U S A*, **101**, 13380-13385.

Larkin, J.C., Brown, M.L. and Schiefelbein, J. (2003) How do cells know what they want to be when they grow up? Lessons from epidermal patterning in Arabidopsis. *Annu Rev Plant Biol*, **54**, 403-430.

Larkin, J.C., Oppenheimer, D.G., Pollock, S. and Marks, M.D. (1993) Arabidopsis GLABROUS1 Gene Requires Downstream Sequences for Function. *Plant Cell*, **5**, 1739-1748.

Larkin, J.C., Young, N., Prigge, M. and Marks, M.D. (1996) The control of trichome spacing and number in Arabidopsis. *Development*, **122**, 997-1005.

Larkins, B.A., Dilkes, B.P., Dante, R.A., Coelho, C.M., Woo, Y.M. and Liu, Y. (2001) Investigating the hows and whys of DNA endoreduplication. *J Exp Bot*, **52**, 183-192.

Laufs, P., Autran, D. and Traas, J. (1999) A chromosomal paracentric inversion associated with T-DNA integration in Arabidopsis. *Plant J*, **18**, 131-139.

Lee, J.Y., Levesque, M. and Benfey, P.N. (2005) High-throughput RNA isolation technologies. New tools for high-resolution gene expression profiling in plant systems. *Plant Physiol*, **138**, 585-590.

Lee, Y., Kim, M., Han, J., Yeom, K.H., Lee, S., Baek, S.H. and Kim, V.N. (2004) MicroRNA genes are transcribed by RNA polymerase II. *Embo J*, **23**, 4051-4060.

Leonhardt, N., Kwak, J.M., Robert, N., Waner, D., Leonhardt, G. and Schroeder, J.I. (2004) Microarray expression analyses of Arabidopsis guard cells and isolation of a recessive abscisic acid hypersensitive protein phosphatase 2C mutant. *Plant Cell*, **16**, 596-615.

Ljung, K., Bhalerao, R.P. and Sandberg, G. (2001) Sites and homeostatic control of auxin biosynthesis in Arabidopsis during vegetative growth. *Plant J*, **28**, 465-474.

Ljung, K., Hull, A.K., Kowalczyk, M., Marchant, A., Celenza, J., Cohen, J.D. and Sandberg, G. (2002) Biosynthesis, conjugation, catabolism and homeostasis of indole-3-acetic acid in Arabidopsis thaliana. *Plant Mol Biol*, **49**, 249-272.

Liang P and Pardee AB. (1992) Differential display of eucaryotic messenger RNA by means of the polymerase chain reaction. *Science* **257,** 967–971

Lieckfeldt E., Simon-Rosin U., Kose F., Zoeller D., Schliep M., Fisahn J. (2007) Gene expression profiling of single epidermal, basal and trichome cells of *Arabidopsis thaliana J Plant Physiol, doi:10.1016/j.jplph.2007.06.017*

Luzzi, V., Mahadevappa, M., Raja, R., Warrington, J.A. and Watson, M.A. (2003) Accurate and reproducible gene expression profiles from laser capture microdissection, transcript amplification, and high density oligonucleotide microarray analysis. *J Mol Diagn*, **5**, 9-14.

Mallory, A.C., Bartel, D.P. and Bartel, B. (2005) MicroRNA-directed regulation of Arabidopsis AUXIN RESPONSE FACTOR17 is essential for proper development and modulates expression of early auxin response genes. *Plant Cell*, **17**, 1360-1375.

Marks, M.D. (1994) Plant development. The making of a plant hair. *Curr Biol*, **4**, 621-623.

Marks, M.D. (1997) Molecular Genetic Analysis of Trichome Development in Arabidopsis. *Annu Rev Plant Physiol Plant Mol Biol*, **48**, 137-163.

Massengill JL, Smith MA, Son DI, O'Dowd DK. (1997) Differential expression of $K_{4\text{-}AP}$ currents and Kv3.1 potassium channel transcripts in cortical neurons that develop distinct firing phenotypes. *J Neurosci,* **17,** 3136–3147

Meijer, M. and Murray, J.A.H. (2000) The role and regulation of D-type cyclins in the plant cell cycle. *Plant Mol Biol*, **43**, 621-633.

Melaragno, J.E., Mehrotra, B. and Coleman, A.W. (1993) Relationship between Endopolyploidy and Cell Size in Epidermal Tissue of Arabidopsis. *Plant Cell*, **5**, 1661-1668.

Morgan, D.O. (1997) Cyclin-dependent kinases: engines, clocks, and microprocessors. *Annu Rev Cell Dev Biol*, **13**, 261-291.

Morita, A., Umemura, T., Kuroyanagi, M., Futsuhara, Y., Perata, P. and Yamaguchi, J. (1998) Functional dissection of a sugar-repressed alpha-amylase gene (RAmy1 A) promoter in rice embryos. *FEBS Lett*, **423**, 81-85.

Mould, M.J., Xu, T., Barbara, M., Iscove, N.N. and Heath, M.C. (2003) cDNAs generated from individual epidermal cells reveal that differential gene expression predicting subsequent resistance or susceptibility to rust fungal infection occurs prior to the fungus entering the cell lumen. *Mol Plant Microbe Interact*, **16**, 835-845.

Nacry, P., Camilleri, C., Courtial, B., Caboche, M. and Bouchez, D. (1998) Major chromosomal rearrangements induced by T-DNA transformation in Arabidopsis. *Genetics*, **149**, 641-650.

Nakazawa, M., Yabe, N., Ichikawa, T., Yamamoto, Y.Y., Yoshizumi, T., Hasunuma, K. and Matsui, M. (2001) DFL1, an auxin-responsive GH3 gene homologue, negatively regulates shoot cell elongation and lateral root formation, and positively regulates the light response of hypocotyl length. *Plant J*, **25**, 213-221.

Nakazono, M., Qiu, F., Borsuk, L.A. and Schnable, P.S. (2003) Laser-capture microdissection, a tool for the global analysis of gene expression in specific plant cell types: identification of genes expressed differentially in epidermal cells or vascular tissues of maize. *Plant Cell*, **15**, 583-596.

Newman, T., de Bruijn, F.J., Green, P., Keegstra, K., Kende, H., McIntosh, L., Ohlrogge, J., Raikhel, N., Somerville, S., Thomashow, M. and et al. (1994) Genes galore: a summary of methods for accessing results from large-scale partial sequencing of anonymous Arabidopsis cDNA clones. *Plant Physiol*, **106**, 1241-1255.

Outlaw, W.H., Jr. and Zhang, S. (2001) Single-cell dissection and microdroplet chemistry. *J Exp Bot*, **52**, 605-614.

Parinov, S. and Sundaresan, V. (2000) Functional genomics in Arabidopsis: large-scale insertional mutagenesis complements the genome sequencing project. *Curr Opin Biotechnol*, **11**, 157-161.

Park, J.E., Park, J.Y., Kim, Y.S., Staswick, P.E., Jeon, J., Yun, J., Kim, S.Y., Kim, J., Lee, Y.H. and Park, C.M. (2007 a) GH3-mediated auxin homeostasis links growth regulation with stress adaptation response in Arabidopsis. *J Biol Chem*, **282**, 10036-10046.

Park, J.E., Seo, P.J., Lee, A.K., Jung, J.H., Kim, Y.S. and Park, C.M. (2007 b) An Arabidopsis GH3 Gene, Encoding an Auxin-Conjugating Enzyme, Mediates Phytochrome B-Regulated Light Signals in Hypocotyl Growth. *Plant Cell Physiol*.

Perazza, D., Herzog, M., Hulskamp, M., Brown, S., Dorne, A.M. and Bonneville, J.M. (1999) Trichome cell growth in Arabidopsis thaliana can be derepressed by mutations in at least five genes. *Genetics*, **152**, 461-476.

Perazza, D., Vachon, G. and Herzog, M. (1998) Gibberellins promote trichome formation by Up-regulating GLABROUS1 in arabidopsis. *Plant Physiol*, **117**, 375-383.

Petalidis, L., Bhattacharyya, S., Morris, G.A., Collins, V.P., Freeman, T.C. and Lyons, P.A. (2003) Global amplification of mRNA by template-switching PCR: linearity and application to microarray analysis. *Nucleic Acids Res*, **31**, e142.

Planchais, S., Perennes, C., Glab, N., Mironov, V., Inze, D. and Bergounioux, C. (2002) Characterization of cis-acting element involved in cell cycle phase-independent activation

of Arath;CycB1;1 transcription and identification of putative regulatory proteins. *Plant Mol Biol*, **50**, 111-127.

Polevoy, V. (1989) Plant physiology. Moscow: *Vysshaya shkola* (in Russian).

Ponce, M.R., Perez-Perez, J.M., Piqueras, P. and Micol, J.L. (2000) A multiplex reverse transcriptase-polymerase chain reaction method for fluorescence-based semiautomated detection of gene expression in Arabidopsis thaliana. *Planta*, **211**, 606-608.

Prestridge, D.S. (1991) SIGNAL SCAN: a computer program that scans DNA sequences for eukaryotic transcriptional elements. *Comput Appl Biosci*, **7**, 203-206.

Ptashne, M. (1992) A Genetic Switch: Phage (Lambda) and Higher Organisms (Cambridge, MA: Cell Press).

Radonic, A., Thulke, S., Mackay, I.M., Landt, O., Siegert, W. and Nitsche, A. (2004) Guideline to reference gene selection for quantitative real-time PCR. *Biochem Biophys Res Commun*, **313**, 856-862.

Ramakers, C., Ruijter, J.M., Deprez, R.H. and Moorman, A.F. (2003) Assumption-free analysis of quantitative real-time polymerase chain reaction (PCR) data. *Neurosci Lett*, **339**, 62-66.

Ramirez-Parra, E., Frundt, C. and Gutierrez, C. (2003) A genome-wide identification of E2F-regulated genes in Arabidopsis. *Plant J*, **33**, 801-811.

Recchi, M.A., Hebbar, M., Hornez, L., Harduin-Lepers, A., Peyrat, J.P. and Delannoy, P. (1998) Multiplex reverse transcription polymerase chain reaction assessment of sialyltransferase expression in human breast cancer. *Cancer Res*, **58**, 4066-4070.

Richert J, Kranz E, Lörz H, Dresselhaus T. (1996) A reverse transcriptase-polymerase chain reaction assay for gene expression studies at the single cell level. *Plant Sci* **114,** 93–99.

Richmond, C.S., Glasner, J.D., Mau, R., Jin, H. and Blattner, F.R. (1999) Genome-wide expression profiling in Escherichia coli K-12. *Nucleic Acids Res*, **27**, 3821-3835.

Riou-Khamlichi, C., Huntley, R., Jacqmard, A. and Murray, J.A. (1999) Cytokinin activation of Arabidopsis cell division through a D-type cyclin. *Science*, **283**, 1541-1544.

Roessner, U., Wagner, C., Kopka, J., Trethewey, R.N. and Willmitzer, L. (2000) Technical advance: simultaneous analysis of metabolites in potato tuber by gas chromatography-mass spectrometry. *Plant J*, **23**, 131-142.

Rogers, R.M.a. (1994) Preparation of genomic DNA from plant tissue. In *Current Protocols in Molecular Biology*: John Wiley & Sons, Inc.

Rosso, M.G., Li, Y., Strizhov, N., Reiss, B., Dekker, K. and Weisshaar, B. (2003) An Arabidopsis thaliana T-DNA mutagenized population (GABI-Kat) for flanking sequence tag-based reverse genetics. *Plant Mol Biol*, **53**, 247-259.

Roxrud, I., Lid, S.E., Fletcher, J.C., Schmidt, E.D. and Opsahl-Sorteberg, H.G. (2007) GASA4, One of the 14-Member Arabidopsis GASA Family of Small Polypeptides, Regulates Flowering and Seed Development. *Plant Cell Physiol*, **48**, 471-483.

Sambrook J., Fritsch E. and Maniatis T. (1989) Molecular cloning: a laboratory manual. (New York, Cold Spring Harbor Laboratory Press)

Schad, M., Lipton, M.S., Giavalisco, P., Smith, R.D. and Kehr, J. (2005) Evaluation of two-dimensional electrophoresis and liquid chromatography--tandem mass spectrometry for tissue-specific protein profiling of laser-microdissected plant samples. *Electrophoresis*, **26**, 2729-2738.

Schad, M., Mungur, R., Fiehn, O. and Kehr, J. (2005) Metabolic profiling of laser microdissected vascular bundles of Arabidopsis thaliana. *Plant methods*, **1**, 2.

Schauer, N., Steinhauser, D., Strelkov, S., Schomburg, D., Allison, G., Moritz, T., Lundgren, K., Roessner-Tunali, U., Forbes, M.G., Willmitzer, L., Fernie, A.R. and Kopka, J. (2005) GC-MS libraries for the rapid identification of metabolites in complex biological samples. *FEBS Lett*, **579**, 1332-1337.

Schellmann, S. and Hulskamp, M. (2005) Epidermal differentiation: trichomes in Arabidopsis as a model system. *Int J Dev Biol*, **49**, 579-584.

Scheres, B. (2002) Plant patterning: TRY to inhibit your neighbors. *Curr Biol*, **12**, R804-806.

Schiefelbein, J. (2003) Cell-fate specification in the epidermis: a common patterning mechanism in the root and shoot. *Curr Opin Plant Biol*, **6**, 74-78.

Schnittger, A., Jurgens, G. and Hulskamp, M. (1998) Tissue layer and organ specificity of trichome formation are regulated by GLABRA1 and TRIPTYCHON in Arabidopsis. *Development*, **125**, 2283-2289.

Schnittger, A., Schobinger, U., Bouyer, D., Weinl, C., Stierhof, Y.D. and Hulskamp, M. (2002 a) Ectopic D-type cyclin expression induces not only DNA replication but also cell division in Arabidopsis trichomes. *Proc Natl Acad Sci U S A*, **99**, 6410-6415.

Schnittger, A., Schobinger, U., Stierhof, Y.D. and Hulskamp, M. (2002 b) Ectopic B-type cyclin expression induces mitotic cycles in endoreduplicating Arabidopsis trichomes. *Curr Biol*, **12**, 415-420.

Schnittger, A., Weinl, C., Bouyer, D., Schobinger, U. and Hulskamp, M. (2003) Misexpression of the cyclin-dependent kinase inhibitor ICK1/KRP1 in single-celled Arabidopsis trichomes reduces endoreduplication and cell size and induces cell death. *Plant Cell*, **15**, 303-315.

Schuppler, U., He, P.H., John, P.C. and Munns, R. (1998) Effect of water stress on cell division and cell-division-cycle 2-like cell-cycle kinase activity in wheat leaves. *Plant Physiol*, **117**, 667-678.

Schutze, K. and Lahr, G. (1998) Identification of expressed genes by laser-mediated manipulation of single cells. *Nat Biotechnol*, **16**, 737-742.

Simillion, C., Vandepoele, K., Van Montagu, M.C., Zabeau, M. and Van de Peer, Y. (2002) The hidden duplication past of Arabidopsis thaliana. *Proc Natl Acad Sci U S A*, **99**, 13627-13632.

Sorin, C., Negroni, L., Balliau, T., Corti, H., Jacquemot, M.P., Davanture, M., Sandberg, G., Zivy, M. and Bellini, C. (2006) Proteomic analysis of different mutant genotypes of Arabidopsis led to the identification of 11 proteins correlating with adventitious root development. *Plant Physiol*, **140**, 349-364.

Spiess, A.N., Mueller, N. and Ivell, R. (2003) Amplified RNA degradation in T7-amplification methods results in biased microarray hybridizations. *BMC Genomics*, **4**, 44.

Stals, H. and Inze, D. (2001) When plant cells decide to divide. *Trends Plant Sci*, **6**, 359-364.

Staswick, P.E., Serban, B., Rowe, M., Tiryaki, I., Maldonado, M.T., Maldonado, M.C. and Suza, W. (2005) Characterization of an Arabidopsis enzyme family that conjugates amino acids to indole-3-acetic acid. *Plant Cell*, **17**, 616-627.

Staswick, P.E., Tiryaki, I. and Rowe, M.L. (2002) Jasmonate response locus JAR1 and several related Arabidopsis genes encode enzymes of the firefly luciferase superfamily that show activity on jasmonic, salicylic, and indole-3-acetic acids in an assay for adenylation. *Plant Cell*, **14**, 1405-1415.

Stevens, C. and La Thangue, N.B. (2004) The emerging role of E2F-1 in the DNA damage response and checkpoint control. *DNA Repair (Amst)*, **3**, 1071-1079.

Stoutjesdijk, P.A., Singh, S.P., Liu, Q., Hurlstone, C.J., Waterhouse, P.A. and Green, A.G. (2002) hpRNA-mediated targeting of the Arabidopsis FAD2 gene gives highly efficient and stable silencing. *Plant Physiol*, **129**, 1723-1731.

Sugimoto-Shirasu, K., Stacey, N.J., Corsar, J., Roberts, K. and McCann, M.C. (2002) DNA topoisomerase VI is essential for endoreduplication in Arabidopsis. *Curr Biol*, **12**, 1782-1786.

Sundaresan, V., Springer, P., Volpe, T., Haward, S., Jones, J.D., Dean, C., Ma, H. and

Martienssen, R. (1995) Patterns of gene action in plant development revealed by enhancer trap and gene trap transposable elements. *Genes Dev*, **9**, 1797-1810.

Szymanski, D.B., Jilk, R.A., Pollock, S.M. and Marks, M.D. (1998) Control of GL2 expression in Arabidopsis leaves and trichomes. *Development*, **125**, 1161-1171.

Szymanski, D.B., Lloyd, A.M. and Marks, M.D. (2000) Progress in the molecular genetic analysis of trichome initiation and morphogenesis in Arabidopsis. *Trends Plant Sci*, **5**, 214-219.

Telfer, A., Bollman, K.M. and Poethig, R.S. (1997) Phase change and the regulation of trichome distribution in Arabidopsis thaliana. *Development*, **124**, 645-654.

Thimm, O., Blasing, O., Gibon, Y., Nagel, A., Meyer, S., Kruger, P., Selbig, J., Muller, L.A., Rhee, S.Y. and Stitt, M. (2004) MAPMAN: a user-driven tool to display genomics data sets onto diagrams of metabolic pathways and other biological processes. *Plant J*, **37**, 914-939.

Thimm, O., Essigmann, B., Kloska, S., Altmann, T. and Buckhout, T.J. (2001) Response of Arabidopsis to iron deficiency stress as revealed by microarray analysis. *Plant Physiol*, **127**, 1030-1043.

Titarenko, E., Rojo, E., Leon, J. and Sanchez-Serrano, J.J. (1997) Jasmonic acid-dependent and -independent signaling pathways control wound-induced gene activation in Arabidopsis thaliana. *Plant Physiol*, **115**, 817-826.

Tomos, A.D. and Sharrock, R.A. (2001) Cell sampling and analysis (SiCSA): metabolites measured at single cell resolution. *J Exp Bot*, **52**, 623-630.

Traas, J., Hulskamp, M., Gendreau, E. and Hofte, H. (1998) Endoreduplication and development: rule without dividing? *Curr Opin Plant Biol*, **1**, 498-503.

Trehin, C., Planchais, S., Glab, N., Perennes, C., Tregear, J. and Bergounioux, C. (1998) Cell cycle regulation by plant growth regulators: involvement of auxin and cytokinin in the re-entry of Petunia protoplasts into the cell cycle. *Planta*, **206**, 215-224.

Van Gelder, R.N., von Zastrow, M.E., Yool, A., Dement, W.C., Barchas, J.D. and Eberwine, J.H. (1990) Amplified RNA synthesized from limited quantities of heterogeneous cDNA. *Proc Natl Acad Sci U S A*, **87**, 1663-1667.

Vandepoele, K., Raes, J., De Veylder, L., Rouze, P., Rombauts, S. and Inze, D. (2002) Genome-wide analysis of core cell cycle genes in Arabidopsis. *Plant Cell*, **14**, 903-916.

Vandepoele, K., Vlieghe, K., Florquin, K., Hennig, L., Beemster, G.T., Gruissem, W., Van de Peer, Y., Inze, D. and De Veylder, L. (2005) Genome-wide identification of potential plant E2F target genes. *Plant Physiol*, **139**, 316-328.

Vaskova D, Spak J, Klerks MM, Schoen CD, Thompson JR, Jelkmann W. (2004) Real-time NASBA for detection of strawberry vein banding virus. *Eur J Plant Pathol,* **110,** 213–221

Vervilet G., Holsters m., Teuchy H., Van Montagu M. And Schell J. (1975) Characterization of different plaque-forming and defective temperate phages in Agrobacterium. J Gen Virol **26**, 33-48

Vitzthum, F., Geiger, G., Bisswanger, H., Brunner, H. and Bernhagen, J. (1999) A quantitative fluorescence-based microplate assay for the determination of double-stranded DNA using SYBR Green I and a standard ultraviolet transilluminator gel imaging system. *Anal Biochem*, **276**, 59-64.

Voelckel C, Baldwin IT. (2003) Detecting herbivore-specific transcriptional responses in plants with multiple DDRT-PCR and subtractive library procedures. *Physiol Plantarum,* **118,** 240–252.

Volkov, R.A., Panchuk, II and Schoffl, F. (2003) Heat-stress-dependency and developmental modulation of gene expression: the potential of house-keeping genes as internal standards in mRNA expression profiling using real-time RT-PCR. *J Exp Bot*, **54**, 2343-2349.

Wagner, C., Sefkow, M. and Kopka, J. (2003) Construction and application of a mass spectral and

retention time index database generated from plant GC/EI-TOF-MS metabolite profiles. *Phytochemistry*, **62**, 887-900.

Walker, J.D., Oppenheimer, D.G., Concienne, J. and Larkin, J.C. (2000) SIAMESE, a gene controlling the endoreduplication cell cycle in Arabidopsis thaliana trichomes. *Development*, **127**, 3931-3940.

Wang, H., Qi, Q., Schorr, P., Cutler, A.J., Crosby, W.L. and Fowke, L.C. (1998) ICK1, a cyclin-dependent protein kinase inhibitor from Arabidopsis thaliana interacts with both Cdc2a and CycD3, and its expression is induced by abscisic acid. *Plant J*, **15**, 501-510.

Wang, G., Kong, H., Sun, Y., Zhang, X., Zhang, W., Altman, N., DePamphilis, C.W. and Ma, H. (2004) Genome-wide analysis of the cyclin family in Arabidopsis and comparative phylogenetic analysis of plant cyclin-like proteins. *Plant Physiol*, **135**, 1084-1099.

Waterhouse, P.M. and Helliwell, C.A. (2003) Exploring plant genomes by RNA-induced gene silencing. *Nat Rev Genet*, **4**, 29-38.

Weingartner, M., Criqui, M.C., Meszaros, T., Binarova, P., Schmit, A.C., Helfer, A., Derevier, A., Erhardt, M., Bogre, L. and Genschik, P. (2004) Expression of a nondegradable cyclin B1 affects plant development and leads to endomitosis by inhibiting the formation of a phragmoplast. *Plant Cell*, **16**, 643-657.

Wienkoop, S., Zoeller, D., Ebert, B., Simon-Rosin, U., Fisahn, J., Glinski, M. and Weckwerth, W. (2004) Cell-specific protein profiling in Arabidopsis thaliana trichomes: identification of trichome-located proteins involved in sulfur metabolism and detoxification. *Phytochemistry*, **65**, 1641-1649.

Weckwerth, W (2006) Metabolomics: Methods and Protocols, in *Methods in Molecular Biology, vol.**358*** (The Humana Press Inc., Totowa, NJ, USA)

Woeste K.E, Vogel J.P., Kieber J.J. (1999) Factors regulating ethylene biosynthesis in etiolated Arabidopsis thaliana seedlings. *PHYSIOLOGIA PLANTARUM*, **105**, 478-484.

Yoshizumi, T., Nagata, N., Shimada, H. and Matsui, M. (1999) An Arabidopsis cell cycle - dependent kinase-related gene, CDC2b, plays a role in regulating seedling growth in darkness. *Plant Cell*, **11**, 1883-1896.

Yu, Y., Steinmetz, A., Meyer, D., Brown, S. and Shen, W.H. (2003) The tobacco A-type cyclin, Nicta;CYCA3;2, at the nexus of cell division and differentiation. *Plant Cell*, **15**, 2763-2777.

Yu, Y.B. and Yang, S.F. (1979) Auxin-induced Ethylene Production and Its Inhibition by Aminoethyoxyvinylglycine and Cobalt Ion. *Plant Physiol*, **64**, 1074-1077.

Zhang, K., Letham, D.S. and John, P.C. (1996) Cytokinin controls the cell cycle at mitosis by stimulating the tyrosine dephosphorylation and activation of p34cdc2-like H1 histone kinase. *Planta*, **200**, 2-12.

Zimmermann, P., Hirsch-Hoffmann, M., Hennig, L. and Gruissem, W. (2004) GENEVESTIGATOR. Arabidopsis microarray database and analysis toolbox. *Plant Physiol*, **136**, 2621-2632.

APPENDIX A

Description of vectors used in this work

Vector	Description	Source
pDONR207	GATEWAY™ Entry vector for PCR products possessing attB recombination sites; Gen^R	Invitrogen
pCR®8/GW/TOPO®	GATEWAY™ Entry vector for TOPO® TA cloning; Spn^R	Invitrogen
pMDC162	GATEWAY™ compatible plant transformation vector for construction of promoter-GUS fusions; contains Kan^R in bacteria and $Hygromycin^R$ in plants	ABRC DNA Stock Center (vector created by M. Curtis; Curtis and Grossniklaus, 2003)

Restriction maps of used vectors

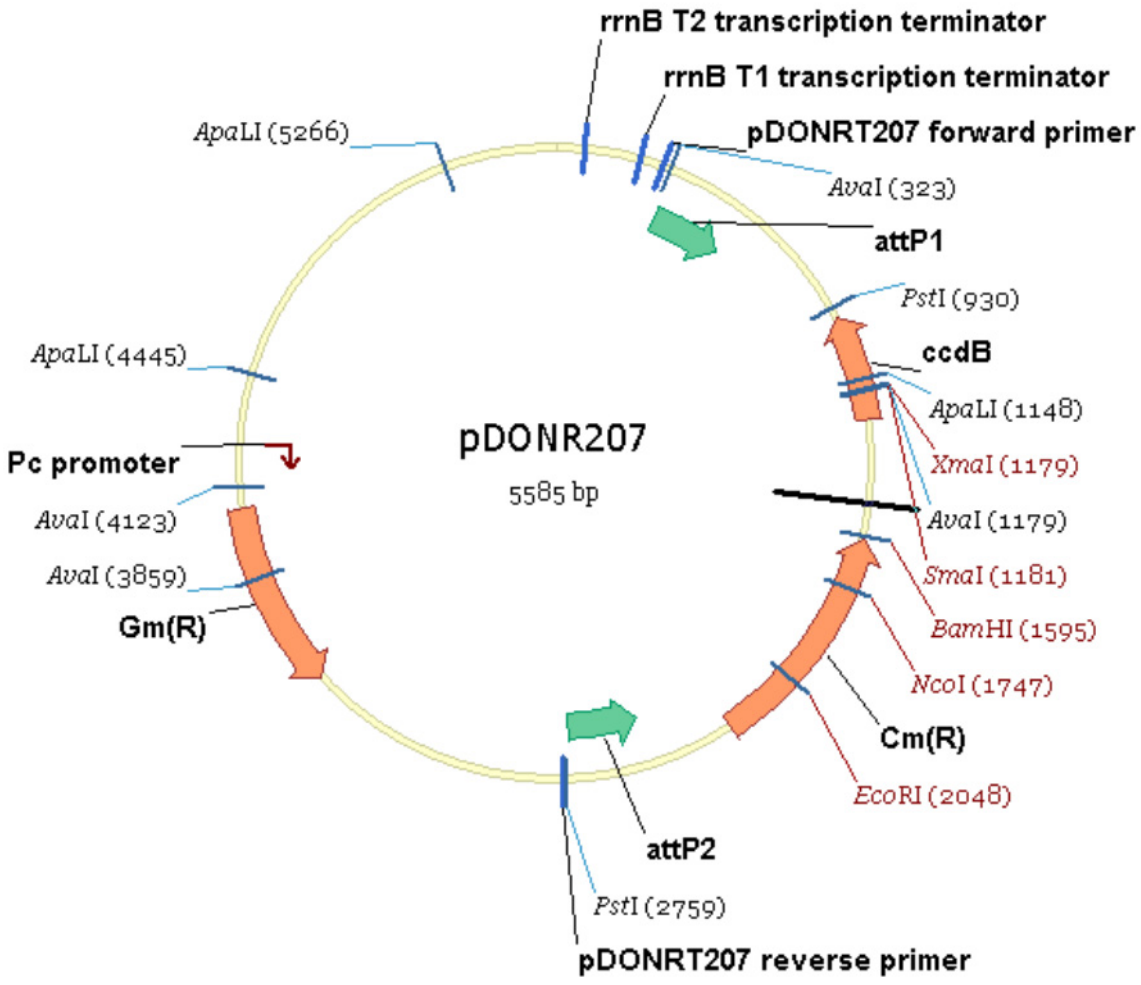

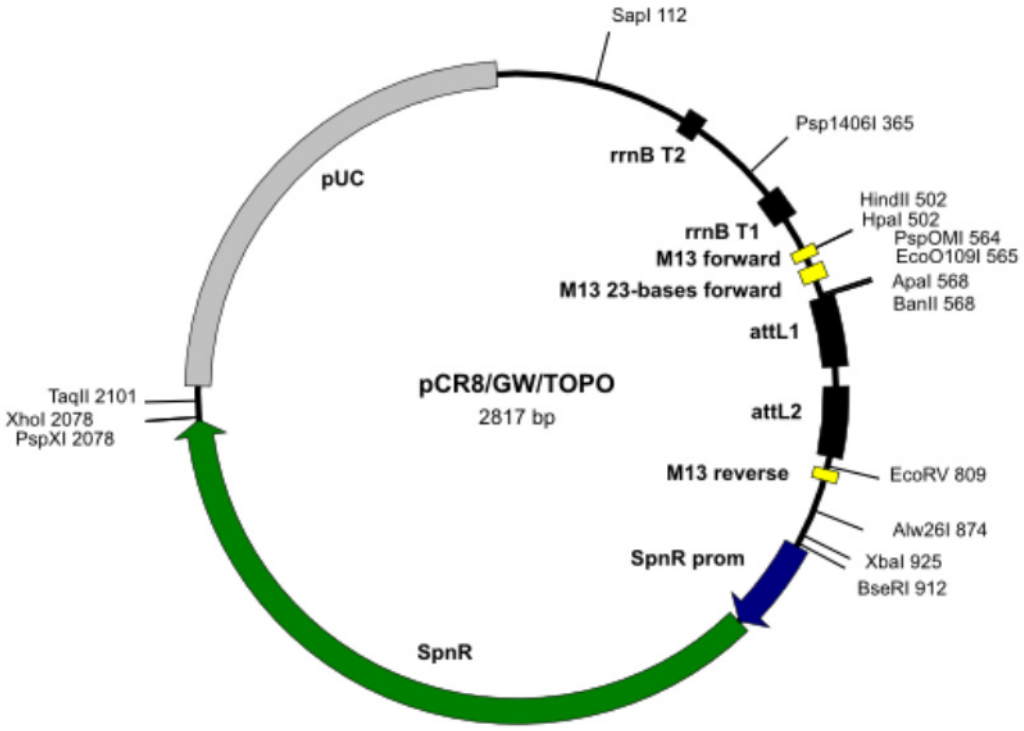
SapI 112
Psp1406I 365
rrnB T2
pUC
HindII 502
HpaI 502
PspOMI 564
EcoO109I 565
rrnB T1
M13 forward
M13 23-bases forward
ApaI 568
BanII 568
attL1
pCR8/GW/TOPO
2817 bp
attL2
TaqII 2101
XhoI 2078
PspXI 2078
M13 reverse
EcoRV 809
Alw26I 874
SpnR prom
XbaI 925
BseRI 912
SpnR

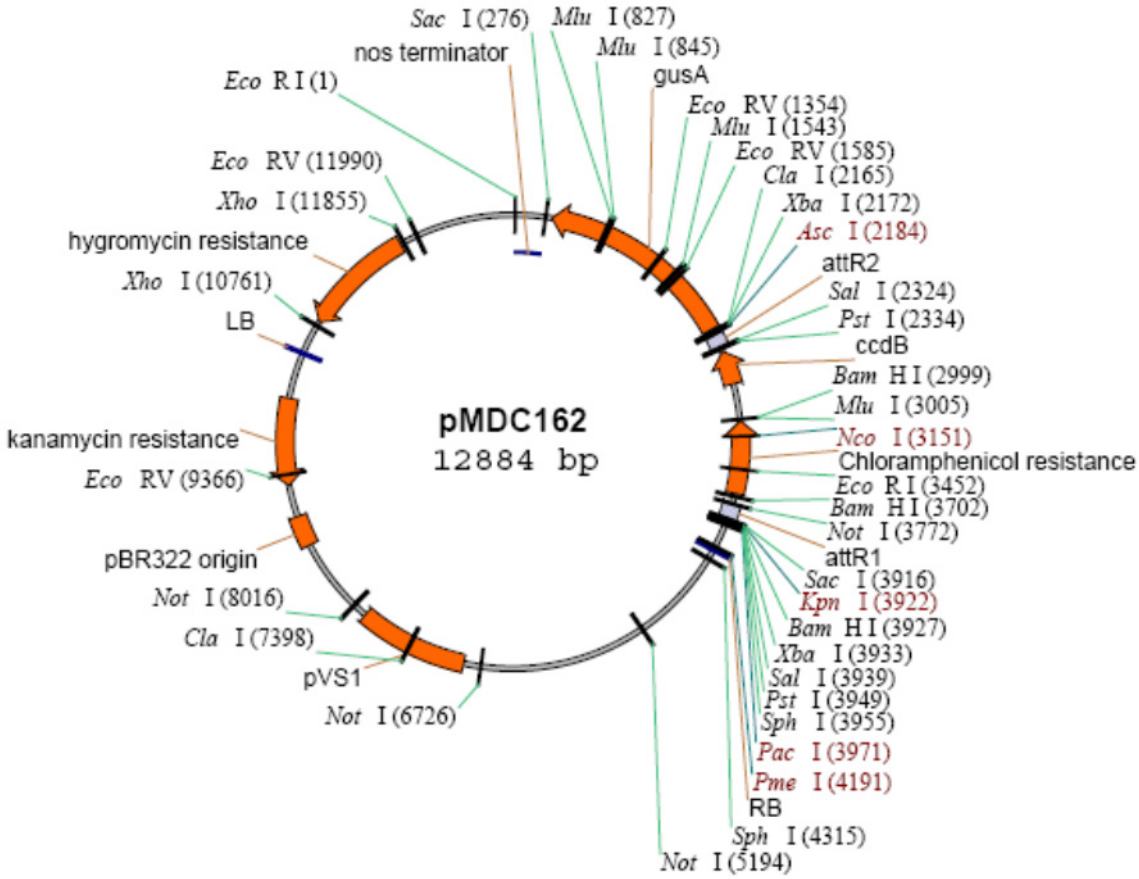
Sac I (276)
Mlu I (827)
nos terminator
Mlu I (845)
Eco R I (1)
gusA
Eco RV (1354)
Mlu I (1543)
Eco RV (11990)
Eco RV (1585)
Cla I (2165)
Xho I (11855)
Xba I (2172)
Asc I (2184)
hygromycin resistance
attR2
Xho I (10761)
Sal I (2324)
LB
Pst I (2334)
ccdB
Bam H I (2999)
pMDC162
12884 bp
Mlu I (3005)
kanamycin resistance
Nco I (3151)
Chloramphenicol resistance
Eco RV (9366)
Eco R I (3452)
Bam H I (3702)
Not I (3772)
pBR322 origin
attR1
Sac I (3916)
Not I (8016)
Kpn I (3922)
Bam H I (3927)
Cla I (7398)
Xba I (3933)
pVS1
Sal I (3939)
Pst I (3949)
Not I (6726)
Sph I (3955)
Pac I (3971)
Pme I (4191)
RB
Sph I (4315)
Not I (5194)

APPENDIX B

Commonly used primers not mentioned in the text

Primers for screening of the knock-out and RNAi lines:

Name	Sequence (5'- 3')	Name	Sequence (5'- 3')
SALK151766FWD RP	GTGAAGAACGCAGTGACACAC	SALK151766REV LP	CGTTCAAGATGACCAAATCTG
2726N2 Fwd	TCATCTCTCTCACAAATCATTTTCTCAG	2726smallREV	GAGGCTCGAGAAAGAGTGAT
SALK_002430 RP	TTGTTCTTGGGTTGTCGAAAC	SALK_002430 LP	AATGAAACTAAGTCCCACTCGC
1698cDNA F	CCTCCTCTATGCTTGCCGTA	1698cDNA R	TAGCCGTAGCCTGGAAGAAA
EF-fwd	TTGACAGGCGTTCTGGTAAGG	EF rev	CAGCGTCACCATTCTTCAAAAA
LBa1	TGGTTCACGTAGTGGGCCATCG	LBb1	GCGTGGACCGCTTGCTGCAACT
Agri 51	CAACCACGTCTTCAAAGCAA	Agri 56	CTGGGGTACCGAATTCCTC
Agri 64	CTTGCGCTGCAGTTATCATC	Agri 69	AGGCGTCTCGCATATCTCAT
SALK_032670 RP	TTCTGGAATTGCACCTCTCTG	SALK_032670 LP	GGGTTGCAACAGACAAAGAAC
GT_5_20762 RP	TGGATATTGAGTTTTAGTTTGGC	GT_5_20762 LP	TCTTGAATTGTTTATTTTTCGTCG
SALK_042431 RP	CCTTAAACCATGTGCAAAACC	SALK_042431 LP	AGGGGCAATTTCGTCAATATC
GABI_218B05 RP	ATGGGCATTCTGGTTGTTTC	GABI_218B05 LP	ATGATATGTGTTGCCACAGGG
GABI ori L	ATATTGACCATCATACTCATTGC		
1523cDNA FWD	AGCCTGAAACGTACCCAATG	1523cDNA REV	AAAAAGGGAACGAAGGGAGA

Primers used for sequencing of GATEWAY clones:

pDONRT207F	TCGCGTTAACGCTAGCATGGATCTC	pDONRT207R	GTAACATCAGAGATTTTGAGACAC
pMDC162Fwd	TAATCGCCTTGCAGCACATCCCC	pMDC162Rev	GGGGATGTGCTGCAAGGCGATTA
GUSfor pMDC162	GTAACGCGCTTTCCCACCAACG		

Primers used for real-time RT-PCR:

2726RT Fwd	TCTTGATGCCTGTGATGAGC	2726RT Rev	CTCCTGGAGTCTTGGATTCG
EF1alpha-fwd	TTGACAGGCGTTCTGGTAAGG	EF1alpha-rev	CAGCGTCACCATTCTTCAAAAA

APPENDIX C

Complete list of genes, differentially expressed between the compared cell types as revealed by filter array hybridization

Supplemental Table 1 List of the genes preferentially expressed in trichome initial cells when compared to pavement cells

AGI code	Annotation
AT1G03870	predicted GPI-anchored protein
AT1G04690	putative K+ channel, beta subunit
AT1G12090	pEARLI 1-like protein
AT1G23290	60s ribosomal protein l27a.
AT1G47900	mysoin-like protein
AT1G50480	10-formyltetrahydrofolate synthetase
AT1G62380	1-aminocyclopropane-1-carboxylate oxidase, putative / ACC oxidase, putative
AT1G62790	protease inhibitor/seed storage/lipid transfer protein (LTP) family protein
AT1G64470	ubiquitin, putative
AT1G64720	membrane related protein CP5, putative
AT1G72150	putative cytosolic factor protein
AT1G76810	translation initiation factor IF-2 like protein
AT2G03480	dehydration-responsive protein-related /// dehydration-responsive protein-related
AT2G31440	expressed protein /// endonuclease-related
AT2G38530	putative nonspecific lipid-transfer protein
AT2G47160	putative anion exchange protein
AT3G09440	heat-shock protein (At-hsc70-3)
AT3G11630	putative 2-cys peroxiredoxin
AT3G12120	omega-6-oleate desaturase
AT3G16980	RNA Polymerase II subunit 14.5 kD, putative
AT3G20320	mce-related family protein
AT3G22440	hydroxyproline-rich glycoprotein family protein
AT3G53420	plasma membrane intrinsic protein 2a
AT4G02380	late embryogenesis abundant 3 family protein / LEA3 family protein
AT4G16720	60S ribosomal protein L15 (RPL15A)
AT4G17900	zinc-binding family protein
AT4G20150	unknown protein
AT4G27260	GH3.5
AT5G04770	amino acid transporter-like protein
AT5G11730	expressed protein, contains Pfam profile PF03267: Arabidopsis protein of unknown function, DUF266
AT5G13240	expressed protein predicted proteins, Schizosaccharomyces pombe
AT5G14540	proline-rich family protein
AT5G15230	GASA4
AT5G17920	5-methyltetrahydropteroyltriglutamate--homocysteine S-methyltransferase
AT5G44790	copper-transporting ATPase RAN1 (RESPONSIVE-TO-ANTAGONIST 1)
AT5G45930	magnesium chelatase subunit of protochlorophyllide reductase
AT5G52920	pyruvate kinase
AT5G53460	NADH-dependent glutamate synthase

Supplemental Table 2 List of the genes more highly expressed in mature trichome cells in comparison to pavement cells

AGI code	Annotation
AT1G07640	Dof-type zinc finger domain-containing protein
AT1G20900	DNA-binding protein-related
AT1G21410	F-box family protein
AT1G21680	expressed protein
AT1G28230	purine permease (PUP1)
AT1G35580	beta-fructofuranosidase, putative / invertase, putative / saccharase, putative / beta-fructosidase, putative
AT1G48750	delta-adaptin, putative
AT1G59650	expressed protein
AT1G67870	glycine-rich protein
AT1G70560	alliinase C-terminal domain-containing protein
AT1G78150	expressed protein
AT2G03640	nuclear transport factor 2 (NTF2) family protein
AT2G14910	expressed protein
AT2G22780	malate dehydrogenase, glyoxysomal, putative
AT2G43340	unknown protein
AT2G47980	expressed protein
AT3G09200	60S acidic ribosomal protein P0 (RPP0B)
AT3G11230	yippee family protein
AT3G17100	expressed protein
AT3G22440	hydroxyproline-rich glycoprotein family protein
AT3G23580	ribonucleoside-diphosphate reductase small chain / ribonucleotide reductase
AT3G51010	expressed protein
AT4G11850	phospholipase D gamma 2 / PLD gamma 2 (PLDGAMMA2) /// phospholipase D gamma 1 / PLD gamma 1 (PLDGAMMA1)
AT4G22710	cytochrome P450 family protein
AT4G27260	auxin-responsive GH3 family protein
AT5G13240	expressed protein
AT5G45820	CBL-interacting protein kinase 20 (CIPK20)
AT5G59310	lipid transfer protein 4 (LTP4)
AT5G62390	calmodulin-binding family protein
AT5G63600	flavonol synthase, putative
AT5G66400	dehydrin (RAB18)

Supplemental Table 3 List of the genes preferentially expressed in mature trichomes in comparison to trichome initial cells

AGI code	Annotation
AT5G66850	protein kinase family protein
AT1G01430	expressed protein
AT1G01620	plasma membrane intrinsic protein 1C (PIP1C) / aquaporin PIP1.3 (PIP1.3) / transmembrane protein B (TMPB)
AT1G02300	cathepsin B-like cysteine protease, putative
AT1G02780	60S ribosomal protein L19 (RPL19A)
AT1G02890	AAA-type ATPase family protein
AT1G03290	expressed protein
AT1G04820	tubulin alpha-2/alpha-4 chain (TUA2) /// tubulin alpha-2/alpha-4 chain (TUA4) /// tubulin alpha-6 chain (TUA6)
AT1G05010	1-aminocyclopropane-1-carboxylate oxidase / ACC oxidase / ethylene-forming enzyme (ACO) (EAT1)
AT1G05180	auxin-resistance protein AXR1 (AXR1)
AT1G05430	expressed protein
AT1G06040	zinc finger (B-box type) family protein / salt-tolerance protein (STO)
AT1G06780	glycosyl transferase family 8 protein
AT1G07010	calcineurin-like phosphoesterase family protein
AT1G07530	scarecrow-like transcription factor 14 (SCL14)
AT1G07600	pentatricopeptide (PPR) repeat-containing protein /// metallothionein-like protein 1C (MT-1C)
AT1G07640	Dof-type zinc finger domain-containing protein
AT1G07790	histone H2B, putative
AT1G07890	L-ascorbate peroxidase 1, cytosolic (APX1)
AT1G07960	thioredoxin family protein
AT1G08200	hypothetical protein
AT1G08340	rac GTPase activating protein, putative
AT1G09330	expressed protein
AT1G09460	glucan endo-1,3-beta-glucosidase-related
AT1G09560	germin-like protein (GLP4) (GLP5)
AT1G09780	2,3-biphosphoglycerate-independent phosphoglycerate mutase, putative / phosphoglyceromutase, putative
AT1G10170	NF-X1 type zinc finger family protein
AT1G10470	two-component responsive regulator / response regulator 4 (ARR4)
AT1G11410	S-locus protein kinase, putative
AT1G11650	RNA-binding protein 45 (RBP45), putative
AT1G11680	obtusifoliol 14-demethylase (CYP51)
AT1G11840	lactoylglutathione lyase, putative / glyoxalase I, putative
AT1G11880	expressed protein
AT1G11910	aspartyl protease family protein
AT1G12550	oxidoreductase family protein
AT1G12740	cytochrome P450 family protein
AT1G12840	vacuolar ATP synthase subunit C (VATC) / V-ATPase C subunit / vacuolar proton pump C subunit (DET3)
AT1G13250	glycosyl transferase family 8 protein
AT1G14840	expressed protein
AT1G15020	thioredoxin family protein
AT1G15040	expressed protein
AT1G15230	expressed protein
AT1G15400	expressed protein
AT1G15820	chlorophyll A-B binding protein, chloroplast (LHCB6)
AT1G16040	expressed protein
AT1G16240	syntaxin 51 (SYP51)
AT1G19530	expressed protein

AT1G20020	ferredoxin--NADP(+) reductase, putative / adrenodoxin reductase, putative
AT1G21120	O-methyltransferase, putative /// O-methyltransferase, putative
AT1G21630	calcium-binding EF hand family protein
AT1G21680	expressed protein
AT1G21750	protein disulfide isomerase, putative
AT1G22740	Ras-related protein (RAB7) / AtRab75 / small GTP-binding protein, putative
AT1G22850	expressed protein
AT1G23310	glutamate:glyoxylate aminotransferase 1 (GGT1)
AT1G23390	kelch repeat-containing F-box family protein
AT1G26920	expressed protein
AT1G27000	bZIP family transcription factor
AT1G27320	histidine kinase (AHK3)
AT1G28140	expressed protein
AT1G28230	purine permease (PUP1)
AT1G29090	peptidase C1A papain family protein
AT1G30110	diadenosine 5',5'''-P1,P4-tetraphosphate hydrolase, putative
AT1G30130	expressed protein
AT1G30720	FAD-binding domain-containing protein /// FAD-binding domain-containing protein
AT1G30750	expressed protein
AT1G30890	integral membrane HRF1 family protein
AT1G34130	oligosaccharyl transferase STT3 subunit, putative
AT1G36310	expressed protein
AT1G36380	expressed protein
AT1G37130	nitrate reductase 2 (NR2)
AT1G43190	polypyrimidine tract-binding protein, putative / heterogeneous nuclear ribonucleoprotein, putative
AT1G43900	protein phosphatase 2C, putative / PP2C, putative
AT1G47210	cyclin family protein
AT1G48350	ribosomal protein L18 family protein
AT1G48380	root hair initiation protein root hairless 1 (RHL1)
AT1G48750	delta-adaptin, putative
AT1G49720	ABA-responsive element-binding protein / abscisic acid responsive elements-binding factor (ABRE)
AT1G51590	mannosyl-oligosaccharide 1,2-alpha-mannosidase, putative
AT1G52600	signal peptidase, putative
AT1G53590	C2 domain-containing protein
AT1G54080	oligouridylate-binding protein, putative
AT1G54130	RelA/SpoT protein, putative (RSH3)
AT1G54320	LEM3 (ligand-effect modulator 3) family protein / CDC50 family protein
AT1G54630	acyl carrier protein, chloroplast, putative / ACP, putative /// acyl carrier protein 3, chloroplast (ACP-3)
AT1G54740	expressed protein
AT1G55150	DEAD box RNA helicase, putative (RH20)
AT1G55360	expressed protein
AT1G56190	phosphoglycerate kinase, putative
AT1G56340	calreticulin 1 (CRT1)
AT1G59650	expressed protein
AT1G60940	serine/threonine protein kinase, putative
AT1G60950	g ferredoxin, chloroplast (PETF)
AT1G60960	metal transporter, putative (IRT3)
AT1G61670	expressed protein
AT1G61870	pentatricopeptide (PPR) repeat-containing protein
AT1G63370	flavin-containing monooxygenase family protein / FMO family protein
AT1G63780	brix domain-containing protein
AT1G64230	ubiquitin-conjugating enzyme, putative
AT1G64950	cytochrome P450, putative /// cytochrome P450, putative
AT1G65040	zinc finger (C3HC4-type RING finger) family protein

AT1G65230	expressed protein
AT1G65660	zinc knuckle (CCHC-type) family protein
AT1G65980	peroxiredoxin type 2, putative /// peroxiredoxin type 2, putative /// peroxiredoxin type 2, putative
AT1G66140	zinc finger (C2H2 type) family protein
AT1G66200	glutamine synthetase, putative
AT1G66260	RNA and export factor-binding protein, putative
AT1G66340	ethylene receptor 1 (ETR1)
AT1G67330	expressed protein
AT1G67870	glycine-rich protein
AT1G67940	ABC transporter family protein
AT1G68190	zinc finger (B-box type) family protein
AT1G68780	leucine-rich repeat family protein
AT1G70160	expressed protein
AT1G70560	alliinase C-terminal domain-containing protein
AT1G70900	expressed protein
AT1G71070	glycosyltransferase family 14 protein / core-2/I-branching enzyme family protein
AT1G72190	oxidoreductase family protein
AT1G73190	tonoplast intrinsic protein, alpha / alpha-TIP (TIP3.1)
AT1G73500	mitogen-activated protein kinase kinase (MAPKK), putative (MKK9)
AT1G73740	glycosyl transferase family 28 protein
AT1G74270	60S ribosomal protein L35a (RPL35aC)
AT1G74470	geranylgeranyl reductase
AT1G74710	isochorismate synthase 1 (ICS1) / isochorismate mutase
AT1G74950	expressed protein
AT1G75200	flavodoxin family protein / radical SAM domain-containing protein
AT1G75410	BEL1-like homeodomain 3 protein (BLH3)
AT1G76180	dehydrin (ERD14)
AT1G77530	O-methyltransferase family 2 protein /// O-methyltransferase family 2 protein
AT1G78100	F-box family protein
AT1G78150	expressed protein
AT1G78660	gamma-glutamyl hydrolase, putative / gamma-Glu-X carboxypeptidase, putative / conjugase, putative
AT1G78730	hypothetical protein
AT1G79440	succinate-semialdehyde dehydrogenase (SSADH1)
AT1G79920	heat shock protein 70, putative / HSP70, putative /// heat shock protein, putative
AT1G80300	adenine nucleotide translocase
AT1G80550	pentatricopeptide (PPR) repeat-containing protein
AT2G01520	major latex protein-related / MLP-related /// major latex protein-related / MLP-related
AT2G01670	MutT/nudix family protein
AT2G02220	leucine-rich repeat transmembrane protein kinase, putative
AT2G03440	nodulin-related| similar to Early nodulin 12B precursor (N-12B)
AT2G03640	nuclear transport factor 2 (NTF2) family protein / RNA recognition motif (RRM)-containing protein
AT2G06850	xyloglucan:xyloglucosyl transferase / xyloglucan endotransglycosylase / endo-xyloglucan transferase (EXT) (EXGT-A1)
AT2G13540	mRNA cap-binding protein (ABH1)
AT2G16380	SEC14 cytosolic factor family protein / phosphoglyceride transfer family protein
AT2G17870	cold-shock DNA-binding family protein
AT2G17990	expressed protein
AT2G18440	expressed protein
AT2G18700	glycosyl transferase family 20 protein / trehalose-phosphatase family protein
AT2G20000	cell division cycle family protein / CDC family protein
AT2G20520	fasciclin-like arabinogalactan-protein (FLA6)
AT2G20580	26S proteasome regulatory subunit S2 (RPN1)
AT2G21160	translocon-associated protein alpha (TRAP alpha) family protein
AT2G22420	peroxidase 17 (PER17) (P17)

AT2G22780	malate dehydrogenase, glyoxysomal, putative
AT2G25490	F-box family protein (FBL6)
AT2G25670	expressed protein
AT2G25950	expressed protein
AT2G25960	unknown protein
AT2G26080	glycine dehydrogenase (decarboxylating), putative / glycine decarboxylase, putative / glycine cleavage system P-protein, putative
AT2G26100	galactosyltransferase family protein|
AT2G26330	leucine-rich repeat protein kinase, putative (ERECTA)
AT2G28960	leucine-rich repeat protein kinase, putative
AT2G29890	villin 1 (VLN1)
AT2G30510	signal transducer of phototropic response (RPT2)
AT2G31090	expressed protein
AT2G31130	expressed protein
AT2G31710	expressed protein
AT2G32580	expressed protein
AT2G34330	expressed protein|
AT2G34680	leucine-rich repeat family protein
AT2G34780	expressed protein
AT2G36060	ubiquitin-conjugating enzyme family protein
AT2G36120	pseudogene, glycine-rich protein
AT2G36530	enolase
AT2G36580	pyruvate kinase, putative /// pyruvate kinase, putative
AT2G37170	aquaporin (plasma membrane intrinsic protein 2B)
AT2G37220	29 kDa ribonucleoprotein, chloroplast, putative / RNA-binding protein cp29, putative
AT2G37520	PHD finger family protein
AT2G37660	expressed protein
AT2G38090	myb family transcription factor
AT2G38700	mevalonate diphosphate decarboxylase (MVD1)
AT2G39000	GCN5-related N-acetyltransferase (GNAT) family protein
AT2G39050	hydroxyproline-rich glycoprotein family protein
AT2G39450	cation efflux family protein
AT2G39470	photosystem II reaction center PsbP family protein
AT2G39770	GDP-mannose pyrophosphorylase (GMP1)
AT2G40280	dehydration-responsive family protein
AT2G40470	LOB domain protein 15 / lateral organ boundaries domain protein 15 (LBD15)
AT2G40890	cytochrome P450 98A3, putative (CYP98A3)
AT2G40920	unknown protein
AT2G40970	myb family transcription factor
AT2G41380	embryo-abundant protein-related
AT2G41430	dehydration-induced protein (ERD15)
AT2G41560	calcium-transporting ATPase 4, plasma membrane-type / Ca2+-ATPase, isoform 4 (ACA4)
AT2G42210	mitochondrial import inner membrane translocase subunit Tim17/Tim22/Tim23 family protein
AT2G42890	RNA recognition motif (RRM)-containing protein
AT2G43030	ribosomal protein L3 family protein
AT2G43090	aconitase C-terminal domain-containing protein
AT2G43150	proline-rich extensin-like family protein
AT2G43340	unknown protein
AT2G43400	electron transfer flavoprotein-ubiquinone oxidoreductase family protein
AT2G43610	glycoside hydrolase family 19 protein
AT2G43670	glycosyl hydrolase family protein 17
AT2G44100	Rab GDP dissociation inhibitor (GDI1)
AT2G44410	unknown protein
AT2G44610	Ras-related GTP-binding protein, putative
AT2G44840	ethylene-responsive element-binding protein, putative
AT2G45520	expressed protein

AT2G45530	zinc finger (C3HC4-type RING finger) family protein
AT2G45960	plasma membrane intrinsic protein 1B (PIP1B) / aquaporin PIP1.2 (PIP1.2) / transmembrane protein A (TMPA)
AT2G46820	expressed protein
AT2G47000	multidrug resistant (MDR) ABC transporter, putative
AT2G47830	cation efflux family protein / metal tolerance protein, putative (MTPc1)
AT2G47910	expressed protein
AT2G47980	expressed protein
AT3G01470	homeobox-leucine zipper protein 5 (HAT5) / HD-ZIP protein 5 / HD-ZIP protein (HB-1)
AT3G01500	carbonic anhydrase 1, chloroplast / carbonate dehydratase 1 (CA1)
AT3G02050	potassium transporter (KUP3)
AT3G02090	mitochondrial processing peptidase beta subunit, putative
AT3G02470	adenosylmethionine decarboxylase family protein
AT3G02520	14-3-3 protein GF14 nu (GRF7)
AT3G03870	expressed protein
AT3G03890	expressed protein
AT3G03960	chaperonin, putative
AT3G04630	expressed protein
AT3G05500	rubber elongation factor (REF) family protein
AT3G05520	F-actin capping protein alpha subunit family protein
AT3G05900	neurofilament protein-related
AT3G05920	heavy-metal-associated domain-containing protein
AT3G05970	long-chain-fatty-acid--CoA ligase / long-chain acyl-CoA synthetase (LACS6)
AT3G06580	galactokinase (GAL1)
AT3G07020	UDP-glucose:sterol glucosyltransferase (UGT80A2)
AT3G07200	zinc finger (C3HC4-type RING finger) family protein
AT3G07350	expressed protein
AT3G09200	60S acidic ribosomal protein P0 (RPP0B)
AT3G09570	expressed protein
AT3G09820	adenosine kinase 1 (ADK1) / adenosine 5'-phosphotransferase 1
AT3G09840	cell division cycle protein 48 (CDC48A) (CDC48)
AT3G09970	calcineurin-like phosphoesterase family protein
AT3G10350	anion-transporting ATPase family protein
AT3G11130	clathrin heavy chain, putative /// clathrin heavy chain, putative
AT3G11230	yippee family protein
AT3G12150	expressed protein
AT3G12380	actin/actin-like family protein
AT3G13800	metallo-beta-lactamase family protein
AT3G14280	expressed protein
AT3G14400	ubiquitin-specific protease 25 (UBP25)
AT3G14940	phosphoenolpyruvate carboxylase, putative / PEP carboxylase, putative
AT3G15070	zinc finger (C3HC4-type RING finger) family protein
AT3G15640	cytochrome c oxidase family protein
AT3G16050	stress-responsive protein, putative
AT3G16400	jacalin lectin family protein
AT3G16950	dihydrolipoamide dehydrogenase 1, plastidic / lipoamide dehydrogenase 1 (PTLPD1)
AT3G17100	expressed protein
AT3G17510	CBL-interacting protein kinase 1 (CIPK1)
AT3G17800	expressed protein
AT3G17900	expressed protein
AT3G17980	C2 domain-containing protein
AT3G18035	histone H1/H5 family protein
AT3G18050	expressed protein
AT3G18490	aspartyl protease family protein
AT3G18780	actin 2 (ACT2)
AT3G20050	T-complex protein 1 alpha subunit / TCP-1-alpha / chaperonin (CCT1)
AT3G20130	cytochrome P450 family protein

AT3G21865	expressed protein
AT3G22440	hydroxyproline-rich glycoprotein family protein
AT3G23580	ribonucleoside-diphosphate reductase small chain / ribonucleotide reductase
AT3G23660	transport protein, putative
AT3G24070	zinc knuckle (CCHC-type) family protein
AT3G24830	60S ribosomal protein L13A (RPL13aB)
AT3G25480	rhodanese-like domain-containing protein
AT3G25500	formin homology 2 domain-containing protein / FH2 domain-containing protein
AT3G25585	aminoalcoholphosphotransferase, putative
AT3G26720	glycosyl hydrolase family 38 protein
AT3G27390	expressed protein
AT3G27430	20S proteasome beta subunit B (PBB1)
AT3G27850	50S ribosomal protein L12-1, chloroplast (CL12-A) /// 50S ribosomal protein L12-3, chloroplast (CL12-C)
AT3G28300	integrin-related protein 14a
AT3G28450	leucine-rich repeat transmembrane protein kinase, putative
AT3G32930	expressed protein
AT3G43980	40S ribosomal protein S29 (RPS29A)
AT3G44600	peptidyl-prolyl cis-trans isomerase cyclophilin-type family protein
AT3G46060	Ras-related protein (ARA-3) / small GTP-binding protein, putative
AT3G47550	zinc finger (C3HC4-type RING finger) family protein
AT3G47640	basic helix-loop-helix (bHLH) family protein
AT3G47650	bundle-sheath defective protein 2 family / bsd2 family
AT3G48100	two-component responsive regulator / response regulator 5 (ARR5) / response reactor 2 (RR2)
AT3G50820	oxygen-evolving enhancer protein, chloroplast, putative / 33 kDa subunit of oxygen evolving system of photosystem II, putative (PSBO2)
AT3G51010	expressed protein
AT3G51610	expressed protein
AT3G51830	phosphoinositide phosphatase family protein
AT3G52150	RNA recognition motif (RRM)-containing protein
AT3G52250	myb family transcription factor
AT3G52930	fructose-bisphosphate aldolase, putative
AT3G53420	plasma membrane intrinsic protein 2A (PIP2A) / aquaporin PIP2.1 (PIP2.1)
AT3G54030	protein kinase family protein
AT3G54920	pectate lyase, putative / powdery mildew susceptibility protein (PMR6)
AT3G54980	pentatricopeptide (PPR) repeat-containing protein
AT3G55120	chalcone-flavanone isomerase / chalcone isomerase (CHI)
AT3G56010	expressed protein
AT3G56230	speckle-type POZ protein-related
AT3G56360	expressed protein
AT3G57050	cystathionine beta-lyase, chloroplast / beta-cystathionase / cysteine lyase (CBL)
AT3G57290	eukaryotic translation initiation factor 3E / eIF3e (TIF3E1)
AT3G58500	serine threonine protein phosphatase PP2A-3 catalytic subunit
AT3G58840	expressed protein
AT3G59320	putative protein hypothetical protein SPCC320.08
AT3G59910	expressed protein
AT3G59920	Rab GDP dissociation inhibitor (GDI2)
AT3G60340	palmitoyl protein thioesterase family protein
AT3G60350	armadillo/beta-catenin repeat family protein / F-box family protein
AT3G60650	expressed protein
AT3G60690	auxin-responsive family protein
AT3G60770	40S ribosomal protein S13 (RPS13A)
AT3G61850	Dof zinc finger protein DAG1 / Dof affecting germination 1 (DAG1) / transcription factor BBFa (BBFA)
AT3G61890	homeobox-leucine zipper protein 12 (HB-12) / HD-ZIP transcription factor 12
AT3G62830	c NAD-dependent epimerase/dehydratase family protein

AT3G62840	small nuclear ribonucleoprotein D2, putative / snRNP core protein D2, putative / Sm protein D2, putative
AT3G63030	putative protein
AT3G63120	cyclin family protein
AT4G00350	MATE efflux family protein
AT4G00400	phospholipid/glycerol acyltransferase family protein
AT4G01050	hydroxyproline-rich glycoprotein family protein
AT4G01100	mitochondrial substrate carrier family protein
AT4G02450	glycine-rich protein
AT4G02930	elongation factor Tu, putative / EF-Tu, putative
AT4G03080	kelch repeat-containing serine/threonine phosphoesterase family protein
AT4G05320	polyubiquitin (UBQ10) (SEN3)
AT4G08180	oxysterol-binding family protein
AT4G08320	tetratricopeptide repeat (TPR)-containing protein
AT4G09670	oxidoreductase family protein
AT4G09960	MADS-box protein (AGL11)
AT4G10340	chlorophyll A-B binding protein CP26, chloroplast / light-harvesting complex II protein 5 / LHCIIc (LHCB5)
AT4G11010	nucleoside diphosphate kinase 3, mitochondrial (NDK3)
AT4G11850	phospholipase D gamma 2 / PLD gamma 2 (PLDGAMMA2) /// phospholipase D gamma 1 / PLD gamma 1 (PLDGAMMA1)
AT4G11970	YT521-B-like family protein
AT4G11980	MutT/nudix family protein
AT4G13020	serine/threonine protein kinase (MHK)
AT4G13940	adenosylhomocysteinase / S-adenosyl-L-homocysteine hydrolase / AdoHcyase (SAHH)
AT4G14020	rapid alkalinization factor (RALF) family protein
AT4G14360	dehydration-responsive protein-related
AT4G14400	ankyrin repeat family protein
AT4G14900	hydroxyproline-rich glycoprotein family protein
AT4G15330	cytochrome P450 family protein
AT4G15390	transferase family protein
AT4G15410	UBX domain-containing protein
AT4G16060	expressed protein
AT4G16430	basic helix-loop-helix (bHLH) family protein
AT4G16720	60S ribosomal protein L15 (RPL15A)
AT4G17390	60S ribosomal protein L15 (RPL15B)
AT4G17480	palmitoyl protein thioesterase family protein
AT4G18480	magnesium-chelatase subunit chlI, chloroplast / Mg-protoporphyrin IX chelatase (CHLI) (CS) (CH42)
AT4G20260	DREPP plasma membrane polypeptide family protein
AT4G20330	transcription initiation factor-related
AT4G21210	expressed protein
AT4G21850	methionine sulfoxide reductase domain-containing protein / SeIR domain-containing protein
AT4G21930	putative protein
AT4G21980	autophagy 8a (APG8a)
AT4G22350	ubiquitin carboxyl-terminal hydrolase family protein /// ubiquitin carboxyl-terminal hydrolase family protein
AT4G22640	expressed protein| various predicted proteins
AT4G22670	tetratricopeptide repeat (TPR)-containing protein
AT4G22710	cytochrome P450 family protein
AT4G23700	cation/hydrogen exchanger, putative (CHX17)
AT4G24220	expressed protein
AT4G24680	expressed protein
AT4G25520	transcriptional co-regulator family protein
AT4G26480	KH domain-containing protein
AT4G26630	expressed protein
AT4G27630	expressed protein /// expressed protein /// importin beta-2 subunit family protein
AT4G27780	acyl-CoA binding protein 2 (ACBP2)

AT4G28990	RNA-binding protein-related
AT4G29790	expressed protein
AT4G30140	GDSL-motif lipase/hydrolase family protein
AT4G30190	ATPase 2, plasma membrane-type, putative / proton pump 2, putative / proton-exporting ATPase, putative
AT4G30390	expressed protein
AT4G30470	cinnamoyl-CoA reductase-related
AT4G31500	cytochrome P450 83B1 (CYP83B1)
AT4G32040	homeobox protein knotted-1 like 5 (KNAT5) / homeodomain containing protein 1 (H1)
AT4G32160	phox (PX) domain-containing protein
AT4G32410	cellulose synthase, catalytic subunit, putative
AT4G32470	ubiquinol-cytochrome C reductase complex 14 kDa protein, putative
AT4G32860	expressed protein|
AT4G34460	guanine nucleotide-binding protein beta subunit (GB1) / GTP-binding protein beta subunit (AGB1) / transducin
AT4G34860	beta-fructofuranosidase, putative / invertase, putative / saccharase, putative / beta-fructosidase, putative
AT4G35100	PIP2.8; putative plasma membrane intrinsic protein
AT4G35260	isocitrate dehydrogenase subunit 1 / NAD+ isocitrate dehydrogenase subunit 1
AT4G36500	expressed protein
AT4G36900	AP2 domain-containing protein RAP2.10 (RAP2.10)
AT4G37550	formamidase, putative / formamide amidohydrolase, putative
AT4G37870	phosphoenolpyruvate carboxykinase (ATP), putative / PEP carboxykinase, putative / PEPCK, putative
AT4G38060	expressed protein
AT4G38430	expressed protein
AT4G39260	glycine-rich RNA-binding protein 8 (GRP8) (CCR1)
AT4G39300	expressed protein
AT4G39460	mitochondrial substrate carrier family protein
AT4G39680	SAP domain-containing protein
AT4G39780	AP2 domain-containing transcription factor, putative
AT4G40060	homeobox-leucine zipper protein 16 (HB-16) / HD-ZIP transcription factor 16
AT5G01090	legume lectin family protein
AT5G01820	CBL-interacting protein kinase 14 (CIPK14)
AT5G02480	expressed protein
AT5G02500	heat shock cognate 70 kDa protein 1 (HSC70-1) (HSP70-1)
AT5G03400	hypothetical protein
AT5G04860	expressed protein
AT5G05100	expressed protein
AT5G06700	expressed protein
AT5G06870	polygalacturonase inhibiting protein 2 (PGIP2)
AT5G08170	porphyromonas-type peptidyl-arginine deiminase family protein
AT5G08450	expressed protein
AT5G08650	GTP-binding protein LepA, putative
AT5G09220	amino acid permease 2 (AAP2)
AT5G10450	14-3-3 protein GF14 lambda (GRF6) (AFT1)
AT5G10980	histone H3
AT5G11500	expressed protein
AT5G11920	glycosyl hydrolase family 32 protein
AT5G12840	CCAAT-binding transcription factor (CBF-B/NF-YA) family protein
AT5G13100	expressed protein
AT5G13800	hydrolase, alpha/beta fold family protein
AT5G14030	translocon-associated protein beta (TRAPB) family protein
AT5G14330	expressed protein
AT5G15850	zinc finger protein CONSTANS-LIKE 1 (COL1)
AT5G15910	dehydrogenase-related
AT5G16710	dehydroascorbate reductase, putative

AT5G17220	glutathione S-transferase, putative
AT5G17380	pyruvate decarboxylase family protein
AT5G18120	expressed protein
AT5G19180	ubiquitin activating enzyme, putative (ECR1)
AT5G19190	putative protein
AT5G19510	elongation factor 1B alpha-subunit 2 (eEF1Balpha2)
AT5G20250	raffinose synthase family protein / seed imbibition protein, putative (din10)
AT5G20290	40S ribosomal protein S8 (RPS8A)
AT5G20490	myosin, putative
AT5G20540	expressed protein
AT5G21170	5'-AMP-activated protein kinase beta-2 subunit, putative
AT5G22350	putative protein
AT5G22780	adaptin family protein
AT5G23060	expressed protein
AT5G24490	30S ribosomal protein, putative
AT5G25270	expressed protein
AT5G26000	myrosinase precursor
AT5G26260	meprin and TRAF homology domain-containing protein / MATH domain-containing protein
AT5G26340	hexose transporter, putative
AT5G26860	Lon protease homolog 2, mitochondrial
AT5G27890	expressed protein
AT5G29000	myb family transcription factor
AT5G35360	acetyl-CoA carboxylase, biotin carboxylase subunit (CAC2)
AT5G37600	glutamine synthetase, putative
AT5G37700	putative protein
AT5G38420	ribulose bisphosphate carboxylase small chain 2b p
AT5G38970	cytochrome P450, putative
AT5G38990	protein kinase family protein /// protein kinase family protein
AT5G39320	UDP-glucose 6-dehydrogenase, putative
AT5G39510	vesicle transport v-SNARE 11 (VTI11) / vesicle soluble NSF attachment protein receptor VTI1a (VTI1A)
AT5G39610	no apical meristem (NAM) family protein
AT5G39740	60S ribosomal protein L5 /// 60S ribosomal protein L5 (RPL5B)
AT5G39990	glycosyltransferase family 14 protein / core-2/I-branching enzyme family protein
AT5G40710	zinc finger (C2H2 type) family protein
AT5G41360	DNA repair protein and transcription factor, putative (XPB2)
AT5G42250	alcohol dehydrogenase, putative
AT5G42300	ubiquitin family protein
AT5G42560	abscisic acid-responsive HVA22 family protein
AT5G43370	inorganic phosphate transporter (PHT1) (PT1)
AT5G44080	bZIP transcription factor family protein
AT5G44810	expressed protein
AT5G44920	Toll-Interleukin-Resistance (TIR) domain-containing protein
AT5G45280	pectinacetylesterase, putative
AT5G45480	expressed protein
AT5G45510	leucine-rich repeat family protein
AT5G45620	26S proteasome regulatory subunit, putative (RPN9)
AT5G45820	CBL-interacting protein kinase 20 (CIPK20)
AT5G46020	expressed protein
AT5G46690	basic helix-loop-helix (bHLH) family protein
AT5G48480	expressed protein
AT5G49280	hydroxyproline-rich glycoprotein family protein
AT5G50920	ATP-dependent Clp protease ATP-binding subunit / ClpC
AT5G51490	pectinesterase family protein
AT5G51570	band 7 family protein
AT5G52470	fibrillarin 1 (FBR1) (FIB1) (SKIP7)
AT5G52840	NADH-ubiquinone oxidoreductase-related

AT5G52840	NADH-ubiquinone oxidoreductase-related
AT5G53460	glutamate synthase (NADH), chloroplast, putative
AT5G54370	late embryogenesis abundant protein-related / LEA protein-related
AT5G54590	protein kinase family protein
AT5G54660	heat shock protein-related
AT5G54890	expressed protein
AT5G56000	heat shock protein 81-4 (HSP81-4) /// heat shock protein, putative /// heat shock protein 81-2 (HSP81-2)
AT5G56010	heat shock protein, putative
AT5G57625	allergen V5/Tpx-1-related family protein
AT5G58100	expressed protein
AT5G58640	selenoprotein-related
AT5G59310	lipid transfer protein 4 (LTP4)
AT5G59710	transcription regulator NOT2/NOT3/NOT5 family protein
AT5G60390	elongation factor 1-alpha / EF-1-alpha /// elongation factor 1-alpha / EF-1-alpha /// elongation factor 1-alpha / EF-1-alpha /// elongation factor 1-alpha / EF-1-alpha
AT5G61020	YT521-B-like family protein
AT5G61410	ribulose-phosphate 3-epimerase, chloroplast, putative / pentose-5-phosphate 3-epimerase, putative
AT5G61820	expressed protein
AT5G62150	peptidoglycan-binding LysM domain-containing protein
AT5G62390	calmodulin-binding family protein
AT5G62460	zinc finger (C3HC4-type RING finger) family protein
AT5G63460	SAP domain-containing protein
AT5G63600	flavonol synthase, putative
AT5G64040	photosystem I reaction center subunit PSI-N, chloroplast, putative / PSI-N, putative (PSAN)
AT5G64080	protease inhibitor/seed storage/lipid transfer protein (LTP) family protein
AT5G64670	ribosomal protein L15 family protein
AT5G66010	heterogeneous nuclear ribonucleoprotein, putative / hnRNP, putative
AT5G66050	expressed protein
AT5G66290	expressed protein
AT5G66400	dehydrin (RAB18)

LIST OF PUBLICATIONS AND PRESENTATIONS September 2007

PUBLICATIONS

A) articles in journals

1. **V.A. Levitskyi, N.G. Mikheieva, V.G. Roguzhinskaya, D.V. Lyzyn, S.O Kryvych.** Influence of Emotionally-painful stress on microcirculation in the cardiac muscle of rats with alimentary hypercholesterolemia. Clinical and experimental pathology.2004.Vol.3, №2.P.318-320 (In Ukrainian)

B) submitted articles

1. **Kryvych S., Nikiforova V., Herzog M., Perazza D., and Fisahn J.** (2007) Gene expression profiling of the different stages of Arabidopsis thaliana trichome development on the single cell level. *Functional Plant Biology*, Submitted

PRESENTATION OF THE RESULTS ON ACADEMIC CONFERENCES

1. **S. Kryvych. J. Fisahn.** Gene expression profiling in different stages of trichome development of *Arabidopsis thaliana*. Abstracts of XVI Berlin botanical Post-Graduates Colloquium "Havel-Spree-Colloquium". Potsdam, Germany. December 3, 2005 (oral presentation)

2. **Kryvych S., Nikiforova V., Fisahn J.** Gene Expression Profiling on the Single Cell Level in Different Developmental Stages of *Arabidopsis thaliana* Trichomes. Abstracts of 3rd International PhD Student Symposium "Horizons in Molecular Biology". Gottingen, Germany. September 14-16, 2006 (oral presentation; poster)

3. **Kryvych S., Nikiforova V., Fisahn J.** Searching for the genes involved in development of *Arabidopsis thaliana* trichomes on the single cell level.
   Abstracts of papers presented at the 2007 meeting on Plant Genomes. March 15- March 18, 2007 Cold Spring Harbor Laboratory Cold Spring Harbor, New York, USA (oral presentation)

ACKNOWLEDGEMENTS

First of all I would like to thank Dr. Joachim Fisahn for providing me an opportunity to carry out this project, for scientific supervision, and critical review of this thesis.

I would like to acknowledge all the members of Biophysical Analysis Group, present and former, for continuous support, appropriate working atmosphere and help not only on scientific topics.

I am thankful to Dr. Dirk Hincha and Transcript Profiling Group guided by him for producing the array filters and to Prof. Martin Hülskamp, University of Cologne for the seeds of *pGL2::GFP* plant line. Furthermore I would like to thank Prof. Dr. Michel Herzog and Dr. Daniel Perazza from Joseph Fourier University of Grenoble for their help on initial stages of the project. I am grateful to Dr. Victoria Nikiforova for the help with filter array hybridization, evaluation of the data, and for critically reading this thesis. I am also grateful to Dr. Andrey Kochevenko for excellent help and support in cloning and histochemical GUS assay. Thanks to Dr. Eugenia Maximova for great help with microscopy, and metabolite profiling team of MPI-MP for GC-MS analysis. Furthermore, I am thankful to Prof. Prof. Hilde-Gunn Opsahl-Sorteberg from the Norwegian University of Life Sciences for the seeds of the SALK_042431 plant line. Thanks also to Tomek Czechowski for the help with real-time RT-PCR and Megan McKenzie for the prompt correction of my terrible English in this thesis.

I am grateful to the members of my PhD evaluation committee: Prof. Lothar Willmitzer, Dr. Victoria Nikiforova and Dr. Wolf-Rüdiger Scheible for productive criticism, useful suggestions and discussions.

I also would like to thank members of the Greenteam of MPI-MP for taking care of my plants and being helpful and patient to me; Joseph Bergstein is appreciated for the wonderful pictures of the plants. Thanks to Dr. Anna Lytovchenko for her useful advice during this work. I am thankful to the administration of the MPI-MP led by Mr. Lothar Grube for help and support in mostly non-scientific but nevertheless important topics during my PhD.

Additional credits are going to Szymanski brothers. Both of them- for creation and support of the good mood in the atmosphere. In particular Jedrzey- for help in evaluation of GC-MS data, continuous providing of various laboratory consumables, answers to unexpected questions, and supply of visual elements for some of my presentations. Witold is appreciated for the excellent help in the laboratory during his time in our group as a student helper.

Thanks to all other people in the institute who had ever helped or supported me and whose names are not mentioned here.

I am thankful to my teachers from Lviv secondary school N45 and Ivano-Frankivsk State Medical Academy. Due to enormous efforts of most of them despite my resistance at least some knowledge remained in my head.

Finally I would like to thank my grandparents and parents for their continuous invaluable support. My wife Maryna Trofimchuk is very much appreciated for support and patience, help in computer processing of some data, and fruitful discussions that were mostly not related to molecular biology. Final credit goes to my son Danylo, born in August this year, for keeping me fit during the final stage of my PhD.